Center for Technology, Policy and Industrial Development

Massachusetts Institute of Technology

Cambridge, MA 02139

A PHARMACOKINETIC/MECHANISM-BASED ANALYSIS OF THE CARCINOGENIC RISK OF ETHYLENE OXIDE

August, 1987 CTPID 87-1

Dale Hattis, Ph.D.

The research underlying this report was supported by the U.S. National Institute for Occpational Safety and Health and the National Institute for Environmental Health Sciences. Any opinions, findings, conclusions, or recommendations are those of the authors, and do not necessarily reflect the views of NIOSH, NIEHS, the Center for Technology, Policy and Industrial Development, or the Massachusetts Institute of Technology.

TABLE OF CONTENTS

V

SUMMARY

In recent years there has been considerable discussion of opportunities to improve the state of the art of carcinogenesis risk assessment by making use of more detailed information on the biological processes involved--including the dynamics of absorption, elimination, and metabolic processing. This report is part of an effort to build an integrated series of pharmacokinetic models for small molecular weight alkylating agents and their precursors. Such models should allow (1) better assessment of the "biologically effective dose" of activated metabolites that is delivered to target tissues by different external exposure levels, routes, and time patterns of exposure, and (2) more appropriate translation of dose units among species. Models of this type will also be of importance for appropriately interpreting information on newer biologcial markers for steps in the carcinogenic process, such as hemoglobin- and DNA-adduct formation.

The summary below first discusses the basic pharmacokinetic modeling approach. Then some results of interspecies comparisons of metabolic processing of ethylene oxide are presented. Finally, I draw the inferences for human risk.

Pharmacokinetic Modeling Approach

The work reported here has a number of features that distinguish it from other current efforts to build pharmacokinetic analysis into quantitative risk assessments:

(1) The models are implemented in an easy-to-use Apple MacIntosh microcomputer-based systems dynamics modeling system (STELLA). Because the system makes extensive use of graphics for representing models and quickly displaying results, it is straightforward for use by people with little experience in programming, and it facilitates the process of understanding the effects of changes in model structure and parameters.

(2) The models are built around assumptions that

- o reaction with glutathione and other sulfhydryl compounds is the primary route of detoxification of ethylene oxide,
- o depletion of tissue glutathione, rather than enzyme saturation, is the primary mechanism capable of generating changes in ethylene oxide elimination rates at high doses. [The data of McKelvey and Zemaitis (1986) provide direct documentation of glutathione depletion in rats and mice after exposures to ethylene oxide in the hundreds of ppm for several hours. It was found in the modeling that these data could be adequately represented without postulating the additional mechanism of enzyme saturation, for which there is no direct evidence.]
- o alveolar ventilation rates in rodents are decreased at high ethylene oxide exposure levels. [It was found in the modeling that the absorption and exhalation data of Tyler and McKelvey (1983) could not be reproduced unless the rats had decreased alveolar ventilation at high exposure levels.]

(3) Diverse sources of data were used in calibrating the adjustable parameters for the models in different species:

- o For rats, alveolar ventilaton rates and ethylene oxide metabolism rates were set to reproduce the data of Tyler and McKelvey (1983) on absorption of ethylene oxide and exhalation after 6 hour exposures to 11, 104, and 1010 ppm.
- o For humans, ethylene oxide metabolism rates were set to reproduce the data of Brugnone et al. (1985) on the absorption of ethylene oxide from alveolar air by exposed workers,
- o For mice, ethylene oxide metabolism rates were set to reproduce the hemoglobin adduct observations of Segerback (1983) and Osterman-Golkar et al. (1976) following intraperitoneal administration of low doses. Given these metabolism rates, low dose alveolar ventilation rates were set to reproduce the

absorption data of Ehrenberg et al. (1984).

Because of the availability of independent data for calibrating the models for each spcecies, no interpsecies extrapolation was required in determining primary metabolism rates.

(4) Extensive sensitivity analysis was undertaken of the effects of different modeling assumptions and parameters. Parallel series of rat, human, and mouse models were constructed incorporating different assumptions about blood/air and tissue/blood partition coefficients, and the distribution of metabolizing activity among tissues. The performance of these model variants was tested where possible with data that were not fully used for primary calibration of metabolism and alveolar ventilation:

- For the rat model variants, expectations were compared with the high-dose glutathione depletion data of McKelvey and Zemaitis (1986), and the hemoglobin adduct data of Osterman-Golkar et al. (1983)
- For the human model variants, expectations were compared with the observed decline with time of the percentage of ethylene oxide absorbed from alveolar air observed by Brugnone et al. (1986) and the hemoglobin adduct data of Calleman et al. (1978),
- For the mouse model variants, expectations were compared with the high-dose glutathione depletion data of McKelvey and Zemaitis (1986)

In general the sensitivity analysis revealed that only very small changes in ultimate human risk projections would result from reasonable changes in modeling assumptions about partition coefficients and the distribution of metabolizing activity among tissues. In one case--the hemoglobin adduct data of Calleman et al. (1978) in human workers--the differences between the expectations of the models and a set of observations/interpretive theory was large enough to require rejection of one or the other. Because

of the significant uncertainties in the exposure levels in the Calleman et al. (1978) data set, and the uncertainties in their interpretive assumptions of in vivo stability of the hemoglobin adducts and red cells containing them, my judgment was to reject the Calleman et al. (1978) data/interpretive assumptions rather than the Brugnone et al. (1985) data and the interpretive assumptions used to construct the pharmacokinetic models.

Pharmacokinetic Modeling Results

The calculated rate constants for systemic elimination of ethylene oxide differ significantly among species. Table S-1 shows the long-term systemic elimination half-lives for ethylene oxide after low dose* exposures. Other things being equal, the longer it takes to eliminate the average molecule of ethylene oxide from the organism, the greater the internal dose (expressed in units of concentration X time) and the more opportunity there will be for reaction with DNA. This indicates that per mole of absorbed dose, one should expect a greater concentration X time of ethylene oxide to be available in humans than in rodents.

Table S-2 shows the results of putting these data were put into a standard allometric scaling equation (Adolf, 1949):

---

*At higher doses, where glutathione is appreciably depleted, ethylene oxide will be eliminated more slowly (longer half-life). The low-dose calculations for Table 5.1 were generally based on exposures to 1 ppm in humans, 11 ppm in rats, or simulated intraperitoneal injection of 2.175×10^{-7} moles of ethylene oxide in mice. None of the models shows appreciable depletion of glutathione under these conditions, nor is there any difference between inhalation and intraperitoneal exposure in the elimination half-life calculated by observing the long term decline in ethlyene oxide concentrations in venous blood.

Table S-1
Apparent Differences in Low Dose Elimination Half-Lives ($T_{1/2}$)
for Ethylene Oxide In Different Species

Model Series (named for rat model)	Values of $T_{1/2}$ (min.) Mouse	Rat	Human
G3BL90 (plain vanilla)	6.16	8.84	39.6
G3BL90-LV* (2X increase in liver metabolism)	6.43	9.21	40.8
G3BL50-LV* (Blood/air of 50, 2X increase in liver metabolism)	6.14	6.84	22.1
G3BL90-LV*-T* (T* set of tissue/blood partition coefficients, 2X increase in liver metabolism)	8.11	11.52	54.8

Table S-2
Allometric Scaling Equations for Elimination Half-Lives for Ethylene Oxide In Different Species

Model Series named for rat model)	Regression Coefficients* log K	m	r	Predicted $T_{1/2}$ for 17.5 Kg Dogs
G3BL90 (plain vanilla)	1.14	.240	.9948	27.5 min.
G3BL90-LV* (2X increase in liver metabolism)	1.16	.239	.9949	28.4 min.
G3BL50-LV* (Blood/air of 50, 2X increase in liver metabolism)	1.01	.170	.9781	16.6 min.
G3BL90-LV*-T* (T* set of tissue/blood partition coefficients, 2X increase in liver metabolism)	1.27	.247	.9937	37.5 min.

---

*For the equation, $\log(T_{1/2}) = m \log(\text{Body Weight})$

$T_{1/2}$ = K (Body Weight)^m

For the models with a blood/air partition coefficient of 90 (our best estimate, based on a direct measurement in human blood by Brugnone et al., 1986) there are excellent linear fits. Moreover the m's that result are very close to the scaling factor of 1/4 that would be expected if, according to the theory of Boxenbaum (1982), elimination rates for chemicals tend to scale with metabolic energy density (metabolic rates per unit of mass).

The allometric relationships in Table S-2 were used to make predictions for the elimination half-life of ethylene oxide in dogs (with an average weight of 17.5 kg). Martis et al. (1982) measured the clearance of ethylene oxide from plasma in four 16-19 kg dogs following intravenous administration of each of two doses--75 or 25 mg/kg. At the higher dose level he measured an average elimination half-life of 36.5 +/- 18.5 (SD) min., while at the lower dose level the average half-life measured was 29.3 +/- 5.7 min. As can be seen in the last column of Table S-2 the latter result at the lower dose is in good agreement with the half-life predicted from the mouse, rat, and human model results using the allometric equation for my "best estimate" G3BL90-LV* series of models. This strengthens the conclusion that the longer elimination half-life predicted by the human model is likely to be correct.

Table S-3 shows the implications of the models for the overall internal dosage that can be expected in humans for brief exposures to relatively low air levels of ethylene oxide. It can be seen that because humans breathe less per unit of body weight, they absorb substantially

Table S-3

Expected Blood and Tissue Doses Following
5 Minute Exposures of Different Species to 1 ppm Ethlene Oxide

Best Estimate Models*

Species	----------Absorption-------- (Moles/kg)	(Moles/kg$^{.75}$)	Blood C X T (Moles/l)-min
Human	3.13×10^{-8}	9.04×10^{-8}	4.36×10^{-6}
Rat	8.53×10^{-8}	6.03×10^{-8}	2.57×10^{-6}
Mouse	2.74×10^{-7}	1.09×10^{-7}	3.77×10^{-6}

The names of these models are: Human--GSH3-LV; Rat--g3BL90-LV*; and Mouse--Mg3BL90-LV*. In all three models, the "LV*" designation indicates that the rate constant for metabolism in the liver has been set at a level twice that in other tissues (to better conform to observations of glutathione depletion in different tissues).

**This is the ultimate amount exhaled by several hours after the 5 minute exposures--after all ethylene oxide absorbed has been disposed of either through metabolism/reaction or exhalation. The approximate half lives of ethylene oxide in the three species are: Human--41 minutes; Rat--9.2 minutes; Mouse--6.4 minutes.

less than mice or rats per body weight. This lower absorption rate per body weight almost exactly offsets the longer elimination half-life, so that the models indicate that the three species will experience quite a similar internal concentration X time from a given low external air level X time.

Conclusions for Human Risk

There is a substantial body of data available on the carcinogenic response of rats (Snellings et al., 1984; Lynch et al., 1984) and mice (NTP, 1987) to ethylene oxide. In both species, for several different organs significant excesses of tumors have been observed in groups exposed to ethylene oxide compared to controls. Pharmacokinetic analysis can contribute to the analysis of such data by improving the measure of "delivered dose" that is used in standard carcinogenesis dose-response modeling.

Table S-4 shows the risk equations that result for different sites, species and sexes, using my preferred measure of "delivered dose"--the long term average blood ethylene oxide concentration--in multistage modeling using Howe and Crump's (1983) "Global82" program.* (Data for

---

*This program calculates maximum likelihood estimates (MLE) for the "q" coefficients in the equation:

$$P(d) = 1 - e^{-(q_0 + q_1 d + q_2 d^2 + \ldots q_k d^k)}$$

Where P(d) is the expected tumor incidence at a particular dose (d). The "q_0" term determines the background tumor incidence, the "q_1" determines the size of the linear dose response term, and q_k's determine the contributions of higher powers of dose. The program also calculates sets of "q" coefficients for predicting upper 95% confidence limits on induced tumor incidence (UCL), based solely on statistical sampling-error uncertainties in the experimental data. All the "q" coefficients are constrained to be positive or zero.

Table S-4
Interspecies Comparison of Overall Carcinogenic Dose Response
--Expressing "Dose" in Average Internal Micromoles/Liter
As Estimated by the "Best Estimate" BL90LV* Series of Models

Sex, Species and Site	---Risk Coefficients---- MLE q_1	q_2	UCL q_1	Overall Induced Cacrcinogenic Transformations per Animal at 1 ppm* MLE	"UCL"**
Female Rats (Snellings et al., 1984)					
Leukemias	.0529	0	.0751		
Brain	.00660	0	.0126		
Total	.0595	0	.0877	.00547	.00807
Male Mice (NTP, 1987)					
Lung	.0225	.00125	.0557		
Harderian Gland	.0192	0	.0301		
Lymphomas	.00386	0	.0097		
Total	.0456	.00125	.0955	.00618	.0129
Female Mice (NTP, 1987)					
Lung	0	.00297	.0198		
Harderian Gland	.0140	0	.0229		
Lymphomas	0	.00215	.0182		
Mammary	.0127	0	.0213		
Uterus	.0026	.00467	.0131		
Total	.0293	.00979	.0953	.00413	.0129

---

*Computed at the equivalent to 1 ppm of approximately .092 umoles/liter long term average internal ETO concentration for rats, and .135 umoles/liter for mice.

**Strictly, this "upper confidence limit", representing the sum of the 95% upper confidence limits seen for a number of different tumor sites, is somewhat more "conservative" (lower probability) than would be obtained by a Monte Carlo simulation of the statistical errors implied for the component data sets.

male rats unfortunately had to be excluded from this analysis because the high backround rates of leukemias rendered the data very difficult to interpret unambiguously). Similar analyses can be found in Section 5.2 using other dose metrics: (1) simple ppm exposure for a given fraction of the time per week, (2) net absorption during exposure [normalized to body weight, (body weight)$^{.75}$, or (body weight)$^{2/3}$], and (3) long term average blood concentration predicted by an alternative series of models (BL50LV*) based on an assumption that the blood/air partition coefficient is only 50, rather than 90.

Because of the differences in positive sites in different species I made comparisons of these data based on the aggregate coefficients including all tumors. As it happened even the simplest of these dose measures--ppm exposure--produced quite consistent results across species. Of the four the poorest consistency was seen for the "alternative" BL50LV* model.

Table S-5 summarises the implications of each of the four dose metrics for overall human cancer risk from 45 year 8-hour/day occupational exposure to 1 ppm ethylene oxide. The "best estimates" in this table are based on the arithmetic mean of the risk coefficients for mice and female rats, where the coefficients for "mice" are themselves the averages of the coefficients for males and females. The "plausible upper limit" estimates are based on the highest 95% upper confidence limit seen in the three species-sex combinations.

In the end it can be seen that in this case the different dose metrics used in the analysis do not lead to markedly divergent estimates of human risk. Even the simplest exposure measure considered--external

Table S-5
"Best Estimates" and "Plausible Upper Limits" for Overall Cancer Risk from Occupational Exposure to 1 ppm Ethylene Oxide

(Exposure for 8 Hours/Day, 5 Days/Week for 45 Years)

Probability Per Individual of Developing at Least One Additional Cancer		
Dose Metric	"Best Estimate"	"Plausible Upper Limit"
PPM in Air (8 hours per day, 5 days/week)	.0045	.013
Net Absorption (Umoles/day) / (Body Weight)^{n}*	.0051	.029
Best Estimate BL90LV* Models Umoles/liter long term average blood ETO conc.	.0065	.019
Alternative BL50LV* Models Umoles/liter long term average blood ETO conc.	.0035	.012

*Where n is .75 for the "Best Estimate" risk and 2/3 for the "Plausible Upper Limit" risk, and where absorption refers to the ethylene oxide absorbed per day on each of 5 days per week of exposure.

air ppm X exposure time--leads to expected risks that are well within a two-fold range of the "best estimate" risks inferred from the pharmacokinetic modeling. At least for a simple direct-acting alkylating agent such as ethylene oxide, the traditional approaches for dose and risk projection across species appear to be sustained by the more elaborate pharmacokinetic-based analysis.

Another conclusion from Table S-5 is of course that the projected risk from working lifetime exposure at the proposed OSHA 8-hour time-weighted-average standard of 1 ppm is appreciable in relation to other cancer risks that have been the subjects of control action in the past. In the light of the mandate of the OSHAct, consideration of the feasibility of a stricter standard is warranted.

Finally, Table S-6 compares the internal doses that can be expected at various levels of exposure for eight hours, with the doses that would be expected if the same ppm-hours were delivered in a 15 minute burst. Starting simply with the 8-hour exposures, it can be seen that relatively little nonlinearity in delivered dose can be expected at exposure levels below 100 ppm. This is basically because if (as the models assume) glutathione concentrations in human tissues are similar to those in rat tissues, the initial store of glutathione in the body is quite large--about .044 moles. Since it takes at least one mole of ethylene oxide to react with one mole of glutathione (neglecting reactions with other sulfhydryls and the continuous replacement of glutathione), a relatively large air concentration for an 8 hour day is required to produce appreciable depletion. For example, at 10 ppm, the approximately 5.44 cubic meters of air taken into the alveoli in an 8 hour work day

Table S-6
Comparison of Predicted Delivered Doses for Constant 8-Hour vs.
High-Level 15 Minute Exposures Presenting the Same External PPM-Hours

ppm	Net Absorption During Exposure (moles/day)	Exhalation of Unchanged ETO After Exposure (moles/day)	Blood C X T (mole/liter)-min per day of exposure	Average Weekly Blood Concentration (umoles/liter) for 5 days exposure/week
Best-Estimate Model (GSH3-LV*. Blood/air partition coefficient = 90*)				
480 minute exposures:				
1	.0001666	5.948E-6	.0004143	.2055
10	.001665	6.041E-5	.004162	2.064
100	.01649	7.073E-4	.04370	21.68
1000	.1472	28.37 E-3	.7480	371.0
15 minute exposures delivering the same ppm-hours/day:				
32	.0002044	4.326E-5	.0004156	.2062
320	.002044	4.353E-4	.004177	2.072
3200	.02044	4.640E-3	.04408	21.86
32000	.2044	9.027E-2	.7917	392.7
Alternative Model (GSH3BL50-LV*. Blood/air partition coefficient = 50*)				
480 minute exposures:				
1	.0001658	2.779E-6	.0002139	.1061
10	.001656	2.823E-5	.002149	1.066
100	.01638	3.325E-4	.02250	11.16
1000	.1390	17.87 E-3	.4011	199.0
15 minute exposures delivering the same ppm-hours/day:				
32	.0001975	3.399E-5	.0002146	.1064
320	.001975	3.423E-4	.002157	1.070
3200	.01975	3.679E-3	.02273	11.27
32000	.1971	8.339E-2	.4373	216.9

---

*See the footnote to Table 4.7, p. 99 for other model specifications.

contains about

(5443 liters)*(10^{-5} moles/25.45 liters at 10 ppm) = 2.1 X 10^{-3} moles ETO

Thus an 8 hour exposure to 10 ppm ethylene oxide is unlikely to produce more than about a 5% depletion of the overall store of glutathione in the body. If, as assumed in the models, this is the chief likely source of nonlinearity*, it follows that there can be only relatively modest nonlinearities in the exposure region up to 10 ppm. For the same reason, the models predict that there will be relatively little difference in hemoglobin- or DNA-adduct formation per ppm-hour of exposure between workers exposed relatively continuously and workers exposed in short high-level bursts.

The fact that emissions from sterilizers and the resulting worker exposures may often occur primarily in short bursts (e.g. when the sterilizers are opened for unloading) suggests that monitoring procedures and control efforts may be usefully directed at limiting the peaks of emissions and worker exposure. Also, in enforcing workplace standards, designing 15 minute limits, to be evaluated at known times of high level exposure, rather than 8-hour time weighted averages, could lead to important savings in the time required for OSHA industrial hygeinists to collect samples. I would suggest that these engineering and administrative considerations should be the driving factors in evaluating

---

*Conceivably enzyme saturation could also produce nonlinearities. However if enzyme saturation were appreciable in rodents at lower doses than required for appreciable glutathione depletion I should not have been able to fit the glutathione depletion results of McKelvey and Zemaitis (1986) as well as I did without including this additional factor.

the desirability of short term exposure limits for ethylene oxide, rather than biological/pharmacokinetic considerations.

There is one remaining caveat that should be attached to this final conclusion, however. Because of a lack of data on blood flows and tissue volumes for the testis, I was unable to test whether the models I have developed would predict the appreciable dose-rate effects seen by Generoso et al. (1986) for dominant lethal mutations. It is not impossible that some special detoxification reactions are present in this tissue that might exhibit saturation behavior at lower dose rates than are seen elsewhere. In the light of the theory developed in Section 2.2 (pp. 21-25), however, one requirement for this would be that at low doses, the metabolism/detoxification in the testis would have to proceed at much faster rates than elimination of ethylene oxide with the venous blood. The modeling to date does not indicate that any other tissue metabolizes ethylene oxide this fast at low doses.

One other possibility is that DNA repair systems in the developing sperm could be saturated by exposure to ethylene oxide at high dose-rates. As described on pp. 26-27, this could lead to a $(\text{dose})^2$ dependence of mutagenic risk for exposures occurring as a single burst.

1. INTRODUCTION

This is the second in a series of carcinogenic risk assessments for small molecular weight alkylating agents based on pharmacokinetic modeling of the likely internal dosage of DNA-reactive substances. An earlier project (Hattis et al., 1986) studied perchloroethylene. It is hoped that models of the kind developed here can improve upon standard risk assessment approaches by (1) better representing high-dose nonlinearities produced by enzyme saturation and other processes, and (2) facilitating better translation of effective dosages between species and between different patterns of exposure (e.g. brief high exposures vs. long-term continuous dosing patterns.)* The practical application of pharmacokinetic prinicples and data to ethylene oxide is a test of the potential helpfulness of this approach, both for risk assessment and for the identification of experimental and epidemiological information that may help reduce residual uncertainties.

1.1 Choice of Ethylene Oxide for Analysis

As illustrated in Figure 1.1, a number of substituted and unsubstituted olefins are at least transiently converted to activated epoxide intermedates which then can react with DNA and other cellular nucleophiles. Ethylene oxide is a relatively simple molecule whose uptake

---

*The latter issue in particular has been the subject of considerable public discussion as different parties have put forward different views on the appropriate form for occupational health standards for ethylene oxide (Sun, 1986).

Figure 1.1

Metabolic Pathways for Perchloroethylene and Some Related Compounds

P450 Metabolism Rearrangement

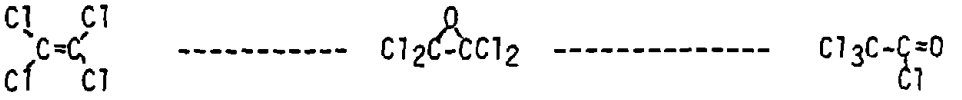

Perchloroethylene — Perchloroethylene Oxide — Trichloroacetyl Chloride

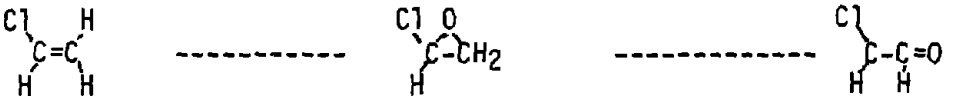

Vinyl Chloride — Chlorooxirane — Cloroacetaldehyde

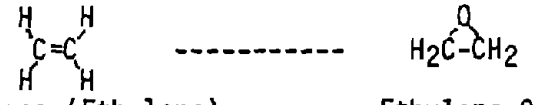

Ethene (Ethylene) — Ethylene Oxide

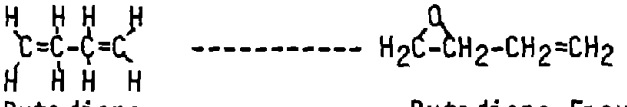

Butadiene — Butadiene Epoxide

and metabolism has been relatively well studied in both rodents and people. Moreover, as the simplest epoxide (and one of the most stable epoxides under physiological conditions*), ethylene oxide may be able to provide helpful clues for the modeling of other epoxides that are harder to study directly.

---

*Kline et al. (1978) report the following pseudo-first-order rate constants for the reaction of various epoxides with water:

	Hydrolysis rate constant, min^{-1}	Indicated water half-life (min)
Measurements at 20°C., pH 7.0:		
ethylene oxide	2.1×10^{-5}	3.3×10^4 (23 days)
tetrachloroethylene oxide	6.0×10^{-2}	11.5
Measurements at 37°C., pH 7.4:		
epichlorohydrin (1,2-epoxy-3-chloropropane)	6.9×10^{-4}	1×10^3 (17 hours)
cis-1,3-dichloropropene oxide	2.4×10^{-3}	290 (4.8 hours)
cis-1-chloropropene oxide	6.3×10^{-2}	11
trans-1-chloropropene oxide	1.6×10^{-1}	4.3
vinyl chloride oxide (chloro-oxirane)	4.6×10^{-1}	1.5
trichloroethylene oxide	5.3×10^{-1}	1.3

1.2 Distinctive Features of the Pharmacokinetic Models Required for Ethylene Oxide

The modeling process in this study revealed two substantial technical "surprises" that required the incorporation of novel features into the ethylene oxide models:

- The basic mechanism producing high-dose nonlinearity is probably not enzyme saturation, but the depletion of glutathione and related sulfhydryl compounds.
- In order to adequately fit ethylene oxide absorption data in rats, I found that there had to be dose-dependent changes in rat breathing rates. The degree of reduction of absorption that could be produced by either glutathione depletion or enzyme saturation at high doses was considerably less than was observed in available experiments.

These are discussed in turn in the subsections below.

1.2.1 Glutathione Depletion as a Cause of Reduced Detoxification Rates at High Doses

My initial expectation was that the pharmacokinetic models for ethylene oxide would be very similar to the models we had just developed for perchloroethylene. For perchloroethlene, as for some other compounds (Ramsey and Andersen, 1985; Gehring et al., 1978), the major nonlinear reaction appeared to be a saturable activation step (mediated by P450 enzymes) that was assumed to take place primarily in the liver. Figure 1.2 is a schematic diagram of the basic perchloroethylene model for rats.

No activation reaction is of course needed for ethylene oxide. However, by analogy, I initially assumed that any nonlinearities in delivered dose as a function of external dose for ethylene oxide would be

Figure 1.2
Basic Structure of the Rat Perchloroethylene Model

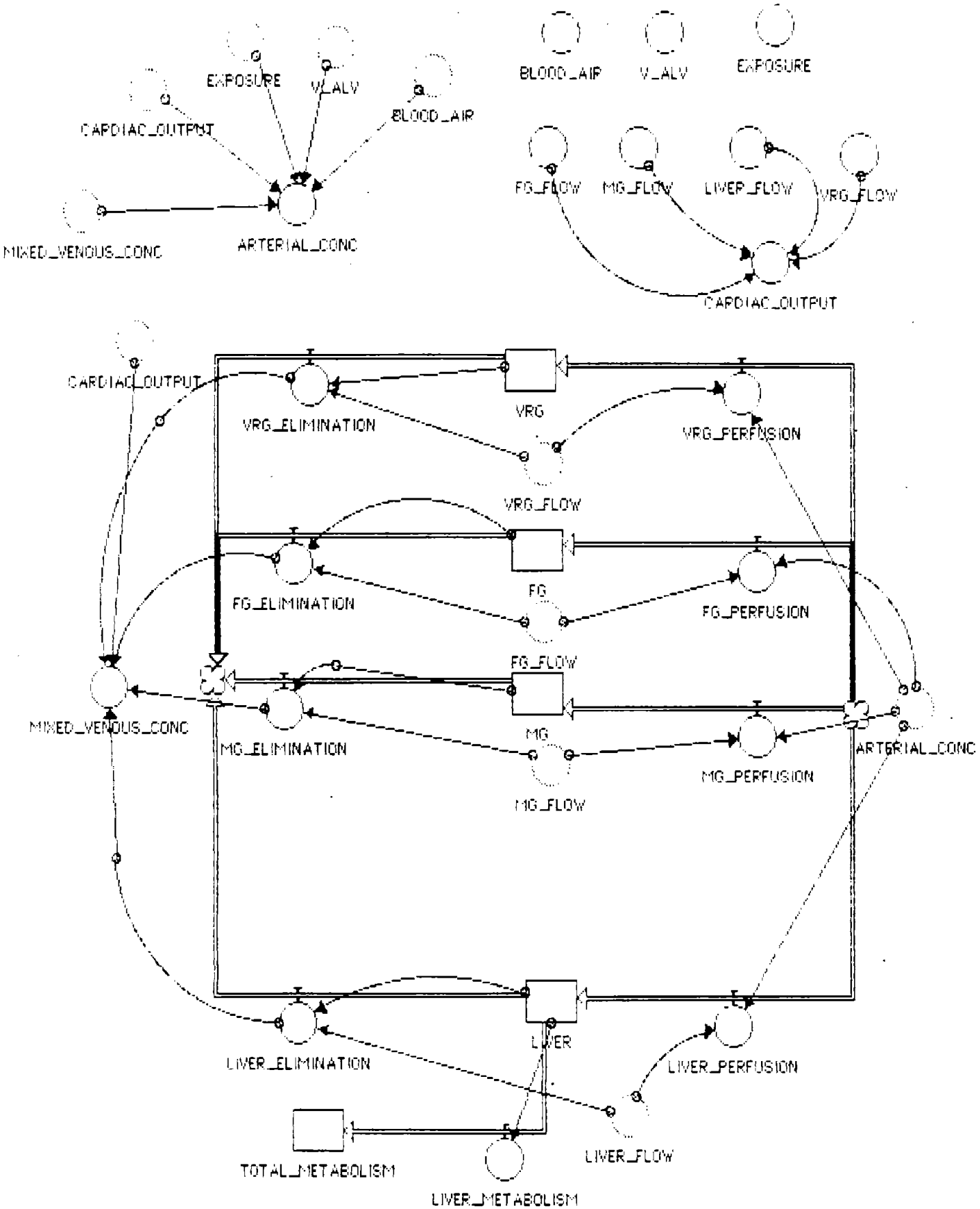

attributable to a saturable detoxification* reaction that occurred primarily in the liver. [This could have been either an enzyme-catalysed hydrolysis (reaction with water to yield ethylene glycol) or a conjugation reaction with glutathione.]

However after some preliminary work had been done along these lines, in reviewing recent literature I found two observations that could not be accommodated within this framework:

(1) After high short term exposures to ethylene oxide in rats and mice (McKelvey and Zemaitis, 1986) there is appreciable depletion of glutathione in a wide variety of tissues--not just the liver. These data are illustrated in Figure 1.3.

(2) Measurements by Brugnone et al. (1986) of ethylene oxide concentrations in human venous blood (presumably drawn from the arm) indicated appreciably lower ethylene oxide levels than would be required to be in equilibrium with simultaneously observed ethylene oxide levels in alveolar air. This suggests that in humans, appreciable ethyene oxide metabolism is likely to take place in the skeletal muscle and/or other tissues that are the source of venous blood drawn from the arm.

We therefore explored the possiblity that the dose-dependent changes in ethylene oxide metabolism seen by Tyler and McKelvey (1983) could be attributable to changes in the availability of glutathione and related sulfhydryl agents in a variety of body tissues. Within each tissue, basal rates of glutathione generation and loss were derived from generally availble information about glutathione turnover in rats (Lauterburg and Mitchell, 1981; Griffith and Meister, 1979). The reaction of ethylene oxide and glutathione was represented by simple bimolecular reaction kinetics, initially assumed to be governed by the same rate constant

---

*Some nonlinearity in detoxification is indicated by data of Tyler and McKelvey (1983), who found an increase in the percentage of absorbed ethylene oxide that is exhaled at high doses (between 100 an 1000 ppm, administered over 6 hours in rats). These data are reproduced in Table 1.1 on page 13 below. Additionally, Generoso et al. (1986) have found high-dose dose rate effects for dominant lethal mutations in mice.

Figure 1.3
Depletion of Glutathione in Various Tissues of Rats by Four Hour Exposures to Different Concentrations of Ethylene Oxide

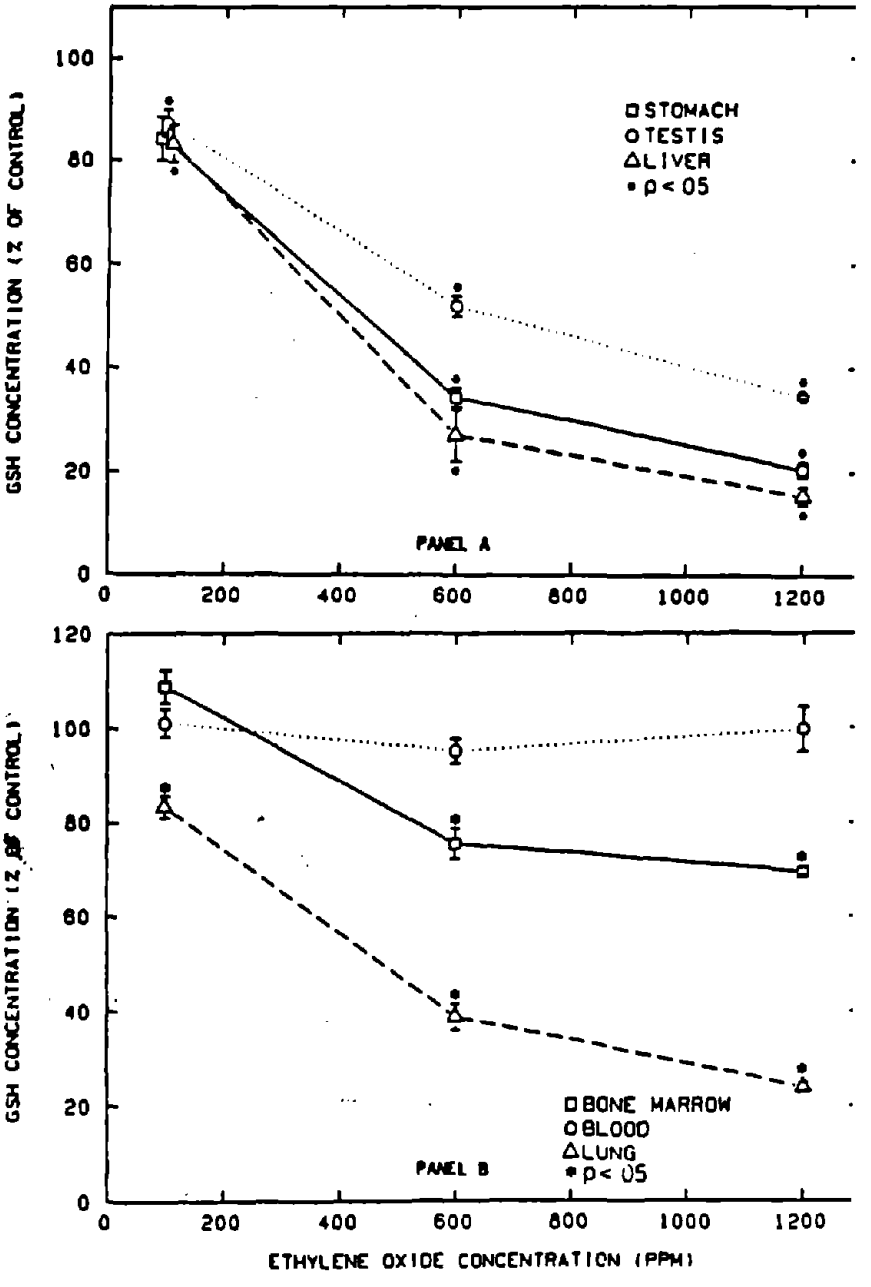

FIG. 1. Tissue GSH levels of Male Fischer-344 Rats Immediately after a Four Hour Exposure to EO.

Source: McKelvey and Zemaitis, 1986

(k_2) in all tissues:

ETO metabolism (moles/minute) = k_2(Moles ETO in Tissue)(Glutathione Concentration)

Given this mechanism, it was not necessary to assume that any of the enzymes responsible for ETO metabolism become appreciably saturated within the dose range that has been studied.

Figure 1.4 shows the more complex schematic diagram representing the ethylene oxide model in rats. Metabolism is assumed to occur in all tissues except the fat and the blood (no data were avaialable on glutathione depletion in fat, and the available information suggested no detectable depletion of glutathione in rat blood). In addition, in comparison with the perchloroethylene model, I have reintroduced an explicit lung compartment (in order to follow glutathione changes in this organ specifically) and finite arterial and venous blood pools. The blood compartments allow one to make comparisons of the model predictions with observations of hemoglobin adduct formation in different species (Osterman-Golkar, 1983; Segerback, 1983; Calleman et al, 1978; Ehrenberg et al., 1974).

There is, of course, a price to be paid for the greater complexity represented in Figure 1.4. There are more independently-adjustable parameters, and therefore greater requirements for information (or assumptions) to adapt the model for different species*. Nevertheless, glutathione-based metabolism and glutathione depletion appear to be common enough features of the toxicology of a number of compounds [e.g. methyl chloride, ethylene dibromide (Dodd et al., 1982; Mann and Darby, 1985)]

---

*The issue of model complexity will be specifically explored in Section 3.6 below.

Figure 1.4
Basic Structure of the Rat Ethylene Oxide Model

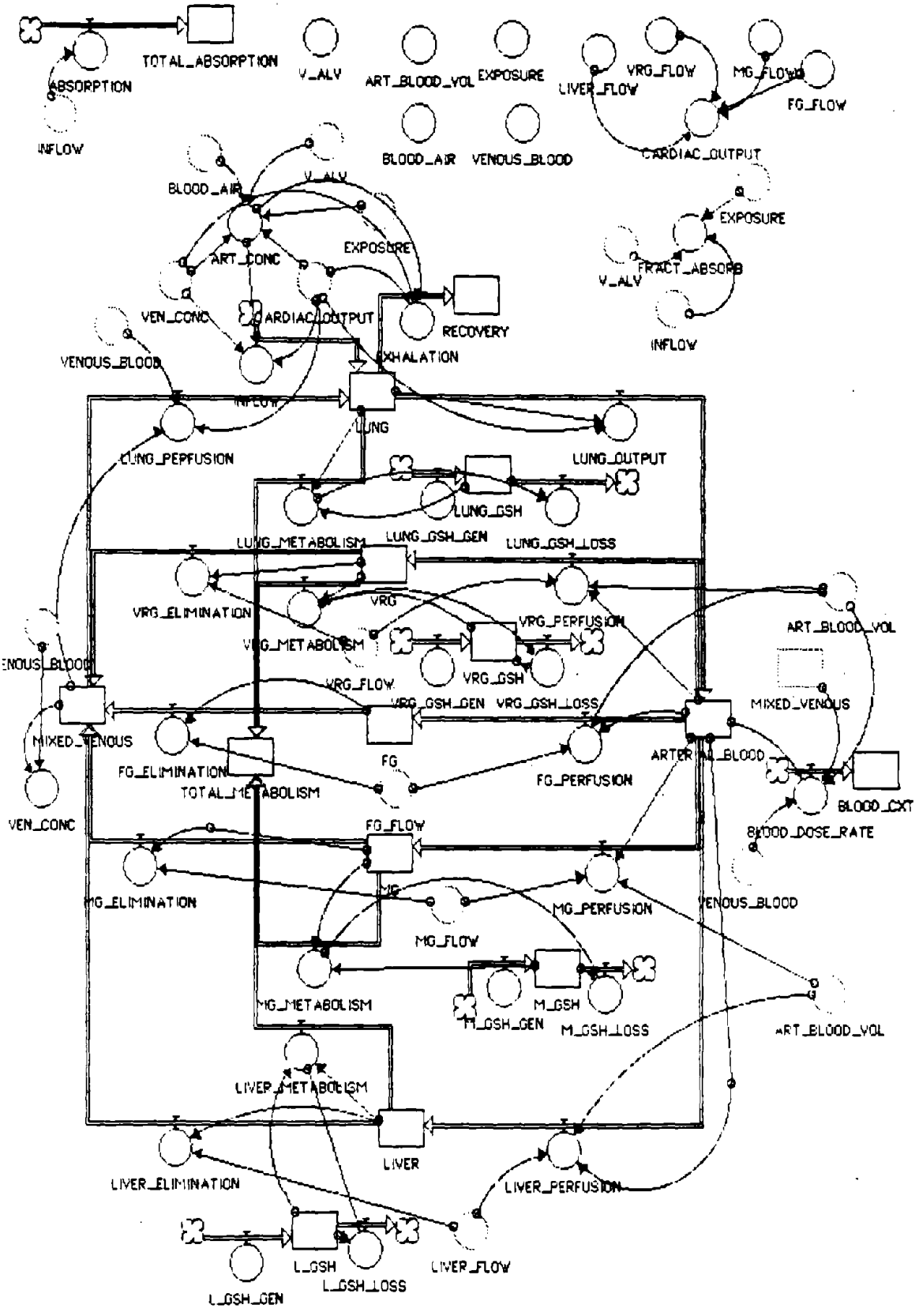

that research on this subject may prove rewarding for pharmacokinetic risk assessment of small molecular weight alkylating agents in general. It is my hope that this initial modeling effort for ethylene oxide may help stimulate relevant experimental research, and indicate ways in which disparate results from different research projects can be integrated into a coherent picture.

1.2.2 Reduced Breathing Rates at High Ethylene Oxide Exposure Levels

Animals respond to a wide variety of irritant gases by decreasing their rate of respiration (Alarie, 1981). [It has even been proposed that the potency of different chemicals for reducing respiration be used as a guide for selecting concentrations that will not produce irritation or other gross toxic effects in humans (Alarie, 1981; Kane et al., 1979; Kane et al, 1980; Alarie, 1981).] As can be seen in Figure 1.5, these effects can persist over at least a three hour exposure period, and they can even increase for exposures that are repeated on subsequent days. Such decereases in respiration at higher doses in animal studies can be expected to reduce the effective delivered dose, both in chronic inhalation bioassays and in the shorter term experiments that are used to derive pharmacokinetic parameters. Other things being equal, unless this effect is detected and accounted for in explicit modeling, it would tend to

(1) distort observed tumor dose response relationships in the direction of high-dose saturation,

(2) often cause an underestimation of carcinogenic potency per unit of delivered dose [since potency is a ratio of effect per unit dosage, overestimation of the actual animal dosage may produce an underestimation of potential human potency at low doses, unless

Figure 1.5

Respiratory Depression for 3 Hour Exposures on Four Successive Days

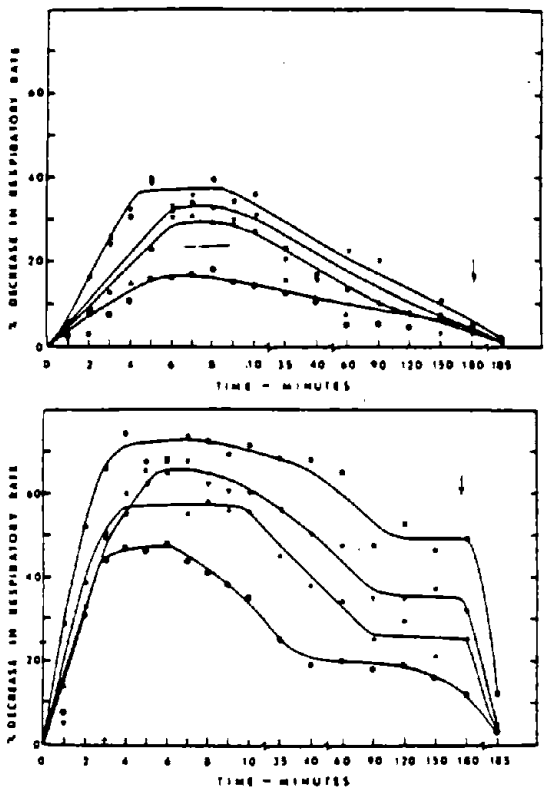

Figure 5 — Time-response relationships for exposure to formaldehyde for 3 hr/day on four consecutive days to 1.0 ppm (upper set) and 3.1 ppm (lower set). The first, second, third and fourth days are designated by • ▲ ▼ ■, respectively. The arrows indicate the end of the exposure periods.

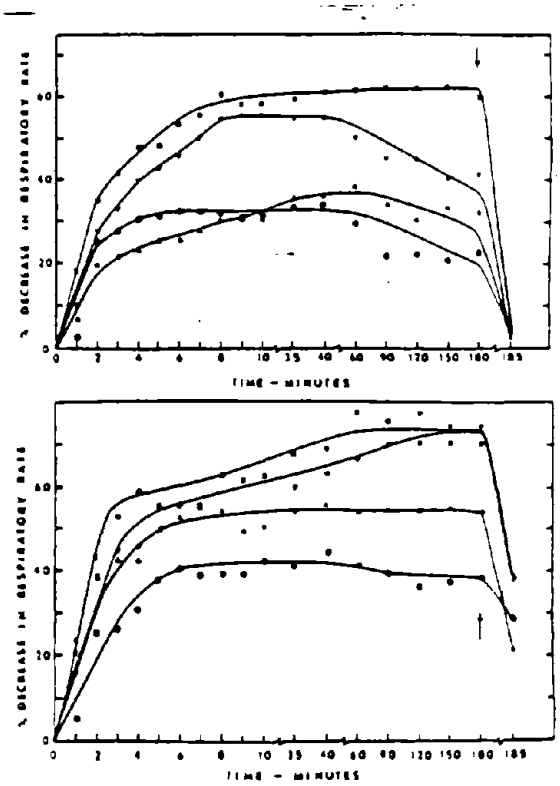

Figure 6 — Time-response relationships for exposure to acrolein for 3 hr/day on four consecutive days to 0.5 ppm (upper set) and 1.7 ppm (lower set). The first, second, third and fourth days are designated by ‡ ▲ ▼ ■, respectively. The arrows indicate the end of the exposure periods.

Source: Kane and Alarie, 1977

this effect is counterbalanced by the misestimation of the dose response relationship produced by effect (1) above], and

(3) cause an underestimation of the metabolic parameters K_m and V_{max} in Andersen-type metabolic rate experiments.

Table 1.1 shows data from a metabolic disposition experiment in rats by Tyler and McKelvey (1982). It is clear from the exhalation data that there is some dose-dependent change in the metabolism of ethylene oxide. And less rapid metabolism at the higher dose rates would tend to also reduce absorption/ppm (see Andersen, 1979). Unfortunately, the observed reduction in absorption per unit of exposure is larger than can be accounted for by the observed pattern of reduced metabolism at high doses. In order to fit these data in the current rat model with the best point estimates of other pharmacokinetic parameters, I found it necessary to postulate reductions in alveolar ventilation of about 23 and 60% for the 104 ppm and 1010 dose rates from the 115 l/minute alveolar ventilation rate needed to fit the observations at 11 ppm for 250 g rats. This tentative conclusion also renders intelligible the finding of Osterman-Golkar et al. (1983) of a slight reduction in hemoglobin adduct formation per ppm-hour of exposure--measured at the end of a two year inhalation bioassay (Table 1.2). If saturation of a metabolizing system or depletion of glutathione were the only process going on, there should be either no observed change or a slight <u>increase</u> in adduct formation per unit dose in these data.

This experience in encountering these two technical surprises in the modeling of ethylene oxide should emphasize the evolving state of the art of pharmacokinetic modeling, even for relatively simple compounds. However, it also indicates that the modeling process can help uncover and

Table 1.1

Net Absorption and Metabolic Disposition of Ethylene Oxide in Rats After 6 Hour Exposures

Exposure Level (ppm)	Net Absorption During Exposure (mg/kg present at end of exposure)	Net Absorption per ppm (mg/kg-ppm)	% Exhaled Unchanged (by 18 hours after end of exposure)
11	2.67	.243	0.5 +/- 0.1*
104	20.2	.194	0.5 +/- 0.1
1010	106.8	.106	2.1 +/- 0.2

---

*Mean +/- standard deviation, four rats per dose level. (Standard errors would be expected to be about half the stated values.)

Source: Tyler and McKelvey, 1982

Table 1.2

Alkylation of Rat Hemoglobin by Ethylene Oxide in a Chronic Inhalation Bioassay

Dose Rate (ppm--30 hr per week)	Degree of alkylation of a histidine-N (nmol/g Hemoglobin)	Alkylation* per ppm (nmol/g-ppm)	% Reduction from 10 ppm ratio of alkylation per ppm
10	12	1.2	----
33	32	0.97	19
100	80	0.80	33

---

*After subtraction of a background level of about 2×10^{-9} mol/g Hb.

Source: Osterman-Golkar et al., 1983

explore unexpected features of biological systems that are of basic scientific interest.

1.3 Structure of the Report

Below, Section 2 presents basic theory for the construction of the pharmacokinetic models. Section 2.1 first reviews the fundamental concepts used in the development of flow-limited models in 2.1. Then section 2.2 developes the general mathematics for assessing potential increases in effective tissue doses of alkylating agents as a function of external dose rates.

Section 3 then reviews the diverse types of data that are available for construction of the models. A final subsection gives a quantitative view of the permissible degree of model complexity given the data at hand.

Using these data, Section 4 shows the process by which the models were articulated and parameters estimated for the various species. Data for rats and humans are presented first, as they were developed together, followed by examination of the generally more limited data available for mice.

Finally Section 5 develops the final conclusions for human risk. Different subsections treat interspecies projection issues and estimated dose rate effects in humans.

2. BASIC PHARMACOKINETIC THEORY FOR ETHYLENE OXIDE MODELS

2.1 Basic Structure of the Pharmacokinetic Models

Pharmacokinetic models are intended to represent and predict the uptake, transfer, metabolism, and excretion of chemicals in biological systems. In the context of risk assessment, the goals are (1) to predict the effective dosage of active metabolites to humans as a function of different levels and time patterns of exposure, and (2) to relate the dosage of active metabolites available to human cells to the dosage available in animal bioassays.

Our models are roughly patterned after those described by Fiserova-Bergerova (1983). Full derivations of the basic equations are presented in our earlier report (Hattis et al., 1986). Relevant exerpts of this report are reproduced as Appendix A.

Briefly, in our models the body is divided into a number of "compartments" representing organs with similar ratios of blood flow to tissue volume. Each compartment is represented as a well-mixed pool. The concentration of ethylene oxide in blood leaving each compartment is assumed to have reached equilibrium with the concentration of ethylene oxide in the compartment. This leads to the following equation for the increase or decrease in the moles of ethylene oxide stored in each compartment:

$$\frac{d(ETO)}{dt} = Q_{tissue}[ETO]_{art} - \frac{Q_{tissue}[ETO]_{tissue}}{V_{tissue}L_{tissue/blood}} - \text{metabolism} \quad (1)$$

moles/min — Input from arterial circulation — Output via venous blood

Where Q_{tissue} is the rate of blood flow to the compartment in liters/minute, $[ETO]_{art}$ and $[ETO]_{tissue}$ are the concentrations of ethylene oxide in arterial blood and tissue, V_{tissue} is the volume of the compartment, and $L_{tissue/blood}$ is the equilibrium ratio of the tissue and blood ethylene oxide concentrations. The "metabolism" term here includes both enzymatic and nonenzymatic reactions with tissue components. As the metabolism component differs appreciably from what was used in the perchloroethylene model, it will be treated in detail below in section 2.2.

Absorption to the lung is represented by setting up a similar equilibrium between the concentrations of ethylene oxide in alveolar air and alveolar blood:

$$[ETO]_{alv\ blood} = \frac{L_{blood/air}(Q[ETO]_{ven\ blood} + [ETO]_{air}V_{alv})}{Q^{*}L_{blood/air} + V_{alv}} \quad (2)$$

Where in this case Q is the total cardiac output of blood (liters/min) and V_{alv} is the amount of air delivered to the alveoli (alveolar ventilation, also in liters/min). The values for the tissue volumes and flows used for the three species can be found in Section 3.1 below. The derivation of air, blood, and tissue partition coefficients is discussed in Section 3.2.

2.2 Mathematical Theory for Deriving Dose-Dependent Changes in the Available Concentration X Time for a Reactive Agent in Tissues

As mentioned earlier, one of the key issues in the public discussion of ethylene oxide standards has been the possible increase in risk associated with the delivery of ethlene oxide in high level, short-term exposures (Sun, 1986). This section derives some general rules for predicting the possible increase in integrated delivered dose X time as a function of the rapidity of delivery. We can do this by comparing what we should theoretically expect for three limiting cases:

(1) exposure at low dose rates (far below levels necessary to produce appreciable saturation of enzymes or depletion of metabolic cofactors such as glutathione) either as a single burst or as at a slow constant rate over time (for at least an 8-hour period) vs.

(2) constant exposure at very high dose rates (well beyond levels that produce maximula saturation of enzymes or profound depletion of metabolic cofactors)

(3) instantaneous delivery of the same total concentration X time as in (2) as a single bolus.

Very Low Constant Dose Rates

At the limit of low dosage, all pharmacokinetic processes can be expected to operate at rates that are directly proportional to the

ethylene oxide concentration*. Within an individual compartment, the rate constants of the processes can be added to obtain an overall rate constant for depletion:

$$\text{overall } \frac{-d[ETO]}{dt} = k_{\text{process a}}[ETO] + k_{\text{process b}}[ETO]..... \quad (4)$$

$$= (k_a + k_b + ...)[ETO] = k_{total}[ETO] \quad (5)$$

Integrating, we obtain a standard exponential decline of ethylene oxide concentration with time after a single burst of exposure:

$$[ETO]_{\text{Time } T} = [ETO]_{\text{Time } 0} e^{-k_{total}T} \quad (6)$$

The overall concentration X time available for reaction with any particular "target" nucleophile within the compartment at low doses can be found with a further integration of $[ETO]_T$ over time:

$$\text{Overall [ETO] X Time} = [ETO]_{\text{Time } 0}/k_{total} \quad (7)$$

$1/k_{total}$ can be thought of as the average residence time of a molecule of [ETO] in the compartment at low doses.

If we have continuous exposure to the ethylene oxide in air, this will be equivalent to a large series of small single doses, and there will

---

*This is because fundamentally the rates of all of these processes at low concentrations are limited by the frequency with which a molecule of the ethylene oxide can be expected to collide with something--either a nucleophile, a molecule of an enzyme, or a small "hole" or receptor on a membrane--and the frequency of all these kinds of collisions depends directly on the number of molecules that are available for such collisions. Chapters 7-11 in the pioneering book of Riggs (1963) provide an excellent detailed treatment of this subject, as applied to passive diffusion among compartments, ordinary chemical reactions, and enzymatic reactions.

be some simple proportionality constant (A) between the external ppm X time and the internal [ETO] X Time.

$$[ETO]_{Internal} \text{ X Time} = A \text{ X } PPM_{External} \text{ X Time}/k_{total} \quad (8)$$

The situation becomes only a little more complex if we add another physiolgical compartment (e.g., the inside of liver cells) coupled with the first compartment (e.g., blood)*.

---

*In that case, we have a transport process that delivers the ethylene oxide to the second compartment at some rate that (at least at low doses) depends directly on the concentration in the first compartment and some transport constant k_{trans}. Given this, and equation (6), it follows that the total quantity of ethylene oxide delivered to the second compartment must be

$$k_{trans}[ETO]_{Time\ 0}/k_{total,\ compartment\ 1} \quad (9)$$

Given this quantity of material placed in compartment 2, the concentration X time product available for reaction with a target molecule in compartment 2 will depend on the volume of compartment 2 and all of the rates of the chemical and physical processes that cause loss from compartment 2. By the same kind of reasoning used earlier:

$$\text{Compartment \#2 [ETO] X Time} = k_{tran}[ETO]_{Time\ 0}/(k_{loss,\ comp.\ 1})(Vol._2)(k_{loss,\ comp.\ 2}) \quad (10)$$

Thus under these low dose conditions, the concentrations X times of the ethylene oxide available for reaction in both compartments can be expected to be linearly related to the amount placed in the first compartment. However, the availability in the two compartments may well be quite different, depending on the transport rate, the volume of the second compartment and the rates of the processes causing loss from the second compartment.

Very High Constant Dose Rates

As the concentrations of ethylene oxide in external air and in the first compartment are increased, one or more of the processes that deplete concentration may tend to operate at slower rates than would be expected from equation 4. This is because either (A) a reactant, such as glutathione, is appreciably decreased in concentration or (B) an appreciable proportion of the molecules of a catalyst (either an enzyme or a saturable transport system) become occupied*. As the dose rate increases the average residence time of a molecule of the ethylene oxide in the body will increase, and the ratio between the internal concentration and the concentration of ethylene oxide in external air will increase. At the limit of very high dosage a vanishingly small portion of the ethylene oxide is processed by the saturable pathway(s), and the relationship between external ppm concentration and internal dose rate becomes:

$$[ETO]_{internal,\ highest\ dose} = (A \times PPM_{External})/(k_{non\text{-}sat}) \qquad (13)$$

---

*The mathematical form for analysis of the second type of situation is well known as classical Michaelis-Menten enzyme kinetics:

$$\text{rate of depletion of ETO} = V_{max}[ETO]/(K_m + [ETO]) \qquad (11)$$

V_{max}/K_m is the maximum rate of the reaction when all the enzyme molecules are fully occupied with substrate at high concentrations of [ETO]. K_m, known as the 'Michaelis Constant, is the concentration of substrate at which the reaction proceeds at one half of V_{max}. As in equation (8), at low doses there will be a simple linear relationship between the concentration of [ETO] within the compartment and the concentration in the external air:

$$[ETO]_{low\ dose} = (A \times PPM)/(k_{tot\ ns} + V_{max}/K_m) = Q \times PPM \qquad (12)$$

If we compare this equation with equation (8), it is clear that we can determine from first prinicples the maximum increase in the ratio of internal to external dosage that can occur as we go from very low to very high doses:

$$\frac{\text{High dose maximum } [ETO]_{intern}/PPM_{extern}}{\text{Low dose minimum } [ETO]_{intern}/PPM_{extern}} = \frac{k_{total}}{k_{non\text{-}sat}} \qquad (14)$$

Thus if, at low doses, non-saturable processes dispose of one third of the total available ethylene oxide, then the maximum high dose increase in the ratio of internal to external dose rate is 3.

For a volatile chemical like ethylene oxide, exhalation via the lung must always constitute at least one nonsaturable pathway of loss. In turn, for a given concentration of ethylene oxide in the systemic ciruculation, the rate of loss by exhalation will be determined by the blood/air parttion coefficient, alveolar ventilation, and cardiac output. If we also know the rate of (potentially saturable) metabolism in the in the body, we can therefore determine the maximum high increase in systemic persistence of ethylene oxide--and changes in the ratio of blood dose rate to external dose rate directly follow. Table 2.1 shows the fraction of absorbed ethylene oxide that is expected to be lost via exhalation after short low-dose exposures for our best-estimate models in humans, rats, and mice. On the basis of these data, we can conclude that the maximum departure from high-dose linearity that can be attributable to systemic ethylene oxide internal dose X time availability is about 4-6 fold in humans and mice, and about 10 fold in rats.

We can also apply the same type of analysis at the level of individual tissues. In this case, the limiting non-saturable process is

Table 2.1

Expected Uptake, Metabolism, and Exhalation Expected Following 5 Minute Exposures of Different Species to 1 ppm Ethlene Oxide

Best Estimate Models*

Species	Absorption (Moles)	Exhalation** (Moles)	Percent Exhaled
Human	2.19×10^{-6}	4.99×10^{-7}	22.8
Rat	2.13×10^{-8}	2.20×10^{-9}	10.3
Mouse	6.84×10^{-9}	1.11×10^{-9}	16.2

For future reference, the names of these models are: Human--GSH3-LV; Rat--g3BL90-LV*; and Mouse--Mg3BL90-LV*. In all three models, the "LV*" designation indicates that the rate constant for metabolism in the liver has been set at a level twice that in other tissues (to better conform to observations of glutathione depletion in different tissues).

**This is the ultimate amount exhaled by several hours after the 5 minute exposures--after all ethylene oxide absorbed has been disposed of either through metabolism/reaction or exhalation. The approximate half lives of ethylene oxide in the three species are: Human--41 minutes; Rat--9.2 minutes; Mouse--6.6 minutes.

simply the loss of ethylene oxide via the venous blood. This is in turn determined by the ratio of blood flow to tissue volume and the tissue/blood partition coefficient:

$$k_{non\text{-}sat} = Q_{tissue}/(V_{tissue}L_{tissue/blood}) \qquad (15)$$

In order for there to be an appreciable increase at high doses in the ratio of tissue concentration X time to blood concentration X time, this $k_{non\ sat}$ must be low relative to the rate constant for saturable routes of metabolism (k_{metab}) at low dosages. As discussed in Section 1 (p. 8 above) the metabolism of ethylene oxide via reaction with glutathione (and, by proxy, other related tissue sulfhydryl compounds) depends on the concentration of glutathione in the tissue and a rate constant we choose to call k_2. Table 2.2 compares the rate constants for non-saturable loss from tissues with the sulfhydryl reaction pathway as estimated in our models for muscle and liver in the three species*. It can be seen that unless our estimates of tissue metabolism rates are grossly wrong, in all cases saturable metabolic pathways of loss of ethylene oxide operate at rates that are rather small relative to the non-saturable route of loss with outgoing blood. Therefore we can expect very little in the way of nonlinearity in the relationship between tissue dose (concentration X time) and blood dose (concentration X time).

---

*Unfortunately we do not have available tissue volumes and blood flow rates for the testis, and thus we were not able to separately represent this tissue in our models. Estimates for the muscle group are included here to show what happens in a tissue that has a much lower rate of perfusion than liver.

Table 2.2
Comparison of Rate Constants for Loss of Ethylene Oxide from Tissues

Non-Saturable Loss ($k_{non-sat}$) Via Blood vs. "Saturable" Loss Via Reaction with Glutathione and Other Sulfhydryls (k_{sat})

Best Estimate Models*

All Rate Constants are in Units of Min^{-1}

Species	------Liver------		------Muscle------	
	$k_{non-sat}$	k_{sat}	$k_{non-sat}$	k_{sat}
Human	.82	.12	.16	.010
Rat	3.9	.55	.16	.048
Mouse	5.3	.97	.35	.078

For future reference, the names of these models are: Human--GSH3-LV; Rat--g3BL90-LV*; and Mouse--Mg3BL90-LV*. In all three models, the "LV*" designation indicates that the rate constant for metabolism in the liver has been set at a level twice that in other tissues (to better conform to observations of glutathione depletion in different tissues).

Instantaneous Delivery of a High Dose

For limiting very high dose rates, so long as nonsaturable pathways are capable of disposing of an appreciable amount of ethylene oxide, the case of instantaneous delivery does not differ from what we would expect for high continuous dose rates. There is one special circumsance, however, in which we can do another kind of analysis for the instantaneous delivery case that is uninformative for a continuous pattern of dosage. That circumstance is where nonsaturable pathways are essentially absent. This could conceivably be the case for the repair of DNA adducts--where there is no obvious analogy to inherently first order nonsaturable processess such as exhalation or loss from a tissue with blood flow.

If there are no or only very minor alternative nonstaturable routes of loss of a specific type of DNA adduct, then the decline in adduct numbers after an initial large burst of adduct generation will be essentially linear with time (at the maximum processing rate of the repair enzyme, V_{max}). If the starting concentration of adducts is $[C]_0$, then at least initially (until the initial high concentration declinces so much that the enzyme is not appreciably saturated),

$$[C]_t = [C]_0 - V_{max}t \qquad (16)$$

To a first approximation, then, a plot of adduct concentration X time will look like a triangle with height equal to $[C]_0$, and a base equal to $[C]_0/V_{max}$. Since the area of a triangle is equal to 1/2 times the base times the height, it follows that the interanal concentration X time product (and therefore the amount of DNA adducts available to potentially

cause permanent changes in DNA information at the times of cell division) will be approximately proportional to the square of the initial dose:

$$\text{DNA mutations} = k\,[C]Xt = k[C]\beta/2V_{max} \qquad (17)$$

It is possible that this kind of mechanism can explain the dose rate effects observed for dominant lethal mutations by Generoso et al. (1986).

To summarize, there are some extreme circumstances under which enzyme saturation can give rise to as much as a $[\text{Dose}]^2$ dependence of DNA adduct concentration X time for high, short term exposures. However, at the limit of low dosage, no departures from basic linearity can be expected. Where nonsaturable processes compete with saturable process, changes in the slope of the realationship between dose and DNA reaction between the limits of low and high doses can be predicted from the ratio of the low-dose rates of the saturable and non-saturable processes.

3. OVERVIEW AND FIRST-ORDER IMPLICATIONS OF THE DATA AVAILABLE FOR MODELING

3.1 Basic Physiological Variables

Pharmacokinetic models are intended to represent and predict the uptake, transfer, metabolism, and excretion of chemicals in biological systems. In the context of risk assessment, the goals are (1) to predict the effective dosage of active metabolites to humans as a function of different levels and time patterns of exposure, and (2) to relate the dosage of active metabolites available to human cells to the dosage available in animal bioassays.

Fundamental to the construction of physiologically-based models is a division of the body into a small number of "compartments" with roughly similar characteristics of basic chemical exchange with blood (as determined by the ratio of blood flow to tissue volume). In the models developed here, tissues are divided into the following five groups:

- Vessel Rich Group containing the brain, kidney, coronary, adrenals, and thyroid tissues as well as additional small viscera,
- Muscle Group containing the lean body tissue: muscle, skin, and tongue,
- Fat Group containing the perirenal and subcutaneous fat and the marrow,
- Liver (distinguished from the vessel rich group because of its often key role in metabolism), and
- Lung.

Table 3.1 shows the volumes and perfusion rates of these groups of tissues used in our human model. These are patterned after the "shoeworker" set of human models presented in our perchloroethylene report

Table 3.1
Human Tissue Group Volumes and Flows--"Shoeworker" Level of Activity

Compartment	Volume* (V) (liters)	Blood Flow (Q) (liters/min.)	Intrinsic Clearance Rate (Q/V) (min^{-1})
Lung	.464	8.4	18
"Arterial Blood Pool"	.674	8.4	12
"Venous Blood Pool"	1.348	8.4	6.2
Vessel Rich Group	3.551	3.87	1.09
Liver	2.476	1.224	.49
Muscle Group	34.76	2.61	.075
Fat Group	15.02	0.69	.046
Total	58.3	8.4	

---

*All volumes include the blood associated with the different tissue groups. The skeleton, and connective tissue (the "Vessel Poor Group" in the human perchloroethylene models) has been excluded from the system for simplicity and because of lack of data on partition coefficients, etc.). The .1 l/minute of blood flow that went to the vessel poor group in the perchloroethylene models was added to the fat group for purposes of ethylene oxide modeling.

(Hattis et al., 1986)--that is, for exercise conditions representing those observed by Brugnone et al. (1980) in a group of 8 artificial leather workers (alveolar ventilation of about 11.38 liters/minute). We think the general activity level in these workers is likely to be similar to the light work of hospital staff and others who would normally be exposed to ethylene oxide.* For comparison, Tables 3.2 and 3.3 show the tissue volumes and flows for our basic rat and mouse models.

The derivation of most of these numbers can be found in our earlier report (Hattis et al., 1986), however there are some significant differences from the perchloroethylene models to accommodate different needs for information for comparison of model results with available observations. In particular, lung tissue and arterial and venous pools of blood have been included in order to allow the models to make predictions of hemoblobin adduct formation in blood and glutathione depression in the lung. These changes, however, introduce relatively quickly-exchanging compartments into the model (as can be seen in the ratios of blood flow to tissue volume) and therefore it was necessary to reduce the step time used in running the models (to .05 to .1 minute for the human model, .025 minute for the rat model, and .15 minute for the mouse model).

For purposes of examining the nonlinearity in male dominant lethal mutations observed by Generoso (1986) it would also be desirable to separate out the relevant tissue in the testis for modeling. However I could not readily find needed data on blood flows and tissue volumes for

---

*During the measurements two of the workers were preparing paint, five were tending a machine that smeared colored polyurethane solution onto cotton cloth, and one was checking the finished product. It should be noted that the individual alveolar ventilation data in these ten minute measurements show nearly a two-fold variation (from 8.3 to 16.0 liters per minute). However this spread would presumably be less if the authors had sampled for a longer time or corrected for differences in body weight among the workers.

Table 3.2
Rat Tissue Group Volumes and Flows

Compartment	Volume* (V) (milliliters)	Blood Flow (Q) (ml/min.)	Intrinsic Clearance Rate (Q/V) (min^{-1})
Lung	1.5	94	62.7
"Arterial Blood Pool"	2.4	94	39.2
"Venous Blood Pool"	4.8	94	19.6
Vessel Rich Group	11	47.9	3.83
Liver	10	23.5	2.35
Muscle Group	187.5	14.1	0.0752
Fat Group	17.5	8.5	0.486
Total	235	94	

Table 3.3
Mouse Tissue Group Volumes and Flows

Compartment	Volume* (V) (milliliters)	Blood Flow (Q) (ml/min.)	Intrinsic Clearance Rate (Q/V) (min^{-1})
Lung	.15	19.0	127
"Arterial Blood Pool"	.24	19.0	79.2
"Venous Blood Pool"	.48	19.0	39.6
Vessel Rich Group	1.1	9.69	7.75
Liver	1.5	4.75	3.17
Muscle Group	17.5	2.85	0.163
Fat Group	2.5	1.71	0.684
Total (VRG, Liver Muscle, Fat)	23.5	19.0	

the testis. Given such data, a future pharmacokinetic modeling project could be specifically directed at mutagenic risks from ethylene oxide.

3.2 Partition Coefficients

The determination of appropriate blood/air and tissue/blood partition coefficients for ethylene oxide was unexpectedly challenging. This section is divided into three parts, describing three different approaches that were tried to arrive at a sensible set of estimates for ethylene oxide's partition coefficients.

3.2.1 An Attempt to Estimate Partition Coefficients from the Regression Analysis Used Earlier for Perchloroethylene (Hattis et al., 1986)

As for perchloroethylene, no one seems to have directly measured ethlene oxide's tissue/blood or tissue/air partition coefficents. I had expected to use the same generalized regression analysis of tissue partition coefficients in relation to oil/air and water/air coefficients that was developed earlier for perchloroethylene.* Table 3.4 shows this analysis, and Table 3.5 shows the partition coefficients it would indicate for ethylene oxide--based on an aqueous buffer/air partition coefficient measured by Filser and Bolt (1984) of 62 and an oil/air partition

---

*Based on a set of measured blood/air and tissue/air partiton coefficients for human tissues for 24 chemicals, for each tissue a multiple regression analysis was done using a model equation of the form:

(footnote continued on the following page)

Table 3.4
Regression Analysis Results for Human Tissue/Gas Partition Coefficients
(Based on the 24 Chemicals Listed in Table 3.6)

Dependant Variable	Oil/gas Coefficient	Water/gas Coefficient	Intercept	R^2
*fat/gas	.7354 (.0311)**	------	18.72	.962
fat/gas	.7304 (.0343)	2.61 (6.80)	16.94	.962
*muscle/gas	.0249 (.0010)	-------	1.073	.965
muscle/gas	.02443 (.0011)	.2429 (.2142)	.9071	.967
*kidney/gas	.01382 (.0012)	.680 (.2338)	1.282	.908
*liver/gas	.03329 (.0012)	.5212 (.2386)	.7657	.978
*blood/gas	.007025 (.0008)	1.091 (.1576)	-.228	.906

*Used for calculation of perchloroethylene partition coefficients.

**The numbers in parentheses are the standard errors of the oil/gas and water/gas coefficients given immediately above.

Table 3.5
Ethylene Oxide Tissue/Gas and Tissue/Blood Partition
Coefficients Calculated from the Equations in Table 3.4

	$L_{Tissue/Gas}$		$L_{Tissue/Blood}$	
Tissue	Best Estimate	Range (+/- 1 Std. Error*)	Best Estimate	Range**
Fat	38.8	37.9-39.6	.57	.49-.68
Muscle (MG)	16.6	3.32-29.9	.24	.04-.52
Kidney (VRG)	43.8	29.3-58.3	.65	.38-1.01
Liver	34.0	19.2-48.8	.50	.25-.84
Blood	67.6	57.8-77.4		

---

*The ranges in this column were calculated by adding or subtracting one standard error from each of the oil/gas and water/gas coefficients in table 3.4. This procedure is likely to somewhat overstate the actual "1 standard error" range of the estimates.

**The low ends of the ranges in this column were computed by dividing the tissue/gas best estimate value - 1 SEM by the blood/gas best estimate value + 1 SEM. The high end of these ranges were computed by dividing the tissue/gas best estimate value + 1 SEM by the blood/gas best estimate value - 1 SEM.

coefficient of 27.3*.

The fact that ethylene oxide is a relatively hydrophilic compound (oil/water partition coefficient of about .44) clearly causes problems in using the regression analysis results derived from our earlier set of 24 chemicals. Unfortunately that data set contained a large number of very hydrophobic aliphatic and chlorinated hydrocarbons, and no relatively hydrophilic ketones or alcohols. As can be seen in Table 3.6 the most hydrophilic material in the group has an oil/water partition coefficient of about 20 (not even close to the 0.44 of ethylene oxide) and most are in the hundreds or thousands. The lack of relatively hydrophilic materials means that the estimates of the water/gas coefficients for some of the tissues in Table 3.4 rest on relatively minor perturbations of the major relationship between the tissue/gas and oil/gas coefficients.

(footnote continued from previous page)

$$L_{Tissue/Gas} = a*L_{Oil/gas} + b*L_{Water/gas} + c \qquad (18)$$

Where, for each chemical, $L_{tissue/gas}$ is the partition coefficient between the tissue and air, $L_{Oil/gas}$ is the partition coefficient between a standard oil and air (often olive oil), and $L_{water/gas}$ is similarly the partition coefficient between water and air. Kidney tissue was used to represent the vessel rich group, and muscle tissue was taken to represent the muscle group.

*Chaigneau (1986) measured the solubility of ethylene oxide in various solvents at 22-23° C. He found that 135 ml of ethylene oxide dissolved per ml of water, and that 60 ml of ethylene oxide dissolved per ml of olive oil. These numbers indicate an oil/water partition coefficient of 60/135 = .44. (We have no reason to suspect that the relative solubility of ethylene oxide in these two media would be markedly different at 37° C.) Combined with the Filser and Bolt (1984) measurement of a buffer/air partition coefficient of 62, this implies an oil/air partition coefficient of .44 X 62 = 27.3.

The oil/water partition coefficient of .44 derived from Chaigneau's measurements is roughly consistent with an octanol/water partition coefficient of .5 given by Hansch and Leo (1979), but considerably different from the oil/water partition coefficient of only .03 implied by the oil/air measurement of 1.83 given by Filser and Bolt (1984) and their buffer/air measurement of 62.

Table 3.6
Hydrophobic Character of the Chemicals Used in the Earlier Regression Analysis (Table 3.4)

CHEMICAL	Partition Coefficients H2O/GAS	OIL/GAS	OIL/H2O
Methylene Chloride	7.20	152.0	21
1,1,1-Trifluoro-2-Chloroethane	.54	24.0	44
1,1-Difluoro-2-chloroethylene	.28	14.0	50
Fluroxene	.85	48.0	68
Teflurane	.32	29.0	91
Chloroform	3.75	400.5	107
Enflurane	.78	98.0	126
Servoflurane	.36	53.0	147
Isoflurane	.62	97.0	156
Benzene	2.80	476.5	170
N-Pentane	.25	47.0	188
Methoxyflurane	4.50	950.0	211
Halothane	.79	220.0	278
2,2-Dimethylbutane	.25	71.0	284
Methyl Chloroform	.93	356.0	383
2-Methylpentane	.25	103.0	412
3-Methylpentane	.25	118.0	472
N-Hexane	.25	146.0	584
Toluene	2.20	1,425.5	648
Trichloroethylene	1.50	819.0	546
Methylcyclopentane	.25	202.0	808
Cyclohexane	.25	293.0	1170
3-Methylhexane	.25	311.0	1240
N-Heptane	.25	452.0	1810

*Where more than one measurement of the blood/gas partition coefficient was available, the different values were averaged.

Sources: Perbellini et al., 1985; Fiserova-Bergerova, 1983; Fiserova-Bergerova et al., 1984

Particularly in the case of muscle, the water/gas regression coefficient is not even statistically significant, with a standard error almost as larger as the estimate of the coefficient itself. The resulting best estimate for the muscle/blood partition coefficient of only .24 in Table 3.5 seems highly implausible. Taken on its face, it would suggest that even though muscle is a mostly aqueous medium (like all body tissues with the possible exception of fat) only a very small proportion of the water in muscle is as available for dissolving ethylene oxide as the water in blood. To have this degree of uncertainty in the muscle/blood coefficient is likely to have a substantial effect on the modeling, because the muscle group represents half or more of the total body mass.

3.2.2 An Attempt to Estimate Partition Coefficients from the Logarithmic Regression Analysis of Seybold et al. (1986)

As another possible input, Dr. Michael Vargas generously provided a multiple regression analysis for rat partition coefficients based on 25 sets of data gathered by Dr. Andersen's group (Seybold et al., 1986). These workers chose to use a logarithmic form for their analysis--that is,

$$\log_{10}(\text{tissue/air}) = a*\log_{10}(\text{saline/air}) + b*\log_{10}(\text{oil/air}) + c \quad (19)$$

The chemicals here were the same types of relatively hydrophobic chlorinated hydrocarbons that gave rise to the analysis shown in Table 3.4. Table 3.7 shows the results of the Seybold et al. (1986) logarithmic regression analysis, and Table 3.8 shows the partition coefficients that this analysis would imply for ethylene oxide.

Table 3.7
Logarithmic Regression Analysis Results for Rat Tissue/Gas Partition Coefficients from Seybold et al., 1986

Dependant Variable	Oil/gas Coefficient	Water/gas Coefficient	Intercept	R^2
fat/gas	1.027	-.046	-.119	.970
	(.045)	(.061)	(.098)	
muscle/gas	.477	.365	-.374	.938
	(.043)	(.058)	(.094)	
liver/gas	.574	.302	-.278	.945
	(.044)	(.060)	(.096)	
blood/gas	.426	.515	-.070	.954
	(.039)	(.054)	(.086)	

*The numbers in parentheses are the standard errors of the coefficients given immediately above.

Table 3.8
Ethylene Oxide Tissue/Gas and Tissue/Blood Partition Coefficients Calculated from the Equations in Table 3.7 (Log-Linear Regression Analysis of Seybold et al. 1986)

	$L_{Tissue/Gas}$		$L_{Tissue/Blood}$	
Tissue	Best Estimate	Range (+/- 1 Std. Error*)	Best Estimate	Range**
Fat	18.8	12.6-28.0	.64	.30-1.36
Muscle (MG)	9.2	6.3-13.5	.32	.15-.66
Kidney (VRG)	ASSUME SAME AS LIVER		ASSUME SAME AS LIVER	
Liver	12.2	8.3-18.1	.42	.20-.88
Blood	29.2	20.5-41.4		

---

*The ranges in this column were calculated by adding or subtracting one standard error from each of the oil/gas and water/gas coefficients in table 3.7. This procedure is likely to somewhat overstate the actual "1 standard error" range of the estimates.

**The low ends of the ranges in this column were computed by dividing the tissue/gas best estimate value - 1 SEM by the blood/gas best estimate value + 1 SEM. The high end of these ranges were computed by dividing the tissue/gas best estimate value + 1 SEM by the blood/gas best estimate value - 1 SEM.

In past work Fiserova-Bergerova (1984) and others have used similar logarithmic model equations. The benefit of using a logarithmic form is that it tends to give more equal weight to data from chemicals with relatively large and relatively small tissue/air partition coefficients, whereas an additive model (equation 18) tends to be much more strongly influenced by data points for chemicals with high tissue/air partition coefficients.* However, the difficulty with the logarithmic form is that because the addition of the logarithms of two numbers is equivalent to multiplying the numbers, the logarithmic model implies a multiplicative interaction between the affinity of a chemical for the oil and water components of a compound mixture--and this appears unlikely on theoretical grounds.**

In the case of the estimates in Table 3.5, this kind of difficulty appears to produce estimates of blood/gas and tissue/gas partition coefficients that are considerably lower than those produced by other methods. In particular, it would be very odd if the blood/gas partition coefficient were as low as 29, in view of the measured saline/gas

---

*This is because ordinary least squares regression analysis minimizes the square of the difference between the predictions of the model equation and the value of the dependent variable for specific points. For measurements of tissue/air partition coefficients, where the error of the measurement is likely to be positively correlated with the absolute value of the measurement, relatively high measurements with correspondingly higher errors will implicitly be given greater weight. Presumably this problem could be corrected within a linear model by giving different weights to the different points, but such methodology has not yet been applied to the determination of partition coefficients.

**Consider, for example, that a particular tissue behaves as if it were 5% fat (oil) and 95% water and nothing else (the regression relationship has no intercept). Now consider a chemical with oil/air and water/air partition coefficients of 10 and 0.1 respectively. An additive model will predict that the mixture should have an overall tissue/air partition coefficient of

(footnote continued on the following page)

coefficient of 62. As will be seen below, Brugnone et al. (1986) have measured the blood/gas coefficient for human blood and report a value of 90 (with a standard deviation of 20).

3.2.3 Estimation of Partition Coefficients from the New Data and Regression Analysis of Fiserova-Bergerova and Diaz (1986)

Fortunately, the recent literature contains a new source of data with human blood and tissue partition coefficients for several relatively hydrophilic materials [Fiserova-Bergerova and Diaz (1986)]. These include five alcohols (methanol, ethanol, 1-propanol, 2-propanol, and isobutanol) and two ketones (acetone and 2-butanone). Fiserova-Bergerova and Diaz (1986) analysed their expanded data set of tissue/blood partition coefficients for 35 chemicals using an arithmetic model with the fat/blood

---

(footnote continued from the previous page)

$$L_{tissue/air} = \underset{\text{oil portion}}{.05*100} + \underset{\text{water portion}}{.95*.1} = 5 + .095 = 5.1 \qquad (20)$$

Another chemical with the same solubility in oil, but with a water/air partition coefficient of 1 would be expected to have a tissue/air partition coefficient of about 6.

On the other hand, a logarithmic model would imply

$$L_{tissue/air} = 10^{a}*.1^{b} = 10^{2a}*10^{-b} = 10^{3a-b} \qquad (21)$$

Another chemical with the same solubility in oil, but with a water/air partition coefficient of 1 would be expected to have a tissue/air partition coefficient 10^{b} times larger:

$$L_{tissue/air} = 1000^{a}*1^{b} = 10^{3a} \qquad (22)$$

Whatever the "a" and "b" constants are in a model like this, it makes no sense that that the contribution of the oil portion of the tissue to the overall tissue/air partition coefficient should be multiplicatively influenced by the contribution from the aqueous portion.

partition coefficient as the single independent variable:

$$\text{tissue/blood} = a*\text{fat/blood} + b \qquad (23)$$

The resulting regression coefficients are reproduced as Table 3.9, and the tissue/gas partition coefficients implied for ethylene oxide are given in Table 3.10.

The results in Table 3.10, together with the blood/air partition coefficient of 90 measured by Brugnone et al. (1986), were used for the bulk of the modeling. However, even these estimates are not without some doubtful qualities on their face. They are very largely influenced by the intercepts in Table 3.9 (and for this reason, whether one assumes a fat/blood partition coefficient of exactly .44 as we have, or some other reasonable value, makes very little difference). I am particularly dubious that the muscle/blood partition coefficient for ethylene oxide could be as low as .47.

Fiserova-Bergerova and Diaz (1986) provide a helpful table (their Table 4) comparing measured tissue-gas partition coefficients with those calculated from their regression equations for the 28 compounds other than the seven hydrophilic chemicals whose primary data they report in earlier tables. In the same spirit, Table 3.11 compares tissue/blood partition coefficients calculated from their direct blood/gas and tissue/gas observations in their Tables 1 and 2 with tissue/blood partition coefficients calculated from their regression equations. The regression predictions are shown in parentheses below the direct observations in Table 3.11. It can be seen that in all cases the regression equation for muscle predicts tissue/blood partition coefficients that are considerably

Table 3.9
Fiserova-Bergerova and Diaz (1986) Regression Analysis Results
for Human Tissue/Gas Partition Coefficients

Analysis of 35 Chemicals, Including Six Hydrophilic Compounds

Dependant Variable	Number of Chemicals	Fat/gas Coefficient	Intercept	R^2	SD
muscle/blood	34*	.0326	.4504	.928	.702
kidney/blood	35	.0211	.6442	.945	.421
brain/blood	35	.0372	.5199	.940	.779
liver/blood	27**	.0452	.5770	.919	.997
lung/blood	30	.00461	1.0701	.541	.702

*An outlying data point for one compound (2,2-dimethylbutane) was excluded.

**The six hydrophilic compounds could not be included in the data set used because extensive in vitro metabolism occurred during the process of equilibration of the system.

Table 3.10
Ethylene Oxide Tissue/Blood Partition Coefficients Calculated from the Equations in Table 3.9, Assuming a Fat/Blood Partition Coefficient of .44

Values Used for Most Modeling

Tissue	$L_{Tissue/Blood}$
Muscle	.47
Brain	.54*
Kidney	.65*
Liver	.60
Lung	1.07

---

*These values for the brain and kidney were combined to yield an averaged tissue/blood partition coefficient for the vessel rich group of about .595

Table 3.11
Comparison of Measured and Regression-Predicted Tissue/Blood Partition Coefficients for Seven Hydrophilic Compounds*

Based on Data from Fiserova-Bergerova and Diaz (1986)

Compound	---------Tissue/Blood Partition Coefficients---------			
	Fat/Blood	Muscle/Blood	Kidney/Blood	Lung/Blood
Methanol	.142	.805 (.455)	.833 (.647)	1.066 (1.071)
Ethanol	.161	.638 (.456)	.706 (.648)	.880 (1.071)
2-Propanol	.250	.698 (.459)	.700 (.649)	.820 (1.071)
1-Propanol	.310	.710 (.460)	.718 (.651)	.855 (1.072)
Acetone	.439	.770 (.465)	.745 (.653)	.816 (1.072)
Isobutanol	.717	.634 (.474)	.686 (.659)	.739 (1.073)
2-Butanone	1.30	.824 (.493)	.856 (.672)	.824 (1.076)
AVERAGE	.530	.726 (.466)	.749 (.654)	.857 (1.072)

---

*The numbers are all tissue/blood partition coefficients. The values outside of parenteses represent the averages calculated from five measurements each of tissue/gas partition coefficients in Table 2 and ten measurements of blood/gas partition coefficients in Table 3 of Fiserova-Bergerova and Diaz (1986). The values in parentheses immediately below each measurement represent the predictions of the Fiserova-Bergerova and Diaz (1986) regression equations (see Table 3.9).

less than indicated by the direct observations. Similarly, the predictions for kidney/blood partition coefficients are all too low, albeit by relatively small amounts, and the lung/blood coefficients are all at least a little too high. The reason for the disappointing performance of the regression analysis for these hydrophilic compounds is very likely that the ordinary least squares fitting procedure gives small weight to the points with relatively low values of the dependent variables (tissue/blood partition coefficients). It thus tolerates deviations of predictions from observations that, while small in absolute terms, are large in relative terms and therefore potentially misleading for pharmacokinetic modeling. In section 4, I will therefore do some sensitivity analysis, utilizing the average values at the bottom of Table 3.11 as an alternative set of tissue/blood partition coefficients (with liver set equal to kidney for these purposes, but fat kept at its same value of .44 from Chaigneau's (1985) oil and water partition coefficient observations). These will be designated the "T*" models.

3.3 Absorption, Exhalation, and Blood Level Data after Exposure to Ethylene Oxide

I present these data below first for rats, then for humans and finally for mice. This somewhat unusual order reflects the sequence I followed in developing the models. Our initial focus on the rat was determined by the salience of the available rat data for exploring possible high-dose nonlinearities.

3.3.1 Observations in Rats

The primary absorption and exhalation data that were used in modeling have already been presented in Table 1.1 on page 13 above. Tyler and McKelvey (1983) exposed male Fischer 344 rats averaging 250 g in weight to various concentrations of radiolabelled ethylene oxide in air for 6 hours (four rats were used at each exposure level). During exposure the ethylene oxide concentration in the chambers was measured every 15 minutes, resulting in the averages of 11, 104 and 1010 ppm shown in the first column of Table 1.1. At the end of exposure, the animals were transferred to Roth metabolism cages for collection of exhaled air and excreta. The data on "Net Absorption During Exposure" in Table 1.1 represent the total radioactivity retained by the animals at the end of the 6 hour exposure period. This is not exactly what might be termed "total absorption" because it does not include any ethylene oxide that was exhaled unchanged during the 6 hour period. Finally, the data on "% Exhaled Unchanged" in the final column of Table 1.1 represent only the ethylene oxide that was exhaled unchanged after the end of the exposure period. Ventilation rates were not directly measured. However, after four hours at the highest exposure level the authors report a gasping type of breathing pattern.

Also at the highest exposure level, there was a decrease in the percentage of radioactivity excreted in the urine, and a change in the percentages of urinary radioactivity represented by different metabolites (Table 3.12). This reinforces the conclusion that some appreciable amount of reactant depletion or enzyme saturation must be taking place at the

Table 3.12
Percentage of Recovered Radioactivity in Various Urinary Fractions
(Mean +/- SD)

Chromatogram Fraction	Exposure Level 11 ppm	104 ppm	1010 ppm
AV1	8.1 +/- .5	6.8 +/- .8	28 +/- 2.5*
AV10	16 +/- 1.7	18 +/- 1.7	26 +/- 3.9**
AV16	69 +/- 3.5	70 +/- 2.2	36 +/- 4.2**
AV34	1.7 +/- .3	2.2 +/- .5	3.8 +/- 1.6

*Signficantly different from 11 ppm (P less than .05) and from 104 ppm (P less than .01).

**Significantly different from 11 ppm and from 104 ppm (P less than .01).

highest exposure level. The authors report that "AV16" chromatographs similarly to a likely derivative of the glutathione conjugate of ethylene oxide--N-acetyl-S-(2-hydroxyethyl) cysteine (Jones and Wells, 1981).

Another potential source of data on this subject is the extensive pharmacokinetic work of Filser and Bolt (1984). These authors exposed rats by inhalation or by intraperitoneal injection and measured changes in ethylene oxide concentrations in exposure chambers. Unfortunately, they provide their raw observations only in graphs that are difficult to translate accurately into actual numbers. Their final numerical results are in terms of their own pharmacokinetic model that treats the animal as if it were a single compartment with no change in breathing rate as a function of dose, and further contains adjustments for body weights that make it impossible to reconstruct the original experimental conditions and data. Because of this, I found it impossible to utilize this otherwise very promising source of information. It is worth noting, however, that they find no evidence of saturation behavior in the gross absorption of ethylene oxide from their chambers.

More directly useful are some observations by Osterman-Golkar et al. (1983). Fisher 344 rats were given intraperitoneal injections of labeled ethylene oxide and the degree of alkylation of a specific histidine nitrogen in hemoglobin was measured in blood taken five hours later:

Amount Injected (umole/kg)	Alkylation of Histidine-N (moles/g Hemoglobin)	Hb Alkylation per Amt. injected
2.77	$.29 \times 10^{-10}$	1.04×10^{-11}
20.4	1.4×10^{-10}	$.69 \times 10^{-11}$

It can be immediately seen that either there are some appreciable nonlinearities in this system (even at these relatively low doses) or

experimental errors are on the order of 50%. As will be seen later in examining similar data from mice, the latter explanation is more likely.

Nevertheless, these data provide the most direct estimates of the concentration X time of ethylene oxide that is available internally in the rat system. Osterman-Golkar et al. (1983) measured the reactivity of ethylene oxide with this residue of hemoglobin in red cells in parallel experiments in vitro. The in vitro experiments yielded a bimolecular rate constant of .27 (+/- .05) X 10^{-4} l/g Hb-hr. Dividing the obseved alkylation in vivo by this rate constant, and converting hours to minutes, we find that the low dose produces an internal ethylene oxide concentration X time of about 6.4 X 10^{-5} (moles/liter)-min., and the higher dose produces about 3.1 X 10^{-4} (moles/liter)-min. Parallel measurements were also made by Osterman-Golkar et al. (1983) in aged rats at the end of a two-year bioassay. These data have already been reproduced as Table 1.2 on p. 14 above.

3.3.2 Observations in Humans

Brugnone and coworkers (1985, 1986) have contributed the most helpful recent information on the processing of ethylene oxide in humans. Ten hospital sterilization workers were monitored during work--external air concentrations were measured simultaneously with alveolar air concentrations. Commendably, Brugnone et al. (1985) provide their raw data on each worker. The second and third columns of Table 3.13 present the averages of these data for the ten workers at various times after the start of exposure. Based on these averages, the final column shows the

Table 3.13
Observations of Brugnone et al. (1985) on the Percentage Absorption of Ethylene Oxide From Alveolar Air in Workers

Averages of Observations for Ten Workers at Each Time Point

Time After Start of Exposure (hr)	Environmental Air Concentration (C_i) (ug/liter)	Alveolar Air Concentration (C_a) (ug/liter)	Percent Absorbed From Alveoli [100X ($1-C_a/C_i$)]
1	1.89	.285	84.5
2	2.05	.45	78.0
3	4.52	1.13	75.0
4	3.03	.88	71.0
5	2.79	.70	74.9
6	2.80	.68	75.7
7	3.08	.73	76.3
8	5.03	1.19	76.3
3-8 Ave	3.54	.885	75.0

percentage of alveolar ethylene oxide absorbed at various times. The absolute level of continuing absorption after the establisment of equilibrium (3-8 hours) is a direct indication of the equilibrium ratio of the rate of metabolic processing to the overall rate of loss of ethylene oxide--including metabolism and exhalation. The exhalation rate in turn is directly determined by the blood/air partition coefficient, which Brugnone et al. (1980) report to be 90 (+/- 20, SD). Thus this set of observations will allow (in Section 4) a calculation of the internal rate of processing of ethylene oxide in humans. Further, it will be seen in Section 4 that the observed rate of approach to the long term equilibrium provides some helpful information for judging the plausibility of different combinations of human blood/air and tissue/blood partition coefficients.

The same data can be interpreted in another way to provide different information. Instead of averaging across workers at specific times, one can average across the eight hours of exposure for individual workers. Table 3.14 shows these results, arranged in order of increasing environmental concentrations. The upper half of the table gives averages of observations taken after all eight hours of exposure, whereas the lower part of the table includes only the five observations taken after hours 4-8 (well after the establishment of equilibrium, to within experimental error). Overall it can be seen that there is remarkably little interindividual variation in the percentage of ethylene oxide absorbed. Moreover there is no discernable tendency for absorption to be less for workers exposed to greater environmental concentrations. This indicates

Table 3.14
Observations of Brugnone et al. (1985) on the Percentage Absorption of Ethylene Oxide From Alveolar Air in Individual Workers

Subject	Environmental Air Concentration (C_i) (ug/liter)	Alveolar Air Concentration (C_a) (ug/liter)	Percent Absorbed From Alveoli [100X ($1-C_a/C_i$)]
Averages of Observations After Each of 8 Hours of Exposure			
MA	1.96	.56	71.4
PI	2.71	.64	76.4
FI	2.79	.80	71.3
FR	2.82	.75	73.4
GE	2.89	.56	80.6
MO	3.10	.77	75.2
MI	3.43	.71	79.3
OR	3.55	.76	78.6
RI	3.60	.93	74.2
MS	4.71	1.10	76.6
Averages of Observations After Hours 4-8 of Exposure			
MA	2.38	.70	70.6
OR	2.68	.64	76.1
PI	3.00	.78	74.0
FR	3.10	.76	75.5
GE	3.26	.70	78.5
MO	3.44	.86	75.0
FI	3.64	1.06	70.9
MI	3.66	.74	79.8
MS	3.86	.86	77.7
RI	4.44	1.26	71.6

that at these levels of exposure,* the workers' rates of metabolism of ethylene oxide are not markedly saturated. Because of the limited range of air levels to which the workers were exposed, the latter inference would be relatively weak on basis of the data in Table 3.14 alone. However it is a straw in the wind that will be seen to be more strongly indicated by the results of the modeling in Section 4. It also suggests a methodology that could be used to confirm the model predictions. If there is to be appreciable high-dose slowing of metabolism (as would be expected to occur if there were appreciable saturation of metabolic enzymes or depletion of glutathione in the body as a whole) then the amount of ethylene oxide exhaled from the alveoli must rise at higher dose levels, and the percentage absorbed from the alveoli must be correspondingly reduced.

Before ending the discussion of the Brugnone et al. findings, one other result should be mentioned that had a significant effect on the modeling--although in the end I was not able to adequately reproduce it in the final models. Brugnone et al. (1986) measured ethylene oxide concentrations in the venous blood, and report finding a ratio of venous blood concentration to alveolar air concentration of 12-17. Because the blood/air partition coefficient measured by Brugnone et al. (1986) is 90, the normal expectation would be that the <u>arterial</u> blood concentration must be 90 times the alveolar air concentration. However, if Brugnone et al. measure a concentration ratio of 12-17 between venous blood (presumably drawn from the arm) and alveolar air, the implication is that the on the order of [90 - (12 to 17)]/90 = 81-87% of the ethylene oxide must be

---

*1 ug/l of ethylene oxide = .578 ppm at 37°C. Therefore the 2-5 ug/l range of exposures seen in the Brugnone et al. worker group corresponds to about 1-3 ppm.

removed on its passage from the arterial circulation through the muscle and other tissues of the arm to the draining vein. From this I concluded that significant metabolism must be ocurring in the large "muscle group" (muscle and skin) compartment. This reinforced the observations of Tyler and Zemaitis (1986) of significant reaction with glutathione in many body tissues (see Figure 1.3 on p. 7 above and Section 3.3 below) and all the models developed in Section 4 provide for reaction with glutathione in the muscle at rates comparable with the rates of reaction in other non-hepatic tissues. Even though the muscle group has a relatively low concentration of glutathione, because the muscle group has a much larger volume than the other compartments, the models imply that it may be a major contributor to the overall disposal of ethylene oxide in the body.

Calleman et al. (1978) have made some hemoglobin adduct formation measurements in humans that are analogous to those in rats by Osterman-Golkar et al. (1983) (see Section 3.3.1). (The adducts measured in this case were at the N-3 positiion of histidine. In vitro experiments indicate that ethylene oxide forms this adduct with a rate constant of .14 X 10^{-4} 1/g Hb-hr.) Unfortunately there is considerable room for doubt about the actual exposure levels experienced by these workers. All but one of the workers reportedly spent a considerable (but undocumented) proportion of their workdays outside of the sterilization rooms. Moreover, according to the authors,

> "Another factor that detracts somewhat from the applicability in our present study of the measurements recorded by Dukelberg and Hartmetz (1977) is that those measurements were made during the summer of 1976, while the blood samples were drawn at the end of 1977; i.e. they are average tissue doses during the period August-November 1977. However no known alterations in the working conditions have been carried out since the measurements of the air-concentration of ethylene oxide were undertaken (Dunkelberg and Hartmetz, personal communication)."

The data are reproduced in Table 3.15. Given the uncertainties in actual exposure, it is not surprising that there are wide differences in the alkylation observed per estimated exposure for different individuals. Also bothersome is the fact that the individual for whom exposures are reportedly known with most confidence has the largest ratio of alkylation to estimated exposure. I will consider these data in Section 4, but they will not be the primary basis for calibrating the human models.

3.3.3 Observations in Mice

The Ehrenberg group in Sweden has also provided extensive data on absorption, hemoglobin adduct formation, and DNA adduct formation at relatively low exposure levels (Ehrenberg et al., 1974 and 1977; Segerback, 1983) in mice. Unfortunately, they do not supply any exhalation data or absorption/adduct formation data at exposure levels in the 100 ppm - 1000 ppm range which proved informative for nonlinearities in the rat.

Table 3.16 shows absorption data and exposure conditions from the original experiments of Ehrenberg et al. (1974). 6-8 week old male CBA mice were exposed to labeled ethylene oxide in closed chambers unsupplemented with additional ethylene oxide during the exposure periods. Accordingly, concentrations decreased during exposure--approximately linearly according to a statement by the authors in the text of their report. It can be seen in the last column of Table 3.16 that absorption per concentration X time of exposure was quite variable--differing by over

Table 3.15
Observations of Calleman et al. (1978) of Hemoglobin Histidine Alklylation in Workers

Subject	Estimated ppm-hours exposure per week* "Maximal"	"Probable"	nmoles ETO per gram hemoglobin	Alkylation per "probable" exposure (nmole/g-ppm-hr)
H	"0" (Control)		less than .05	
I	"0" (Control)		less than .05	
E	490	250	0.5	.0020
D	625	310	2.6	.0084
C	1560	1560	14.3	.0092
A	2500	1250	6.4	.0051
B	2500	1250	3.6	.0029

---

*The "maximal" exposures are based on average measurements in the workplace. However, all of the subjects except C reportedly "do chores outside of the sterilization rooms during a substantial part of their workdays."

Data Source: Calleman et al., 1978

Table 3.16
Absorption of Inhaled Ethylene Oxide by Mice

---ETO Concentrations (ppm)--- Average (ppm)	Range (beginning to end of exposure)	Exposure Duration (min.)	Net Absorbed During Exposure (umole/kg)	Absorption per ppm-min. of exposure (umole/kg)
1.15	2.2 to 0.1	75	4.5	.052
3.5	7 to 0	107	15	.040
6.5	9.7 to 3.3	60	12	.031
6.5	10 to 3	75	30	.062
7.4	9.7 to 5.1	60	13	.029
29	35 to 23	82	100	.042
33	57 to 9	75	140	.057

Data Source: Ehrenberg et al., 1974

two-fold from experiment to experiment. No explanation for this appreciable experimental variability in absorption is offered by the investigators. In section 4, I use these data to calculate alveolar ventilation rates for mice in this range of exposures.

Ehrenberg et al. (1974) also present measurements of alkylation of miscellaneous tissue proteins and of DNA in kidney. However because of the small number of counts in the DNA experiments, and the availability of later measurements based on a single well-defined protein (hemoglobin) I elected not to try to use this information for modeling.

Following up these observations, Ehrenberg (1977) cites unpublished data as indicating that

> "Direct exposure of mice to ethene oxide gives 30 X 10^{-3} nmol hydroxyethylcysteine per g haemoglobin and per ppm-hr."

Data of Segerback (1983) on the relative amounts of cysteine-S alkylation in comparison to histidine alkylation indicate that the second order rate constant for the cysteine-S alkylation is likely to be about 3.1 times the rate constant for reaction with histidine-N-tau, or 5.27 X 10^{-4} 1/g Hb-hr. Dividing this into the reported amount of hydroxyethylcysteine observed for inhalation exposure per ppm-hour gives us an expectation of 5.7 X 10^{-8} mole/liter-hr (or 3.4 X 10^{-6} mole/liter-min) of internal ethylene oxide concentration per ppm-hr of external exposure. The fact that these observations were never published in detail, however, and some hints by the authors of technical difficulties with cysteine-S alkylation in later papers indicates that this result should be treated with some reserve.

In a more extensive presentation, Osterman-Golkar et al. (1976) measured the overall alkylation of hemoglobin following intraperitoneal

injection of various doses of ethylene oxide. The bimolecular rate constant for this reaction is reported to be 1.8 X 10^4 l/g Hb-hr. More recently, Segerback (1983) has published results based on the formation of a specific adduct (at the tau position of histidine) after intraperitioneal injection of ethylene oxide. The in vitro bimolecular rate constant for this subset of overall alkylation is reported to be .17 X 10^4 l/g Hb-hr. It is informative to juxtapose the results of the five experiments reported in these two papers. The final column of Table 3.17 shows the indicated internal exposure of the hemoglobin in red cells (in moles/liter-minute per umole/kg of ethylene oxide injected) in the different studies. It can be seen that with the exception of the higher-dose point of Segerback (1983) there is reasonably good agreement between the studies. For purposes of the modeling in Section 4, I chose to tune the mouse metabolism rates for ethylene oxide to reproduce the average blood dose for the the three lowest-dose points in this table. This essentially assumes that the higher-dose point of Segerback is an outlier because of some experimental error, and that the highest dose point of Osterman-Golkar may possibly be somewhat inflated relative to the relationship at low doses because of significant glutathione depletion or enzyme saturation at this level of administration. Section 4 will present the results of model simulations on this point.

In the same experiments, Segerback (1983) also made some measurements of the alkylation at the N-7 position of guanines in DNA in liver, spleen and testis five and 23-24 hours after the injections. Because of appreciable reductions in DNA alkylation at the later time point, the original degree of alkylation was back-calculated assuming a simple exponential decay of DNA alkylation with time (this would be expected if

Table 3.17
Alkylation of Mouse Hemoglobin by Ethylene Oxide
after Intraperitoneal Injections

umol/kg Injected	Hemoglobin alkylation observed (nmol/g Hb)	Indicated Internal Concentration X Time of ETO Available in vivo (mole/liter-min)*	Internal ETO CXT (mol/l-min) per umol/kg ETO injected
Data from Osterman-Golkar et al., 1976--Total hemoglobin alkylation			
5.4	.20	6.67×10^{-5}	1.23×10^{-5}
14.4	.50	1.67×10^{-4}	1.16×10^{-5}
840	37	1.23×10^{-2}	1.46×10^{-5}
		Average	1.28×10^{-5}
Data from Segerback, 1983--Alkylation of a specific histidine in hemoglobin			
8.7**	.032	1.13×10^{-4}	1.30×10^{-5}
44	.32	1.13×10^{-3}	2.57×10^{-5}
		Average	1.93×10^{-5}
		Average of all data points	1.54×10^{-5}
		Average of three lowest-dose points	1.23×10^{-5}

---

*Obtained by dividing the hemoglobin alkylation data in the second column by the appropriate rate constant for the reaction between ethylene oxide and hemoglobin in red cells observed in vitro--3×10^{-6} l/g Hb-min for the total alkylation data of Osterman-Golkar et al. (1976), or 2.83×10^{-7} l/g Hb-min for the specific histidine alkylation data of Segerback (1983).

**Segerback (1983) expresses some doubts about the actual amount injected in the case of this experiment.

all originally-formed N-7 guanine adducts at different positions on DNA were repaired at a single uniform rate. This is not unreasonable, but experience in other DNA adduct studies indicates that it is not necessarily so either.) Table 3.18 presents these observations, together with calculations of the apparent concentration X time of ethylene oxide available to the DNA based on a bimolecular rate constant for the ETO/DNA-guaninine N7 reaction of .96 X 10^{-4} l/g DNA-hr. The average concentration X time seen in these tissue DNA adduct experiments is slightly less than the concentration X time indicated in the same experiments in the hemoglobin adduct studies, although this conclusion must be quite tentative in the light of the variability seen in both types of data. Nevertheless, as will be seen in section 4, this result can be broadly expected where (1) tissue/blood partition coefficients are less than 1 and (2) metabolism occurs primarily in the tissues.

3.4 Glutathione Depletion by Ethylene Oxide

Figure 1.3 on p. 7 above has already presented in graphical form the results of some experiments by McKelvey and Zemaitis (1986) on reductions in glutathione concentration immediately following four hour exposures to ethylene oxide in Fischer-344 rats. The same paper also presents similar data for Swiss-Webster mice. Hoping to learn more about the details of these results, and any further work along the same lines that might not have been published, I contacted Dr. Zemaitis. He graciously provided the data in numerical form (Table 3.19) from Mr. McKelvey's notebooks, which will allow a more accurate comparison of model predictions with the

Table 3.18
Alkylation of Mouse DNA at the N-7 Position of Guanine after Intraperitoneal Injections of Ethylene Oxide

umol/kg injected	DNA N-7 Guanine shortly after injection (extrapolated) (nmol/g DNA)		Indicated internal concentration X time of ETO available in vivo (mole/liter-min)	Internal ETO C X T per mg/kg injected (mole/l-min per mg/kg)
8.7*	Liver	.24	1.5×10^{-4}	1.72×10^{-5}
	Spleen	.083	$.52 \times 10^{-4}$	$.62 \times 10^{-5}$
	Testis	.11	$.69 \times 10^{-4}$	$.79 \times 10^{-5}$
44	Spleen	.87	5.4×10^{-4}	1.23×10^{-5}
			Average of all data points	1.09×10^{-5}
			Average of lowest dose points	1.04×10^{-5}

---

*Segerback (1983) expresses some doubts about the actual amount injected in the case of this experiment.

Data Source: Segerback (1983)

Table 3.19
Depletion of Glutathione Immediately After 4 Hour Exposures
To Varous Concentrations of Ethylene Oxide

Glutathione Concentrations in Exposed Animals as % of Control
(Numbers in Parentheses are Standard Errors)

Experiments in Rats	ppm Ethylene Oxide Exposure		
	100	600	1200
Bone Marrow	108.8 (3.5)	75.4 (3.3)	69.3 (0.8?)
Blood	101.0 (3.0)	95.1 (2.6)	99.6 (4.8)
Lung	83.3 (2.3)	38.7 (2.8)	23.8 (1.0)
Stomach	84.2 (4.3)	34.3 (1.9)	20.4 (1.5)
Testis	87.2 (2.7)	52.0 (2.0)	34.5 (0.5)
Liver	83.1 (3.7)	27.0 (4.9)	15.3 (1.8)

Experiments in Mice	ppm Ethylene Oxide Exposure		
	100	450	900
Blood	91.3 (5.1)	50.4 (4.9)	39.8 (6.3)
Lung	78.1 (3.6)	35.5 (4.4)	14.1 (8.3?)
Stomach	96.5 (4.6)	42.4 (2.3)	28.5 (3.6)
Testis	96.7 (2.7)	88.1 (1.4)	63.9 (2.1)
Liver	80.7 (2.4)	41.3 (5.5)	16.3 (3.0)

observations. No other unpublished data were available. Mr. McKelvey's studies were to have been part of his Ph.D. work, but tragically he died suddenly before completing them. Dr. Zemaitis, who was his thesis advisor, submitted the data for publication.

3.5 Basic Data on Glutathione Levels and Glutathione Turnover

One of the first questions that is of interest in assessing the significance of the glutathione depression data in the previous section is how much of the overall metabolism of ethylene oxide might be accounted for by reaction with glutathione? How many moles of glutathione must be lost in the body as a whole in order to produce the observed depressions in tissue levels, and how does this compare with the amount of ethylene oxide we can expect to have been absorbed during exposure? To begin to answer these questions, we need to assemble information on the standing stocks of glutathione in various tissues and the rates at which these stocks "turn over" (are lost and replaced by new synthesis) under normal conditions.

Absolute values of the concentrations of glutathione measured by McKelvey and Zemaitis (1986) in the absense of ethylene oxide exposure are shown in the third columns of Table 3.20 (for rats) and Table 3.21 (for mice).* The fourth columns of these tables show aggregate amounts of glutathione projected for the various compartments of the pharmacokinetic models. The values here for the different compartments are incorporated

---

*The values in the third column represent the averages of the two "control" measurements for each tissue given in McKelvey and Zemaitis' tables.

Table 3.20
Stocks of Glutathione in Different Rat Tissues and Compartments and Indicated Losses after 4-Hour Exposure to 1200 ppm ETO

Tissue group and tissue	Volume (ml)	Basal GSH conc. (umoles/g)	Basal Pool of GSH in compartment (umoles)	After 4 hr 1200 ppm ETO exposure GSH conc. (umoles/g)	Minimal* GSH loss (umoles)
Lung	1.5	1.025	1.54	.16	1.2
VESSEL-RICH GROUP					
Kidney		.51		.42	
Brain		1.12		.74	
Stomach (?)**		1.74		.51	
Spleen		2.08		1.08	
Bone Marrow		2.70		1.70	
Testis		2.92		1.03	
Total, VRG	11 app.	1.84***	20.2	.99	9.3
FAT GROUP	17.5	?	?	?	?
MUSCLE GROUP					
Heart		1.47		.99	
Skeletal Muscle		.75****			
Skin		?			
Total, MG	187.5 Assume	.75 app.	140	Assume .50	app. 46?? *****
Liver	10	4.26	42.6	.73	36.1
OTHER					
Blood	7.2******	.94	6.8	.98	0
Skeleton, Connective tissue		?	?	?	
	235		211+	app.	93

---

*Assuming no resynthesis of GSH during the four hours.
**It is not entirely clear that the stomach should be counted as part of the vessel-rich group.
***Based on an average of all organs shown except the stomach.
****Based on data of Griffith and Meister, 1979
*****Based on the approximately 33% reduction in glutathione level observed in the heart. There is, of course, an excellent chance that the heart muscle is not representative of skeletal muscle.
******Arterial and venous blood pools only--other blood is treated as part of the tissue compartments.

Table 3.21
Stocks of Glutathione in Different Mouse Tissues and Compartments and Indicated Losses after 4-Hour Exposure to 900 ppm ETO

Tissue group and tissue	Volume (ml) (ml)	Basal GSH conc. (umoles/g)	Basal Pool of GSH in compartment (umoles)	After 4 hr 900 ppm ETO exposure GSH conc. (umoles/g)	Minimal* GSH loss (umoles)
Lung	.15	1.175	.176	.16	.15
VESSEL-RICH GROUP					
Kidney		.31		.27	
Brain		1.12		.76	
Stomach (?)**		1.68		.52	
Spleen		2.225		1.42	
Bone Marrow		Not reported			
Testis		3.525		2.07	
Total, VRG	1.1	app. 1.85***	2.035	1.43	.46
FAT GROUP	2.5	?	?	?	?
MUSCLE GROUP					
Heart		.98		.28	
Skeletal Muscle		.78****			
Skin		?			
Total, MG	17.5	Assume .78	app. 13.65		app. 9.75? *****
Liver	1.5	4.855	7.28	.67	6.27
OTHER					
Blood	.72******	.62	.45	.16	.33
Skeleton, Connective tissue		?	?	?	
	23.5		23.6+	approx.	17

*Assuming no resynthesis of GSH during the four hours.
**It is not entirely clear that the stomach should be counted as part of the vessel-rich group.
***Based on an average of all organs shown except the stomach.
****Based on data of Griffith and Meister, 1979
*****Based on the approximately 33% reduction in glutathione level observed in the heart. There is, of course, an excellent chance that the heart muscle is not representative of skeletal muscle.
******Arterial and venous blood pools only--other blood is treated as part of the tissue compartments.

into the models as the starting levels of glutathione at the beginning of the simulations. Unfortunately McKelvey and Zemaitis (1986) do not report measurements for skeletal muscle, so I have used data from Griffith and Meister (1979) for skeletal muscle and the muscle group as a whole (including muscle and skin). It appears that even though muscle has a relatively modest concentration of glutathione, the large volume of the muscle group implies that this compartment contains a substantial proportion of the standing stock of glutathione in the body.

The fifth columns of Tables 3.20 and 3.21 show McKelvey and Zemaitis' observations of glutathione levels in various tissues after the highest exposures to ethylene oxide. Based on these data, and a rather questionable assumption that skeletal muscle glutathione depression will resemble the depression of glutathione observed in the heart, the final columns of Tables 3.20 show conservative calculations of the umoles of glutathione lost in different compartments, assuming that none of the glutathione lost through reaction with ethylene oxide has been replaced by enhanced synthesis or reductions in other routes of loss of glutathione. This calculation is conservative because it assumes that none of the glutathione lost through reaction with ethylene oxide will have been replaced by enhanced synthesis or reductions in other routes of loss within the four hour period of exposure. It of course also excludes any additional reaction between glutathione and the portion of the ethylene oxide remaining in the rats after the end of the four hours of exposure.

Even on this conservative basis, it is clear that glutathione reaction must account for a not-insignificant fraction of the ethylene oxide absorbed. McKelvey and Zemaitis (1986) unfortunately did not measure overall absorption in these experiments, but Tyler and McKelvey's

earlier work (see Table 1.1) indicates that absorption by rats exposed to 1010 ppm for six hours (6060 ppm-hours) amounts to about 606 umoles per 250 g rat. In the McKelvey and Zemaitis experiment, where rats were exposed to 1200 ppm for four hours (4800 ppm-hours), the minimal estimate of 93 umoles of glutathione loss per 250 g rat probably represents at least a fifth of the absorbed ethylene oxide. The dynamic modeling in section 4 will allow a refinement of this initial crude estimate.

There has been a great deal of work in recent years on the normal synthesis and degradation of glutathione, particularly in the liver (Kaplowitz and Ookhtens, 1985; Reed, 1986; Lauterburg and Mitchell, 1981; Lunn et al, 1979; Joshi et al., 1986), and the effects of external agents on glutathione levels (Mann and Darby, 1985; Morton and Mitchell, 1985; Pierson and Mitchell, 1986; Dodd et al., 1982). There appears to be a substantial transfer of glutathione among organs. Glutathione is exported from the liver, and this export reportedly accounts for a substantial portion of the glutathione in the systemic circulation. Substantial amounts of glutathione are taken up from the ciruculation and used by the kidney and gut (Kaplowitz et al., 1985).

Another interesting phenomenon that is sometimes seen in studies of glutathione levels in the liver and some other organs after depletion of glutathione is a modest (10-40%) "overshoot" of basal levels that can last at least a day or two after the initial inhibition has been reversed (Mann and Darby, 1985). Figure 3.1 (from McKelvey and Zemaitis, 1986) shows that this occurs in some cases for ethylene oxide in mice. This indicates that tissues respond to lowered glutathione levels by either increasing synthesis or uptake of glutathione or reducing loss via moderately long-lasting functional changes. Unfortunately, however, the nature of

Figure 3.1

Recovery of Glutathione Levels After Ethylene Oxide or DEM

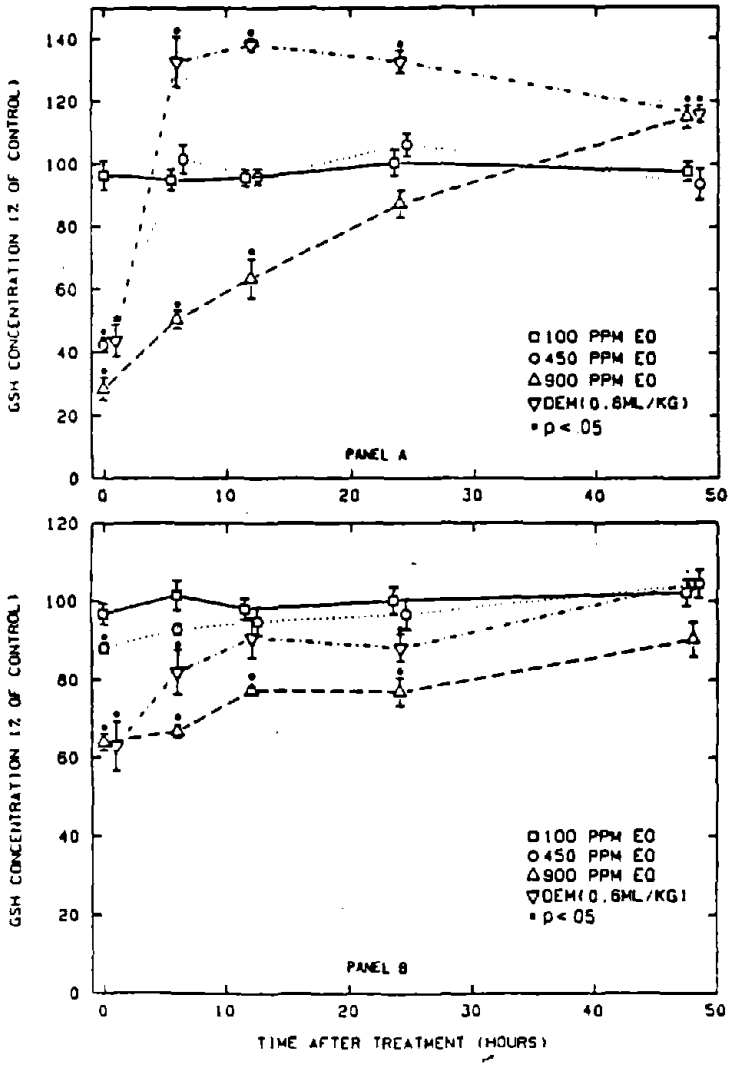

FIG. 2. Stomach (Panel A) and Testis (Panel B) GSH Levels in Male Swiss-Webster Mice After a Four Hour EO Exposure or DEM Injection.

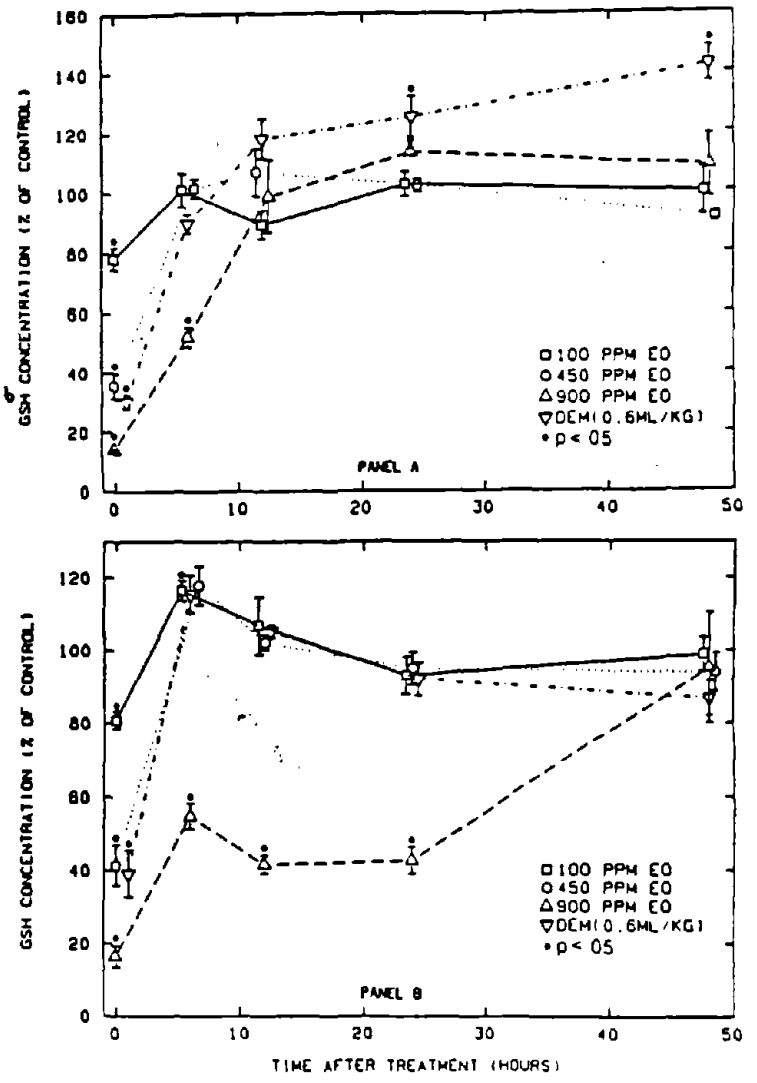

FIG. 3. Lung (Panel A) and Liver (Panel B) GSH Levels in Male Swiss-Webster Mice after a Four Hour EO Exposure or DEM Injection.

Source: McKelvey and Zemaitis, 1986

these changes has not yet been well worked out--and exactly how strong they are, and when they occur after the start of how much lowering of glutathione levels are impossible to say on the basis of available information.

In developing the ethylene oxide models, I made the judgment that attempting to incorporate the interorgan transfers of glutathione, or the complexities of the overshoot of basal glutathione levels after inhibition, would considerably complicate the modeling process with probably little reward in terms of accuracy for describing the behavior of the metabolism of ethylene oxide. I believe it stretches the available data resources enough even to attempt a much simpler treatment of disseminated metabolism in different tissues. All of the modeling of glutathione levels used to date incorporates a simple uniform rate of synthesis of glutathione in each tissue. Glutathione is lost from each tissue by processes other than ethylene oxide reaction at a rate that depends simply on the glutathione concentration:

$$-d[GSH]/dt = k_{GSH\ elim.}[GSH] \qquad (24)$$

The paper I found most directly useful in beginning to model the normal turnover of glutathione in a wide variety of tissues was by Griffith and Meister, (1979). These workers administered an inhibitor of glutathione synthesis* to rats and mice, and measured the decline in glutathione levels over time. Assuming that glutathione synthesis was complete and instantaneous after the administration of inhibitor, the decline should be exponential with time:

---

*The inhibitor was buthionine solfoximine, which is described as "a potent selective inhibitor of gamma-glutamylcysteine synthetase."

$$[GSH]_t = [GSH]_0 e^{-kt} \qquad (25)$$

where $[GSH]_0$ is the basal concentration in a particular tissue, and t is the time after administration of the inhibitor. The only evidence on these assumptions is the time profile of glutathione depression itself in liver and kidney, which looks reasonbly steep over at least the first couple of hours after BSO administration (Figure 3.2). On this basis, Table 3.22 shows calculations of the rate constants for loss of glutathione in different tissues of rats and mice. To the degree that the assumptions of instantaneous and complete inhibition of glutathione synthesis are not met, the rate constants calculated in this table may be understated. Some of the lower turnover rates are also suspect because the very modest amounts of reduction observed makes the calculation of turnover rates subject to potentially large statistical errors. However, these rate constants were the ones incorporated into the models for the basal turnover of glutathione in the various tissues.

As indicated earlier, in the models a basal equilibrium was set up for each tissue between glutathione generation and glutathione loss. The basal loss was simply set equal to the appropriate rate constant from Table 3.22 times the amount of glutathione in the compartment; glutathione generation was set at a constant level that exactly balanced this rate of loss in the absence of exposure to ethylene oxide. The rate constants for kidney were used for the vessel rich group in rats and mice, even though the kidney constitutes only a portion of the vessel rich group and has a particularly rapid rate of turnover (the kidney does not primarily synthesize its own glutathione but absorbs it from the blood). In the

Figure 3.2

Decline of Glutathione Levels After Adninistration of BSO

Swiss-Webster Mice

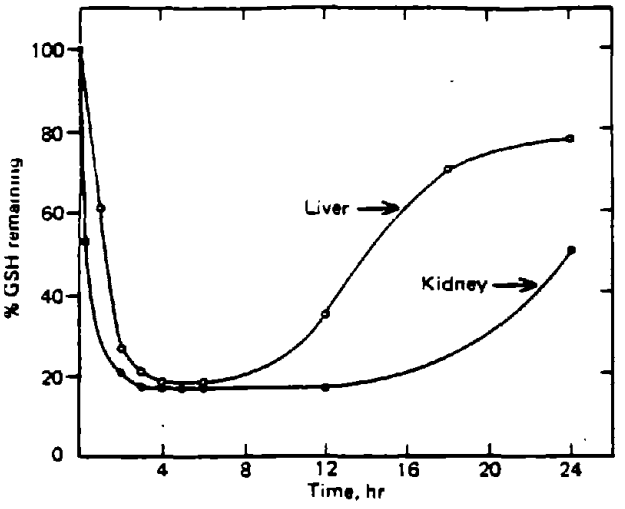

FIG. 1. Levels of GSH in kidney and liver after administration of BSO (4 mmol/kg) to mice (starved for 12 hr) by intraperitoneal injection of 100 mM solution.

Source: Griffith and Meister, 1979

Table 3.21
Calculations of Rate Constants for Normal Glutathione Turnover

Tissue	GSH concentration in untreated controls (umol/g)	GSH Concentration 2 hours after BSO injection (umol/g)	Indicated rate constant for GSH turnover (min^{-1})
Experiments in Rats (young 90-100g rats, injected with 4 mmol/kg s.c.)			
Kidney	2.56	.59	.0122
Liver	4.51	1.37	.0099
Pancreas	1.66	1.05	.0038
Skeletal Muscle	.75	.63	.0014
Experiments in Mice			
Kidney	4.13	.75	.0142
Liver	7.68	2.67	.0088
Pancreas	1.78	.81	.0066
Skeletal Muscle	.78	.52	.0034
Brain	2.08	1.93	.0006
Heart	1.35	1.19	.0010
Lung	1.52	1.42	.0006
Spleen	3.43	3.46	-
Small intest. mucosa	2.94	2.40	.0017
Colon mucosa	2.11	1.83	.0012
Plasma	28.4 uM	9.3 uM	.0093

case of lung tissue, however, the relatively complete regeneration of glutathione by 6 hours after the end of exposure to diethyl maleate in the McKelvey and Zemaitis (1986) experiments suggested a more rapid turnover than the very low value suggested by the data of Griffith and Meister (1979). A rate constant of .006 min^{-1} was selected (corresponding to a half life of 2 hours) in the light of these data.

Unfortunately I could find no comparable data for human tissues--either on the standing stocks of glutathione or normal turnover with the exception of some work in red cells in vitro (Lunn et al., 1979). To construct the human models, I chose to assume that humans had the same concentrations of tissue glutathione as rats, but that the turnover rates were less--in all cases scaled down in porportion to metabolic rates per weight of tissue. Because metabolic rates per body weight scale approximately to the .25 power of body weight, this resulted in an assumption that human basal glutathione synthethis and utilization rates are about one quarter the rates in rats--$(.25\ kg/70\ kg)^{.25} = .244$.

4. TESTING AND REFINEMENT OF THE INITIAL MODELS FOR ETHYLENE OXIDE

This section derives the basic models for rats, humans, and mice. In each case I also explore the fit to the data of a number of model variants (these variants are described in Section 4.1.2 below). The differences in risk predictions between the model variants that are reasonably compatible with the available data will provide insight into the sensitivity of the conclusions to different reasonable interpretations of the data.

4.1 Articulation of the Rat Model

Table 4.1 shows the equations for the basic rat model (designated "G3BL90"). The schematic diagram was presented earlier in Figure 1.4 on page 9 above.

4.1.1 Fitting the Adjustable Parameters for the Basic Rat Model

In fitting the model (and model variants) to the available absorption and ethylene oxide exhalation data of Tyler and McKelvey (1983), there are essentially three categories of adjustable parameters:

- "k_2"--this is the constant relating the rate of metabolism of ethylene oxide to the concentration of glutathione in a particular tissue, as described in the equation at the top of page 8 above. For the initial models, it was treated as uniform for all tissues (as if the reaction were passive). In this equation the concentration of glutathione stands as a proxy for glutathione plus all the other sulfhydryl compounds in the tissue that may also be reacting with ethylene oxide. Implicitly we assume that the concentrations of these other sulfhydryl compounds is directly proportional to the concentration of glutathione.

Table 4.1
Equations for the Basic Rat Model (G3BL90)

□ ARTERIAL_BLOOD = ARTERIAL_BLOOD - VRG_PERFUSION -
LIVER_PERFUSION + LUNG_OUTPUT - FG_PERFUSION - MG_PERFUSION
INIT(ARTERIAL_BLOOD) = 0
□ BLOOD_CXT = BLOOD_CXT + BLOOD_DOSE_RATE
INIT(BLOOD_CXT) = 0 {initial value...}
□ FG = FG + FG_PERFUSION - FG_ELIMINATION
INIT(FG) = 0
□ LIVER = LIVER + LIVER_PERFUSION - LIVER_ELIMINATION -
LIVER_METABOLISM
INIT(LIVER) = 0
□ LIVER_CXT = LIVER_CXT + LIVER_CONC
INIT(LIVER_CXT) = 0 {initial value...}
□ LUNG = LUNG - LUNG_OUTPUT + LUNG_PERFUSION + INFLOW -
LUNG_METABOLISM - EXHALATION
INIT(LUNG) = 0
□ LUNG_CXT = LUNG_CXT + LUNG_CONC
INIT(LUNG_CXT) = 0 {initial value...}
□ LUNG_GSH = LUNG_GSH + LUNG_GSH_GEN - LUNG_GSH_LOSS
INIT(LUNG_GSH) = 1.54E-6 {1.5 G OF LUNG AT 1.025 MICROMOLES/G}
□ L_GSH = L_GSH - L_GSH_LOSS + L_GSH_GEN
INIT(L_GSH) = 4.26E-5 {Moles/liter. Equal to 10 g liver tissue at 4.26
micromoles per gram, after McKelvey and Zemaitis.}
□ MG = MG + MG_PERFUSION - MG_ELIMINATION - MG_METABOLISM
INIT(MG) = 0
□ MIXED_VENOUS = MIXED_VENOUS + VRG_ELIMINATION + LIVER_ELIMINATION
LUNG_PERFUSION + FG_ELIMINATION + MG_ELIMINATION
INIT(MIXED_VENOUS) = 0
□ M_GSH = M_GSH - M_GSH_LOSS + M_GSH_GEN
INIT(M_GSH) = 1.4E-4 {187.5 G MUSCLE GROUP TISSUE AT .75 MICROMOLES/
G}{BASAL RATE DATA FROM GRIFFITH AND MEISTER, 1979}
□ RECOVERY = RECOVERY + EXHALATION
INIT(RECOVERY) = 0 {initial value...}
□ TOTAL_ABSORPTION = TOTAL_ABSORPTION + ABSORPTION
INIT(TOTAL_ABSORPTION) = 0 {initial value...}
□ TOTAL_METABOLISM = TOTAL_METABOLISM + LIVER_METABOLISM +
MG_METABOLISM + LUNG_METABOLISM + VRG_METABOLISM
INIT(TOTAL_METABOLISM) = 0 {Initial value...}
□ VRG = VRG + VRG_PERFUSION - VRG_ELIMINATION - VRG_METABOLISM
INIT(VRG) = 0
□ VRG_CXT = VRG_CXT + VRG_CONC
INIT(VRG_CXT) = 0 {initial value...}
□ VRG_GSH = VRG_GSH + VRG_GSH_GEN - VRG_GSH_LOSS
INIT(VRG_GSH) = 2.02E-5 {initial value...} {11 g at about 1.84 micromoles
per gram}
○ ABSORPTION = IF (INFLOW > 0) THEN INFLOW ELSE 0
○ ART_BLOOD_VOL = .0024 {LITERS}
{ARTERIAL BLOOD VOLUME}
○ ART_CONC = BLOOD_AIR*(CARDIAC_OUTPUT*VEN_CONC + V_ALV *(
EXPOSURE *10^(-6)/25.45))/(CARDIAC_OUTPUT*BLOOD_AIR +V_ALV) {
MOLES/LITER}
○ BLOOD_AIR = 90
○ BLOOD_DOSE_RATE = (MIXED_VENOUS + ARTERIAL_BLOOD)/(
ART_BLOOD_VOL + VENOUS_BLOOD) {CALCULATES TOTAL BLOOD
CONCENTRATION}
○ CARDIAC_OUTPUT = VRG_FLOW + LIVER_FLOW + MG_FLOW + FG_FLOW {
liters/minute}
○ EXHALATION = IF (VEN_CONC > ART_CONC) THEN CARDIAC_OUTPUT*(
VEN_CONC - ART_CONC) ELSE 0
○ EXPOSURE = IF (TIME < 360) THEN 1 ELSE 0

Table 4.1, continued
Equations for the Basic Rat Model (G3BL90)

- FG_ELIMINATION = (FG * FG_FLOW) / (.0175 * .44)
  {moles/minute} {FG/BLOOD = .44 BASED ON OIL/WATER SOLUBILITY RATIO OBSERVED BY CHAIGNEAU}
  { ([FG_BLOOD] * *f*F[FG]) / (*f*V[FG] * *f*L[FG\BLOOD]) }
- FG_FLOW = .0085 {liters/minute}
- FG_PERFUSION = ARTERIAL_BLOOD * FG_FLOW / ART_BLOOD_VOL
  {moles/minute}
  { [ARTERIAL_BLOOD] * *f*F[FG] / *f*V[arterial blood] }
- FRACT_ABSORB = IF (INFLOW ≥ 0) THEN
  INFLOW / (V_ALV * EXPOSURE * 10 ^(-6)/25.45) ELSE 0
- INFLOW = IF (ART_CONC > VEN_CONC) THEN CARDIAC_OUTPUT*(ART_CONC - VEN_CONC) ELSE 0 {MOLES/MIN}
- LIVER_CONC = LIVER/.01 {MOLES/LITER}
- LIVER_ELIMINATION = (LIVER * LIVER_FLOW) / (.01 * .6)
  {moles/minute}
  { (LIVER * *f*F[LIVER]) / (*f*V[liver] * *f*L[LIVER\BLOOD]) }
- LIVER_FLOW = .0235 {liter/minute}
- LIVER_METABOLISM = (80)*(LIVER)*(L_GSH/.01) {BASIC SECOND ORDER RATE EQUATION.}
- LIVER_PERFUSION = ARTERIAL_BLOOD * LIVER_FLOW / ART_BLOOD_VOL
  {moles/minute}
  { *f*F[LIVER] * ARTERIAL_BLOOD / *f*V[arterial blood] }
- LUNG_CONC = LUNG/.0015 {MOLES/LITER}
- LUNG_GSH_GEN = .006*1.54E-6 {statement goes here...}
- LUNG_GSH_LOSS = .006*LUNG_GSH +.43*LUNG_METABOLISM {LUNG TURNOVER ESTIMATED AS HAVING A T1/2 OF less than 2 HOURS, FROM MCKELVEY AND ZEMAITIS OBSERVATION OF ESSENTIALLY COMPLETE RESTORATION IN 6 HOURS FOR LOW DOSES. 2 hours corresponds to .006.}
- LUNG_METABOLISM = 80*(LUNG)*(LUNG_GSH/.0015)
- LUNG_OUTPUT = LUNG * CARDIAC_OUTPUT /(.0015*1.07)
  {moles/minute}
  { [LUNG] * CARDIAC_OUTPUT / *f*V[lung blood] }
- LUNG_PERFUSION = MIXED_VENOUS * CARDIAC_OUTPUT / VENOUS_BLOOD
  {moles/minute}
  { MIXED_VENOUS * CARDIAC_OUTPUT / *f*V[venous blood] }
- L_GSH_GEN =.0025*4.26E-5
- L_GSH_LOSS = .0025*L_GSH + .43*LIVER_METABOLISM {MOLES/MIN.}
- MG_ELIMINATION = (MG * MG_FLOW) / (.1875 * .47)
  {moles/minute}
  { ([MG] * *f*F[MG]) / (*f*V[MG] * *f*L[MG\BLOOD]) }
- MG_FLOW = .0141 {liter/minute}
- MG_METABOLISM = (80)*(M_GSH)*(MG/.1875) {BASIC SECOND ORDER RATE EQUATION.}
- MG_PERFUSION = ARTERIAL_BLOOD * MG_FLOW / ART_BLOOD_VOL
  {moles/minute}
  { [ARTERIAL_BLOOD] * *f*F[MG] / *f*V[arter]
- M_GSH_GEN = .0014*1.4E-4
- M_GSH_LOSS = .0014*M_GSH + .43*MG_METABOLISM
- VENOUS_BLOOD = .0048 {LITERS}
  {MIXED VENOUS BLOOD VOLUME}
- VEN_CONC = MIXED_VENOUS/VENOUS_BLOOD {MOLES/LITER}
- VRG_CONC = VRG/.011 {MOLES/LITER}
- VRG_ELIMINATION = (VRG * VRG_FLOW) / (.011 * .595)
  {moles/minute}{ VRG * *f*F[VRG] / *f*V[VRG blood] * *f*L[VRG\BLOOD] }{New value of .011 for the volume of vrg is the old value of .0125 less .0015 for lung tissue.}
- VRG_FLOW = .0479 {liter/minute}

Table 4.1, continued
Equations for the Basic Rat Model (G3BL90)

- VRG_GSH_GEN = .0122*2.02E-5 {Turnover rate is high, after kidney as measured by Griffith and Meister is small 100 g rats, even though the VRG contains many tissues with much lower turnover rates.}
- VRG_GSH_LOSS = .43*VRG_METABOLISM + .0122*VRG_GSH
- VRG_METABOLISM = 80*(VRG)*(VRG_GSH/.011) {Basic bimolecular reaction kinetics.}
- VRG_PERFUSION = ARTERIAL_BLOOD * VRG_FLOW / ART_BLOOD_VOL {moles/minute}
  { ƒF[VRG] * ARTERIAL_BLOOD / ƒV[arterial blood] }
- V_ALV = .117 {liters/min.}

- o "k_1"--this is essentially the fraction of total ethylene oxide metabolism that is accounted for by reaction with glutathione. It was assumed to be uniform across all tissues.
- o alveolar ventilation as a function of exposure level.

The iterative trial-and-error procedure for arriving at the values of these parameters for the model G3B190 is illustrated in Table 4.2. First, k_2 and alveolar ventilation at the lowest exposure level are adjusted to give the total absorption and ethylene oxide exhalation observed for the 11 ppm exposure. Next, for the highest dose point, k_1 and the alveloar ventilation at 1010 ppm are adjusted to give the total absorption and ethylene oxide exhalation observed there. Higher values of k_1 lead to more depletion of glutathione (for a given amount of ethylene oxide absorbed), greater persistence of absorbed ethylene oxide in the system, and therefore a greater percentage of absorbed ethylene oxide that will be eventually exhaled. After modification of k_1, correspondence with the intermediate- and low-dose data is reexamined. It can be seen that in the end, with this number of adjustable parameters, it was possible to achieve quite a reasonable fit to all the available absorption and exhalation information. The indication is that approximately 43% of ethylene oxide metabolism is accounted for by direct reaction with glutathione--a reasonable result from first principles, and consistent with the notion that depletion of glutathione and related sulfhydryl compounds could be an important source of nonlinearities in the concentration X time of ethylene oxide available for reaction with other targets at high doses.

Table 4.2
Illustration of the Fitting of Model Parameters to the Absorption And Exhalation Data of Tyler and McKelvey (1983)

ppm (6 hrs)	Alveolar Ventilation (l/min)	Net Absorption During Exposure (Micromoles per 250 g Rat)	Exhalation After Exposure (Micromoles Per 250 g Rat)	% Exhalation of Absorption (+/- SD)
Observations				
11	not measured	15.15*	.0758**	.5 +/- .1
104	not measured	114.6*	.574**	.5 +/- .1
1010	not measured	606.1*	12.74**	2.1 +/- .2
Trial***, k_2 = 100, k_1 = .34				
11	.115	15.49	.05022	.324
Trial, k_2 = 83, k_1 = .34				
11	.120	15.73	.07498	.477
Trial, k_2 = 82, k_1 = .34				
1010	.05	639.1	8.379	1.31
Trials, k_2 = 82, k_1 = .43				
1010	.050	628.6	15.07	2.40
1010	.048	608.2	12.77	2.10
104	.095	120.5	.6433	.533
104	.090	115.0	.5779	.502
11	.120	15.70	.07717	.492
Trials, k_2 = 80, k_1 = .43				
11	.117	15.33	.7715	.503
104	.090	114.7	.6030	.526
1010	.048	607.0	13.10	2.16

---

*Calculated from reported absorption of 2.7, 20.2, and 106.8 mg/kg respectively at the three exposure levels.

**Calculated from absorption and reported % exhalation data (last column).

***Note: Increases in k_2 (the rate of reaction between glutathione and other sulfhydryls and ethylene oxide) tend to increase absorption and decrease ethylene oxide exhalation following exposure; increases in k_1 (the fraction of ethylene oxide metabolism accounted for by glutathione) tend to increase ethylene oxide exhalation following exposure at high doses; increases in the alveolar ventilation rate tend to increase both absorption and exhalation following exposure.

4.1.2 Description of Model Variants for Exploration of Assumptions in the Basic Rat Model

In constructing the basic rat model, I made a number of assumptions whose consequences require exploration via model variants. These include:

- Is it really necessary for rat alveolar ventilation rates to change as a function of exposure level in order to achieve a reasonable fit to the Tyler and McKelvey (1983) data? This will be studied via the "brun" and "brun2" models.
- In the modeling presented in Table 4.2, rats are assumed to maintain the same breathing rates immediately after exposure as they are estimated to have had during exposure--in other words the high-dose breathing rate reductions are assumed to persist for at least a short time (30-60 minutes) after the end of exposure. What happens if the animals return to an assumed basal alveolar ventilation rate of .133 l/min. immediately after the end of exposure? This alternative assumption is incorporated into the "G4" rat models.
- What are the effects of different values of the blood/air partition coefficient? Models whose names include "BL67.6" and "BL50" incorporate blood/air partition coefficients of 67.6 and 50, respectively.
- What differences are produced by the "T*" series of tissue/blood partition coefficients (see pp. 45-46 above). These coefficients are incorporated into models with "T*" in their names. To provide additional insight into the consequences of different tissue/blood partition coefficients models with "TBL1" in their names have all tissue/blood partition coefficients set at 1.
- Finally, as noted above, in the basic model there is an assumption that the "k_2" rate constant for metabolism of ethylene oxide in relation to glutathione concentration is uniform for all tissues. For models with "LV*" in their names, I assume that the "k_2" rate constant for the liver is twice the value for other tissues.

Other details about the different models can be found in Tables 4.3a and 4.3b below.

In the following sections I will use a number of different sets of data to judge the likelihood of these variants:

- The "fit" to the intermediate dose exhalation data point in Tyler/Mckelvey absorption/exhalation rat experiment. (This point is not generally required for derivation of k_2, k_1, and the alveolar ventilation rates for the specific model.) (See Section 4.1.3.)

- The fit of the models to the pattern of change of glutathione levels in lung, liver, and (to some extent) the vessel-rich-group [for both McKelvey and Zemaitis (1986) rat and mouse data--see Sections 4.1.4 and 4.3.]

- The fit of the models to the ethylene oxide concentration X time in the blood inferred from the hemoglobin adduct observations of Osterman-Golkar et al. (1983) following intraperitoneal injections of ethylene oxide into rats (see Section 4.1.5).

- After translation into human models--the fit to the time pattern of % absorption in Brugnone (1986) human observations (see Section 4.2.)

4.1.3 Exploration of the Fit of Model Variants to the Tyler and McKelvey (1983) Absorption and Exhalation Data

Table 4.3 compares the final fit of our basic rat model to the final fits of a number of model variants for the Tyler and McKelvey (1983) data. Table 4.3a includes model variants with uniform k_2's across all tissues, while Table 4.3b includes model variants with liver k_2's set at twice the level of other tissues.

The third and fourth sets of results in Table 4.3a (for the "brun" and "brun2" models) show the basis for my conclusion that alveolar ventilation rates must be lower at higher dose levels. For the "brun" model I adjusted k_1 so that a good fit was achieved with the % exhalation data in the final column. This, however, led the model to "predict" over twice the net absorption of ethylene oxide as was observed

Table 4.3a
Primary Fit of Different Rat Models to the Tyler/McKelvey Data Set
Models with Uniform GSH/ETO Reaction Rates Across Tissues

ppm (6 hrs)	Alveolar Ventilation (l/min)	Net Absorption During Exposure (Micromoles per 250 g Rat)	Exhalation After Exposure (Micromoles Per 250 g Rat)	% Exhalation of Absorption (+/- SD)
Observations				
11	not measured	15.15*	.0758**	.5 +/- .1
104	not measured	114.6*	.574**	.5 +/- .1
1010	not measured	606.1*	12.74**	2.1 +/- .2
Model G3-BL90 (Blood/Air = 90, k_1 = .43, k_2 = 80)				
11	.117	15.33	.07715	.503
104	.09	114.7	.6030	.526
1010	.048	607.0	13.10	2.16
Model G3-BL90-brun (Blood/Air = 90, k_1 = .15, k_2 = 80, no change in breathing rates with increasing dose, but maintaining fit to data on % exhaled)				
11	.117	15.34	.07534	.491
104	.117	144.4	.7941	.550
1010	.117	1318	27.34	2.07
Model G3-BL90-brun2 (Blood/Air = 90, k_1 = 1.0 k_2 = 80, no change in breathing rates with increasing dose, but making maximal attempt to maintain fit to data on moles absorbed)				
11	.117	15.30	.08100	.529
104	.117	139.30	1.746	1.25
1010	.117	719.2	269.7	37.5
Model G3-BL67.6 (Blood/Air = 67.6, k_1 = .42, k_2 = 92)				
11	.12	15.18	.07604	.501
104	.092	114.0	.5919	.519
1010	.049	605.2	12.49	2.06
Model G3-BL90-TBL1 (Blood/Air = 90 but all tissue/blood partition coefficients are set at 1 except for the fat group, k_1 = .44, k_2 = 55)				
11	.112	15.21	.07788	.512
104	.087	114.3	.6177	.540
1010	.0465	607.1	13.17	2.17
Model G4-BL90 (Blood/Air = 90, k_1 = .33, k_2 = 91, breathing rate jumps to .133 l/minute immediately after exposure)				
11	.115	15.34	.06703	.437
104	.0885	114.8	.6124	.533
1010	.0465	605.6	12.06	1.99

---

*Calculated from reported absorption of 2.7, 20.2, and 106.8 mg/kg respectively at the three exposure levels.

**Calculated from absorption and reported % exhalation data (last column).

Table 4.3b
Primary Fit of Different Rat Models to the Tyler/McKelvey Data Set
Comparisons with LV* Models (Enhanced Metabolism in Liver)

ppm (6 hrs)	Alveolar Ventilation (l/min)	Net Absorption During Exposure (Micromoles per 250 g Rat)	Exhalation After Exposure (Micromoles Per 250 g Rat	% Exhalation of Absorption (+/- SD)
Observations				
11	not measured	15.15*	.0758**	.5 +/- .1
104	not measured	114.6*	.574**	.5 +/- .1
1010	not measured	606.1*	12.74**	2.1 +/- .2
Model G3-BL90 (Blood/Air = 90, k_1 = .43, k_2 = 80)				
11	.117	15.33	.07715	.503
104	.09	114.7	.6030	.526
1010	.048	607.0	13.10	2.16
Model G3-BL90-LV* [Blood/Air = 90, rate constant for reaction of glutathione with ETO in the liver is set at twice the value for other tissues, k_1 = .4, k_2 = 130 (liver) or 65 (other tissues)]				
11	.115	15.20	.07467	.491
104	.09	115.2	.6141	.533
1010	.0478	604.6	12.24	2.02
Model G3-BL50-LV* [Blood/Air = 50, rate constant for reaction of glutathione with ETO in the liver is set at twice the value for other tissues, k_1 = .395, k_2 = 172 (liver) or 86 (other tissues)]				
11	.125	15.20	.07715	.508
104	.095	113.8	.6115	.537
1010	.051	605.6	12.84	2.12
Model G3-BL90-T*-LV* [Blood/Air = 90, tissue/blood partition coefficients are the new set presented in the last line of Table 3.11, p. 45 (with liver set equal to kidney, but fat maintained at its original value of .44); additionally, the rate constant for reaction of glutathione with ETO in the liver is set at twice the value for other tissues, k_1 = .42, k_2 = 110 (liver) or 55 (other tissues)]				
11	.112	15.12	.07348	.486
104	.0875	114.1	.6016	.527
1010	.047	605.4	13.19	2.18

---

*Calculated from reported absorption of 2.7, 20.2, and 106.8 mg/kg respectively at the three exposure levels.

**Calculated from absorption and reported % exhalation data (last column).

by Tyler and McKelvey (1983) at the highest exposure level. For the "brun2" model I attempted to maintain consistency with the absorption data by setting k_1 at its highest possible level of 1.0 (clearly no more than 100% of the metabolism of ethylene oxide can be accounted for by reaction with glutathione). Even with this elevated k_1, the model predicted somewhat more absorption than was observed at the highest exposure level. But the major difficulty for the "brun2" model is the departure from the observations of the percentage of absorbed ethylene oxide that was exhaled following exposure. This model over-predicts the exhaled ethylene oxide by over two-fold at the intermediate (104 ppm) exposure level, and by a whopping 18-fold at the highest exposure level. In particular these departures for "brun2" are far beyond the bounds of experimental error in the Tyler and McKelvey (1983) data. Accordingly, these models without change in alveolar ventilation rates as a function of exposure level were not pursued further.

The next two sets of results in Table 4.3a--respectively assuming a blood/air partition coefficient of 67.6 or all tissue/blood partition coefficients set at 1--are both unremarkable, as are all of the results for the "LV*" models in Table 4.3b. There is nothing to exclude them in the Tyler and McKelvey (1983) data.

Some difficulty in achieving a good fit is apparent for the last ("G4") model in Table 4.3a, where breathing rates increase to .133 liters/minute immediately after the end of exposure. It can be seen that while achieving good correspondence to the absorption data, the departure of the best fit model from the exhalation data was appreciable--although

in my judgment* probably not large enough to classify it as excluded by the observations.

4.1.4 The Fit of the Models to the McKelvey and Zemaitis (1986) Data on Changes in Rat Tissue Glutathione Levels

Tables 4.4a and 4.4b show the correspondence of the "predictions" of different models to the pattern of changes of tissue glutathione levels with increasing ethylene oxide air levels observed by McKelvey and Zemaitis (1986). As discussed in Section 3.4 above, these observations were made at the end of four-hour exposures.

It can be seen in Table 4.4a that the basic rat model (G3BL90) predicts glutathione reductions that are quite close to the observations in the lung and (to the degree we can believe the aggregate data) the vessel-rich-group. However, the basic model predicts that there should be about twice as much residual glutathione in the liver as was observed by McKelvey and Zemaitis (1986) at the 600 and 1200 ppm exposure levels.

---

*It would be useful, of course, to be able to put this kind of statement on a somewhat more formal basis than "my judgment". However, there are appreciable difficulties in developing an appropriate statistical testing procedure for the "fit" of model "predictions" to multiple sets of experimental observations. This is particularly true in this case where I do not have access to the raw individual data points and the authors provide limited summary statistics to characterize their experimental errors. Although the authors report standard deviations for their exhalation observations, any testing I might do assuming a normal distribution for the errors in these data would be incomplete because of the lack of information on the experimental errors in the absorption data. An additional difficulty is that the exposure levels themselves were measured with some error--and although the authors report the standard deviations of these measurements, they do not report the number of measurements they made and therefore one cannot calculate the standard errors of the authors' estimates of mean exposures.

Table 4.4a
Depletion of Glutathione Immediately After 4 Hour Exposures
To Varous Concentrations of Ethylene Oxide
Models with Uniform GSH/ETO Reaction Rates Across Tissues

ppm (4 hrs)	Alveolar Ventilation (l/min)*	----Percentage of Basal Glutathione Levels---- Liver	Lung	Vessel-Rich Group	Muscle Group
Observations					
100	Not Measured	83.1	83.3	Incomplete	Not Measured
600	Not Measured	27.0	38.7	Incomplete	Not Measured
1200	Not Measured	15.3	23.8	About 54	Not Measured
Model G3-BL90 (Blood/Air = 90, k_1 = .43, k_2 = 80)					
100	.09	85.5	81.1	93.0	89.6
600	.0573	49.0	42.6	71.8	59.1
1200	.0447	28.2	25.1	55.2	37.3
Model G3-BL67.6 (Blood/Air = 67.6, k_1 = .42, k_2 = 92)					
100	.092	85.6	81.1	93.1	90.0
600	.0585	48.1	42.6	72.0	60.0
1200	.0456	28.4	25.1	55.3	38.0
Model G3-BL90-TBL1 (Blood/Air = 90 but all tissue/blood partition coefficients are set at 1 except for the fat group, k_1 = .44, k_2 = 55)					
100	.087	86.4	89.3	93.3	89.1
600	.056	52.1	61.3	73.5	57.9
1200	.0435	32.5	43.8	58.6	36.9
Model G4-BL90 (Blood/Air = 90, k_1 = .33, k_2 = 91, breathing rate jumps to .133 l/minute immediately after exposure)					
100	.0885	88.6	84.8	94.5	92.1
600	.0558	58.9	51.7	78.3	68.8
1200	.0432	40.5	34.9	65.5	51.3

---

*These alveolar ventilation rates as a function of dose were calculated from the relationships derived for each model from the Tyler and McKelvey (1983) data in Table 4.3. To project the values at 600 and 1200 ppm from the "observed" rates at 104 and 1010 ppm, we used a relationship patterned after the empirical formula of Kane and Alarie (1977): % reduction of breathing rate = k[log (exposure level)].

Table 4.4b
Depletion of Glutathione Immediately After 4 Hour Exposures
To Varous Concentrations of Ethylene Oxide
Comparisons with LV* Models (Enhanced Metabolism in Liver)

ppm (4 hrs)	Alveolar Ventilation (l/min)	----Percentage of Basal Glutathione Levels---- Liver	Lung	Vessel-Rich Group	Muscle Group
Observations					
100	Not Measured	83.1	83.3	Incomplete	Not Measured
600	Not Measured	27.0	38.7	Incomplete	Not Measured
1200	Not Measured	15.3	23.8	About 54	Not Measured
Model G3-BL90 (Blood/Air = 90, k_1 = .43, k_2 = 80)					
100	.09	85.5	81.1	93.0	89.6
600	.0573	49.0	42.6	71.8	59.1
1200	.0447	28.2	25.1	55.2	37.3
Model G3-BL90-LV* [Blood/Air = 90, rate constant for reaction of glutathione with ETO in the liver is set at twice the value for other tissues, k_1 = .4, k_2 = 130 (liver) or 65 (other tissues)]					
100	.09	80.2	85.5	94.8	91.9
600	.0572	36.4	50.5	77.2	66.4
1200	.0444	17.8	31.7	62.2	46.4
Model G3-BL50-LV* [Blood/Air = 50, rate constant for reaction of glutathione with ETO in the liver is set at twice the value for other tissues, k_1 = .395, k_2 = 172 (liver) or 86 (other tissues)]					
100	.095	80.4	85.1	94.6	92.1
600	.0608	35.4	48.9	76.3	66.2
1200	.0475	16.4	29.6	60.3	44.9
Model G3-BL90-T*-LV* [Blood/Air = 90, tissue/blood partition coefficients are the new set presented in the last line of Table 3.11 (p. 45) (with liver set equal to kidney, but fat maintained at its original value of .44); additionally, the rate constant for reaction of glutathione with ETO in the liver is set at twice the value for other tissues, k_1 = .42, k_2 = 110 (liver) or 55 (other tissues)]					
100	.0875	80.9	90.6	94.8	91.1
600	.056	38.1	64.1	77.9	63.6
1200	.0438	19.1	45.7	63.4	42.9

This result is unaffected by changing the blood/air partition coefficient to 67.6. The model where the tissue/blood partition coefficients have been adjusted to 1 performs even a bit more poorly as measured by these data, as does the "G4" model.

It was these data that suggested the creation of the "LV*" series of models, where the rate of reaction between ethylene oxide and glutathione in the liver is set at twice the value for other tissues. As can be seen in Table 4.4b, this change brings the models into appreciably closer alignment with the observations. As was observed in earlier, changing the blood/air partition coefficient (even, in this case, down to 50) does not alter the glutathione depletion behavior of the resulting model. Use of the "T*" set of tissue/blood partition coefficients appears to produce a moderate deterioration in the fit of the model to these data (see especially the result for the lung).

A key route for testing and refining these models further can be found in the final columns of Tables 4.4a and 4.4b. As mentioned earlier, McKelvey and Zemaitis (1986) did not make glutathione measurments in muscle or skin tissue, but because the volume of the muscle group is so large, our models suggest that an appreciable portion of ethylene oxide metabolism takes place there, and the amount of depression of glutathione levels as a function of dose should be readily observable.

4.1.5 Comparison of the Model Predictions to the Hemoglobin Adduct Data of Osterman-Golkar et al. (1983)

As discussed in Section 3.3.1 (pp. 49-50 above) these data from intraperitoneal injection of low doses of ethylene oxide show an internal inconsistency in the ratio of blood concentration X time to administered dose of about 50%. I therefore believe they should be given less weight in judging the models than the data covered in the previous sections, which appear to have less experimental error. Nevertheless, Table 4.5a and 4.5b compare the predictions of the different models with these observations in the same format as was used earlier for the absorption/exhalation and the glutathione depletion data.

It can be seen in Table 4.5 that all of the models come within about 25% of predicting the effective blood concentration X time observed at the lower of the two doses of Osterman-Golkar et al. (1983). On the other hand, they all predict larger blood concentration X time values than observed for the higher intraperitoneal dose--by amounts ranging from 25% to 75%. The data are marginally more compatible with the model based on the "T*" set of partition coefficients. These data also give some support for retaining models based on relatively low blood/air partition coefficients as part of a sensitivity analysis. In my judgment, however, they are not sufficient to overcome the presumption that the most likely value is about 90 on the basis of the direct measurement of this parameter for human blood by Brugnone et al. (1986).

Table 4.5
Blood and Tissue Concentration X Time Expected For Different Models After Intraperitoneal Injections of Low Doses of Ethylene Oxide --Comparison with the Data of Osterman-Golkar et al., (1983)

Micromoles Injected	Micromoles Exhaled	--Tissue Concentration X Time Internal Dose-- (Mole/Liter)-Minutes X 10^{-6} Liver	Vessel-Rich Group	Lung	Blood
Observations					
.6925	Not Measured	Not Meas.	Not Meas.	Not Meas.	64.4
5.1	Not Measured	Not Meas.	Not Meas.	Not Meas.	311
Model G3-BL90 (Blood/Air = 90, k_1 = .43, k_2 = 80)					
.6925	.1026	59.76	45.96	84.30	79.59
5.1	.7580	441.5	339.7	623.0	588.2
Model G3-BL67.6 (Blood/Air = 67.6, k_1 = .42, k_2 = 92)					
.6925	.1193	52.69	39.04	71.82	68.04
5.1	.8815	389.2	288.5	530.6	502.8
Model G3-BL90-TBL1 (Blood/Air = 90 but all tissue/blood partition coefficients are set at 1 except for the fat group, k_1 = .44, k_2 = 55)					
.6925		86.94	64.64	66.13	66.76
5.1	.6088	642.2	477.7	488.8	493.4
Model G4-BL90 (Blood/Air = 90, k_1 = .33, k_2 = 91, breathing rate jumps to .133 l/minute immediately after exposure)					
.6925	.1035	54.25	40.66	74.78	70.71
5.1	.7640	400.5	300.3	552.3	522.2
Model G3-BL90-LV* [Blood/Air = 90, rate constant for reaction of glutathione with ETO in the liver is set at twice the value for other tissues, k_1 = .4, k_2 = 130 (liver) or 65 (other tissues)]					
.6925	.09304	53.73	42.58	77.82	73.45
5.1	.6884	397.5	315.1	575.8	543.5
Model G3-BL50-LV* [Blood/Air = 50, rate constant for reaction of glutathione with ETO in the liver is set at twice the value for other tissues, k_1 = .395, k_2 = 172 (liver) or 86 (other tissues)]					
.6925	.1289	40.99	29.98	55.07	52.44
5.1	.9533	303.2	221.8	407.4	387.9
Model G3-BL90-T*-LV* [Blood/Air = 90, tissue/blood partition coefficients are the new set presented in the last line of Table 3.11 (with liver set equal to kidney, but fat maintained at its original value of .44); additionally, the rate constant for reaction of glutathione with ETO in the liver is set at twice the value for other tissues, k_1 = .42, k_2 = 110 (liver) or 55 (other tissues)]					
.6925	.08169	61.96	48.29	56.21	66.20
5.1	.6045	458.3	357.3	416.0	489.9

4.1.6 Summary of Tentative Conclusions from the Fit of the Rat Model Variants to Three Types of Data

The results of the modeling to this point are relatively encouraging. All of the data have been accommodated within an overall model structure with only modest needs for ad hoc adaptations of assumptions. The following conclusions are indicated:

- o There is a firm conclusion from the Tyler and McKelvey (1983) data that rat alveolar ventilation rates decline markedly at higher ethylene oxide exposure levels. Moreover, using the declines in alveolar ventilation rates calculated from these data, we obtain glutathione depletion in different tissues that are at least in the ballpark of what was observed by McKelvey and Zemaitis (1986).

- o The latter data suggest a slight adaptation of the original assumptions in the form of a two-fold larger rate constant for the reaction of ethylene oxide with glutathione in the liver, as compared to other tissues. If in fact this is an enzyme-catalyzed, rather than a passive process (as is further indicated by the results in Section 4.2 below) such a difference between the liver and other tissues would not be at all surprising. Indeed, for an enzyme-catalyzed detoxificiation reaction, one might generally expect such differences to be considerably larger than this.

- o The glutathione depletion data are marginally more compatible with models based on the original set of tissue/blood partition coefficients than with the "T*" set.

- o The hemoglobin adduct formation data are marginally more compatible with models based on relatively low values of the blood/air partition coefficient, and with the "T*" set of tissue/blood partition coefficients. The internal variability of these data however, indicates that these last conclusions should carry relatively small weight in the overall analysis.

4.2 Articulation of the Human Model

4.2.1 Construction of Human Model Variants

Table 4.6 gives the equations for the basic human model.

As was discussed in Section 3.3.2 the primary data that are available for constructing the basic human model and model variants are the absorption and exhalation data of Brugnone et al. (1985) and, of course, the measurement of the human blood/air partition coefficient of Brugnone et al. (1986). These data are most directly applicable for setting the "k_2" constants for the rate of reaction between ethylene oxide and tissue glutathione/other sulfhydryls--and k_2 is the only "adjustable" parameter that can be fit to the human data in the construction of the model variants.

Other details of the human model variants needed to be determined either with the aid of exogenous human data (e.g. alveolar ventilation rates, blood flows, and tissue volumes as discussed in Section 3.1) or by projection from rat data (e.g. tissue glutathione levels and rates of turnover, as discussed in Section 3.5). Lacking any very high dose observations that would provide a basis for a direct assessment of the degree of depletion of glutathione in human tissues, I also needed to project the value of k_1 (the fraction of ethylene oxide metabolism accounted for by direct reaction with glutathione) from rats. I did this by associating each human model variant with one of the rat model variants, and using the k_1 derived in the rat model directly in the corresponding human model. The details of this correspondence are included in the footnote at the bottom of Table 4.7, described in Section

Table 4.6
Equations for the Basic Human Model (GSH3)

□ ARTERIAL_BLOOD = ARTERIAL_BLOOD - VRG_PERFUSION - LIVER_PERFUSION + LUNG_OUTPUT - FG_PERFUSION - MG_PERFUSION
INIT(ARTERIAL_BLOOD) = 0

□ BLOOD_CXT = BLOOD_CXT + BLOOD_DOSE_RATE
INIT(BLOOD_CXT) = 0 {initial value...}

□ FG = FG + FG_PERFUSION - FG_ELIMINATION
INIT(FG) = 0

□ LIVER = LIVER + LIVER_PERFUSION - LIVER_ELIMINATION - LIVER_METABOLISM
INIT(LIVER) = 0

□ LIVER_CXT = LIVER_CXT + LIVER_CONC
INIT(LIVER_CXT) = 0{initial value...}

□ LUNG = LUNG - LUNG_OUTPUT + LUNG_PERFUSION + INFLOW - LUNG_METABOLISM - EXHALATION
INIT(LUNG) = 0

□ LUNG_GSH = LUNG_GSH + LUNG_GSH_GEN - LUNG_GSH_LOSS
INIT(LUNG_GSH) = 4.76E-4 {464 G OF LUNG AT 1.025 MICROMOLES/G}

□ L_GSH = L_GSH - L_GSH_LOSS + L_GSH_GEN
INIT(L_GSH) = 1.055E-2 {Moles/liter. Equal to 2476 g liver tissue at 4.26 micromoles per gram, after McKelvey and Zemaitis.}

□ MG = MG + MG_PERFUSION - MG_ELIMINATION - MG_METABOLISM
INIT(MG) = 0

□ MIXED_VENOUS = MIXED_VENOUS + VRG_ELIMINATION + LIVER_ELIMINATION LUNG_PERFUSION + FG_ELIMINATION + MG_ELIMINATION
INIT(MIXED_VENOUS) = 0

□ M_GSH = M_GSH - M_GSH_LOSS + M_GSH_GEN
INIT(M_GSH) = 2.61E-2 {34,756 G MUSCLE GROUP TISSUE AT .75 MICROMOLES/G}{BASAL RATE DATA FROM GRIFFITH AND MEISTER, 1979}

□ RECOVERY = RECOVERY + EXHALATION
INIT(RECOVERY) = 0 {initial value...}

□ TOTAL_ABSORPTION = TOTAL_ABSORPTION + ABSORPTION
INIT(TOTAL_ABSORPTION) = 0 {initial value...}

□ TOTAL_METABOLISM = TOTAL_METABOLISM + LIVER_METABOLISM + MG_METABOLISM + LUNG_METABOLISM + VRG_METABOLISM
INIT(TOTAL_METABOLISM) = 0 {initial value...}

□ VRG = VRG + VRG_PERFUSION - VRG_ELIMINATION - VRG_METABOLISM
INIT(VRG) = 0

□ VRG_CXT = VRG_CXT + VRG_CONC
INIT(VRG_CXT) = 0{initial value...}

□ VRG_GSH = VRG_GSH + VRG_GSH_GEN - VRG_GSH_LOSS
INIT(VRG_GSH) = 6.53E-3 {3551 g at about 1.84 micromoles per gram. THE 3.551 LITER VOLUME USED HERE IS THE ORIGINAL VRG VOLUME OF 6.037 LESS THE LUNG VOLUME OF .464 AND THE ARTERIAL AND VENOUS BLOOD POOL VOLUMES OF .674 AND 1.348 LITERS }

○ ABSORPTION = IF (INFLOW > 0) THEN INFLOW ELSE 0

○ ALVBLOOD_CONC = BLOOD_AIR*(CARDIAC_OUTPUT*VEN_CONC + V_ALV *(EXPOSURE *10^(-6)/25.45))/(CARDIAC_OUTPUT*BLOOD_AIR +V_ALV) { MOLES/LITER}

○ ART_BLOOD_VOL = .674 {LITERS} {ARTERIAL BLOOD VOLUME}

○ BLOOD_AIR = 90

○ BLOOD_DOSE_RATE = (MIXED_VENOUS + ARTERIAL_BLOOD)/(ART_BLOOD_VOL + VENOUS_BLOOD) {CALCULATES TOTAL BLOOD CONCENTRATION}

○ CARDIAC_OUTPUT = VRG_FLOW + LIVER_FLOW + MG_FLOW + FG_FLOW { liters/minute}

○ EXHALATION = IF (VEN_CONC > ALVBLOOD_CONC) THEN CARDIAC_OUTPUT*(VEN_CONC - ALVBLOOD_CONC) ELSE 0

Table 4.6, continued
Equations for the Basic Human Model (GSH3)

- EXPOSURE = IF (TIME≤90) THEN 1.09 ELSE IF (TIME≤150) THEN 1.18 ELSE IF (TIME≤210) THEN 2.61 ELSE IF (TIME≤270) THEN 1.75 ELSE IF (TIME≤330) THEN 1.61 ELSE IF (TIME≤390) THEN 1.62 ELSE IF (TIME≤450) THEN 1.78 ELSE IF (TIME≤480) THEN 2.91 ELSE 0 (ppm)
- FG_ELIMINATION = (FG * FG_FLOW) / (15.024 * .44) {moles/minute} {FG/BLOOD = .44 BASED ON OIL/WATER SOLUBILITY RATIO OBSERVED BY CHAIGNEAU} { ([FG_BLOOD] * ƒF[FG]) / (ƒV[FG] * ƒL[FG\BLOOD]) }
- FG_FLOW = .69 {liters/minute. This is the usual value during activity of .59 plus .1 l/minute to compensate for the absence of the vessel poor group in this model.}
- FG_PERFUSION = ARTERIAL_BLOOD * FG_FLOW / ART_BLOOD_VOL {moles/minute} { [ARTERIAL_BLOOD] * ƒF[FG] / ƒV[arterial blood] }
- FRACT_ABSORB = IF (INFLOW ≥ 0) THEN INFLOW / (V_ALV * EXPOSURE * 10 ^(-6)/25.45) ELSE 0
- INFLOW = IF (ALVBLOOD_CONC > VEN_CONC) THEN CARDIAC_OUTPUT*(ALVBLOOD_CONC - VEN_CONC) ELSE 0 {MOLES/MIN}
- LIVER_CONC = LIVER/2.476{MOLES/LITER}
- LIVER_ELIMINATION = (LIVER * LIVER_FLOW) / (2.476 * .6){moles/minute} { (LIVER * ƒF[LIVER]) / (ƒV[liver] * ƒL[LIVER\BLOOD]) }
- LIVER_EXTRACTION = 1 - LIVER_ELIMINATION/LIVER_PERFUSION {Dimensionless, includes any net storage of ethylene oxide in the liver.}
- LIVER_FLOW = 1.224 {liter/minute}
- LIVER_METABOLISM = (17.1)*(LIVER)*(L_GSH/2.476) {BASIC SECOND ORDER RATE EQUATION.}
- LIVER_PERFUSION = ARTERIAL_BLOOD * LIVER_FLOW / ART_BLOOD_VOL {moles/minute} { ƒF[LIVER] * ARTERIAL_BLOOD / ƒV[arterial blood] }
- LUNG_GSH_GEN = .02*4.76e-4 {moles/min. Rate constant scaled from rat value (divided by (70/.25)^.75)}
- LUNG_GSH_LOSS = .02*LUNG_GSH +.43*LUNG_METABOLISM {liters/min. Assumes, as in rats, that glutathione accounts for about 43% of total tissue reaction with ethylene oxide.}
- LUNG_METABOLISM = 17.1*(LUNG)*(LUNG_GSH/.464)
- LUNG_OUTPUT = LUNG * CARDIAC_OUTPUT /(.464*1.07) {moles/minute} { [LUNG] * CARDIAC_OUTPUT / ƒV[lung] The current equation uses the volume of the lung only, without special inclusion of blood in the lung.}
- LUNG_PERFUSION = MIXED_VENOUS * CARDIAC_OUTPUT / VENOUS_BLOOD {moles/minute} { MIXED_VENOUS * CARDIAC_OUTPUT / ƒV[venous blood] }
- L_GSH_GEN = (6.1e-4)*1.055e-2 {Turnover rate scaled from rat data--see lung}
- L_GSH_LOSS = 6.1e-4*L_GSH + .43*LIVER_METABOLISM {MOLES/MIN. GSH ACCOUNTS FOR 40% OF LIVER METABOLISM. }
- MET_RATE = VRG_METABOLISM + LIVER_METABOLISM + MG_METABOLISM + LUNG_METABOLISM {MOLES/MIN}
- MG_ELIMINATION = (MG * MG_FLOW) / (34.756 * .47) {moles/minute} { ([MG] * ƒF[MG]) / (ƒV[MG] * ƒL[MG\BLOOD]) }
- MG_EXTRACTION = 1 - MG_ELIMINATION/MG_PERFUSION
- MG_FLOW = 2.61 {liter/minute}
- MG_METABOLISM = (17.1)*(M_GSH)*(MG/34.756) {BASIC SECOND ORDER RATE EQUATION.}
- MG_PERFUSION = ARTERIAL_BLOOD * MG_FLOW / ART_BLOOD_VOL {moles/minute}

Table 4.6, continued
Equations for the Basic Human Model (GSH3)

- M_GSH_GEN = (3.4e-4)*2.61e-2 {Scaled from rat--see lung explanation.}
- M_GSH_LOSS = (3.4e-4)*M_GSH + .43*MG_METABOLISM
- VENOUS_BLOOD = 1.348 {LITERS}
  {MIXED VENOUS BLOOD VOLUME}
- VEN_CONC = MIXED_VENOUS/VENOUS_BLOOD {MOLES/LITER}
- VRG_CONC = VRG/3.551 {MOLES/L}
- VRG_ELIMINATION = (VRG * VRG_FLOW) / (3.551 * .595)
  {moles/minute}
  { VRG * ƒF[VRG] / ƒV[VRG blood] * ƒL[VRG\BLOOD] }
- VRG_EXTRACTION = 1 - VRG_ELIMINATION/VRG_PERFUSION
- VRG_FLOW = 3.87 {liter/minute}
- VRG_GSH_GEN = .003*6.53e-3 {Turnover rate is high, after kidney as measured by Griffith and Meister is small 100 g rats, even though the VRG contains many tissues with much lower turnover rates.}
- VRG_GSH_LOSS = .43*VRG_METABOLISM + .003*VRG_GSH
- VRG_METABOLISM = 17.1*(VRG)*(VRG_GSH/3.551) {Basic bimolecular reaction kinetics.}
- VRG_PERFUSION = ARTERIAL_BLOOD * VRG_FLOW / ART_BLOOD_VOL
  {moles/minute}
  { ƒF[VRG] * ARTERIAL_BLOOD / ƒV[arterial blood] }
- V_ALV = 11.38 {liters/minute}

4.2.2 below.

4.2.2 The Fit of Different Human Model Variants to the Absorption Data of Brugnone et al. (1985)

To arrive at the human metabolism rate constant (k_2) and to compare the fit of the different human model variants, I elected to adopt a more quantitative procedure than was needed for the rat data. This procedure was patterned after the least-squares fitting approach that is a standard part of regression analysis. As can be seen in Table 3.13 (page 51 above) I had available eight hourly measurements of the percentage absorption of ethylene oxide from alveolar air. For each model variant and each trial of a value of k_2, I produced a series of 8 hourly "predictions" of the percentage absorbed from the alveoli. I then summed the square of each difference between "predicted" and observed data. As an alternative procedure, I assumed that the data from 3-8 hours represented fluctuations about what was actually a constant near equilibrium level. For the alternative comparisons I therefore substituted 75.0 for the actual hourly levels observed in the third through the eighth hours.

Table 4.7 shows the resulting fits of the different model variants to the data, assuming that the exposure of the workers can be represented as a constant low level throughout the day. This would be appropriate if the differences in air exposure levels seen at different times in Table 3.13 were primarily momentary fluctuations*, or had a large component of

---

*The environmental air measurements were based on instantaneous grab samples from the workers' breathing zones, done in parallel with the alveolar air sampling.

Table 4.7
Comparison of the Best Fit of Various Human Models to the Observations of Brugnone et al. (1985) on the Percentage Absorption of Ethylene Oxide From Alveolar Air in Workers*

Comparisons Based on Constant Exposure of Models to a Constant 1 ppm

Time (hr)	Observed % Abs.	% Absorption Expected For Different Models: GSH3	GSH4	GSH3-TBL1	GSH3-LV*	GSH3BL50-LV*	GSH3-T*-LV*
1	84.9	82.99	80.97	86.59	82.97	79.81	85.08
2	78.0	77.48	77.34	80.43	77.78	77.75	79.34
3	75.0	76.23	76.49	76.90	75.91	77.47	76.65
4	71.0	75.61	76.29	74.87	75.23	77.43	75.39
5	74.9	75.39	76.24	73.71	74.98	77.42	74.80
6	75.7	75.32	76.23	73.04	74.89	77.42	74.52
7	76.3	75.29	76.22	72.65	74.86	77.42	74.39
8	76.3	75.28	76.22	72.43	74.84	77.42	74.33
3-8 Ave	75.0	75.52	76.28	73.93	75.11	77.43	75.01
Dif^2		29.1	48.2	64.1	27.4	85.2	32.8
(sum of squared differences from actual observations)							
$Dif^{2'}$		6.22	25.8	30.0	4.71	61.4	5.79

(sum of squared differences, assuming the 3-8 hour observations were all at the average value of 75)

---

*Explanation of model terminology:

GSH3--Patterned after the rat model G3BL90. Blood/air partition coefficient is 90, k_1 = .43, k_2 = 18.

GSH4--Patterned after the rat model G3BL67.6. Blood/air partition coefficient is 67.6, k_1 = .42, k_2 = 25

GSH3-TBL1--Patterned after the rat model G3BL90-TBL1. Blood/air partition coefficient is 90, but all tissue/blood partition coefficients (except fat) are set at 1; k_1 = .44, k_2 = 8.

GSH3-LV*--Patterned after the rat model G3BL90-LV*. Blood/air partition coefficient is 90, rate constant for reaction of glutathione with ETO in the liver is set at twice the value for other tissues, k_1 = .4, k_2 = 28 (liver) or 14 (other tissues).

GSH3BL50-LV*--Patterned after the rat model G3BL50-LV*. Blood/air partition coefficient is 50, rate constant for reaction of glutathione with ETO in the liver is set at twice the value for other tissues, k_1 = .395, k_2 = 58 (liver) or 29 (other tissues).

GSH3-T*-LV*--Patterned after the rat model G3BL90-T*-LV*. Blood/air partition coefficient is 90, but the tissue/blood partition coefficients are the "T*" set described on pages 45-46 above. The rate constant for reaction of glutathione with ETO in the liver is set at twice the value for other tissues, k_1 = .42, k_2 = 19.8 (liver) or 9.9 (other tissues).

Table 4.8
Comparison of Model Fits, Using An Alternative Interpretation of the Brugnone et al. (1985) Data*

Comparisons Based on Measured Changes in Exposures, Assumed to Occur at the Midpoints Between Hourly Observations

		---------% Absorption Expected For Different Models---------					
Time (hr)	Observed % Abs.	GSH3	GSH4	GSH3-TBL1	GSH3-LV*	GSH3BL50-LV*	GSH3-T*-LV*
1	84.9	82.72	80.42		82.74	78.60	84.98
2	78.0	78.24	77.11	Not	78.14	76.55	79.92
3	75.0	82.60	81.16	done	82.55	79.86	84.00
4	71.0	72.02	72.04		71.79	72.67	73.00
5	74.9	72.24	73.27		71.91	74.32	71.94
6	75.7	73.68	74.64		73.36	75.35	72.98
7	76.3	75.38	75.90		75.10	76.16	74.87
8	76.3	79.97	79.33		79.82	78.59	80.39
Dif^2		89.08	73.01		90.56	73.92	123.6

(sum of squared differences from actual observations)

---

*Explanation of model terminology (note the small differences in the best-fitting values of k_2 in comparison to those in Table 4.7):

GSH3--Patterned after the rat model G3BL90. Blood/air partition coefficient is 90, k_1 = .43, k_2 = 17.1.

GSH4--Patterned after the rat model G3BL67.6. Blood/air partition coefficient is 67.6, k_1 = .42, k_2 = 24.2.

GSH3-LV*--Patterned after the rat model G3BL90-LV*. Blood/air partition coefficient is 90, rate constant for reaction of glutathione with ETO in the liver is set at twice the value for other tissues, k_1 = .4, k_2 = 26.8 (liver) or 13.4 (other tissues).

GSH3BL50-LV*--Patterned after the rat model G3BL50-LV*. Blood/air partition coefficient is 50, rate constant for reaction of glutathione with ETO in the liver is set at twice the value for other tissues, k_1 = .395, k_2 = 58 (liver) or 29 (other tissues).

GSH3-T*-LV*--Patterned after the rat model G3BL90-T*-LV*. Blood/air partition coefficient is 90, but the tissue/blood partition coefficients are the "T*" set described on pages 45-46 above. The rate constant for reaction of glutathione with ETO in the liver is set at twice the value for other tissues, k_1 = .42, k_2 = 19.2 (liver) or 9.6 (other tissues).

experimental error, and for the most part did not reflect true variations in average hourly exposure. The fits using an alternative assumption--that true exposures varied in a stepwise fashion in parallel with the average environmental measurements recorded for each hour in Table 3.13--are shown in Table 4.8 (for this latter intepretation the step changes in exposures were placed at the midpoints between the hourly readings).

Drawing substantive conclusions from these comparisons would have been much more straightforward if I had not thought to do the latter set of comparisons shown in Table 4.8. The comparisons in Table 4.7 strongly suggest that the Brugnone et al. (1985) observations are much more compatible with models incorporating a blood/air partition coefficient of 90 [as Brugnone et al. (1986) actually measured] than with models incorporating blood/air partition coefficients of 67.4 ("GSH4") or 50 ("GSH3BL50-LV*"). This is because the models with the lower blood/air partition coefficients approach equilibrium much more rapidly than is indicated by the progression of first-hour absorption of about 85% and second-hour absorption of 78%. Given a blood/air partition coefficient of 90, these data also indicate a very marginal advantage in the fit of models with the original set of tissue/blood partition coefficients, and against models with the "T*" coefficients.

The comparisons in Table 4.8 seem to tell a different story, however. Here the rapidity with which the models with lower blood/air partition coefficients approach equilibrium causes them to show lesser fluctuations in predicted % absorption in response to the fluctuations in exposure suggested by the raw air sampling data. This is particularly true for the point taken at the third hour after the start of exposure. Here the

environmental measurements (p. 51) suggest that a nearly twofold increase had just taken place in average exposure, as compared with the previous hour. If the increase were actually this extreme, the slower-equilibrating models with a blood/air partition coefficient of 90 indicate that the percentage absorbed should have increased, rather than falling slightly as the absorption data show. The models with lower partition coefficients predict smaller increases, giving them an edge on this point and the point at 8 hours, where a similar increase in the average exposures is reflected in the raw data.

Because of regression-to-the-mean effects, measurement errors and very short term fluctuations will tend to cause the actual fluctuations in environmental air concentrations to be overstated in data of this sort. Just how large the overstatement might be, however, is difficult to assess by readily available techniques. (This might be a good subject of future statistical method development.) My judgment is that the comparisons in Table 4.7 are likely to be closer to revealing the truth about blood/air partition coefficients, but clearly in the light of the alternative interpretation of Table 4.8, blood/air partition coefficients as low as 50 cannot be said to be excluded by these data.

4.2.3 Comparisons With the Hemoglobin Adduct Data of Calleman et al. (1978)

As was discussed in Section 3.3.2 (pp. 55-7 above), these data show great variability, and there is reason to doubt the precision of the exposure measurements. Nevertheless the data in Table 3.15 provide

another possible point of comparison with the human model variants.

To do this comparison, however, I need to mention one key set of interpretive assumptions--that is that hemoglobin adducts are stable *in vivo* and that the red cells carrying them have a conventional life time of 18 weeks. Under these conditions, as discussed by Calleman et al. (1978), the average red cell should be 9 weeks old, and therefore have 9 weeks of accumulated exposure to whatever average concentration of ethylene oxide has been available in the blood during that period. Following these assumptions, the data in the last column of Table 3.15 indicate that each ppm-hour of exposure should give rise to the following integral of blood concentration X time:

$$\frac{[.002 \text{ to } .0092 \text{ (nmol/g Hb-ppm-hour)/9 weeks}]}{.14 \times 10^{-4} \text{ 1/g Hb-hour}}$$

$$= 16 \text{ to } 73 \times 10^{-9} \text{ (moles/liter)-hour in blood/ppm-hour in air}$$

Calleman et al. (1978) make a similar calculation in their Table 3, providing an average value of 44×10^{-9} (moles/liter)-hour in blood per ppm hour in air. For an eight-hour day, these figures translate into an average of 2.1×10^{-5} (moles/liter)-minutes per ppm-day of exposure, with a range of 7.6×10^{-6} to 3.5×10^{-5} for the five individuals studied.

The predictions of the different human models for the blood concentration X time for every 8 hours of worker exposure to 1 ppm in air are shown in Table 4.9. It can be seen that the average concentration X time inferred from the observations of Calleman et al. (1978) is ten to twenty times less than the predictions of the various models. The

Table 4.9
Concentration X Time of Ethylene Oxide in the Blood
Predicted by the Different Human Model Variants

For One-Day 8 Hour Exposures to 1 ppm ETO in Air

Model	Blood Concentration X Time
GSH3	4.067×10^{-4}
GSH4	2.984×10^{-4}
GSH3-TBL1	4.608×10^{-4}
GSH3-LV*	4.143×10^{-4}
GSH3BL50-LV*	2.139×10^{-4}
GSH3-T*-LV*	4.239×10^{-4}

predictions of the models themselves differ by only about two-fold, indicating that uncertainties in my assumptions of partition coefficients or liver metabolism in relation to metabolism elsewhere in the body make relatively little difference to the results. Clearly something is seriously wrong either with the alveolar absorption observations of Brugnone et al. (1985) that were used to calibrate the metabolism rates in the human models, or with the exposure measurements and assumptions of adduct/red cell persistence used to interpret the hemoglobin adduct measurements of Calleman et al. (1978).

If the exposure/hemoglobin adduct observations of Calleman et al. (1978) were to prove correct, this would indicate that the current models appreciably understate the rate of metabolism of ethylene oxide in humans. This would lead to overestimation of the average persistence of ethylene oxide in the body and overstatement of the resulting tissue concentration X time (and, ultimately, cancer risks) by the indicated 10-20 fold or so.

I can imagine one way in which the Brugnone et al. (1985) measurements could be misleading. That is if they do not truly represent alveolar air, but instead include an appreciable contamination from the physiological "dead space" air that has not been effectively exposed to alveolar blood, and which would be expected to have a several fold higher concentration of unabsorbed ethylene oxide. The Brugnone group has been taking alveolar air samples for many years (Brugnone et al., 1980a and 1980b). In their 1986 paper, they describe their procedure as follows:

> "Air samples were collected in stoppered glass tubes with screw caps at both ends, and with an interior volume of 70 ml. Standing in the work place, and after a normal inspiration, workers forced expiration, keeping the glass tube between their lips. The tube was immediately sealed with the two caps after the end of the expiration. One instantaneous environmental air sample was collected at the same

> time as every alveolar air sampling. Instantaneous environmental samples were collected in glass tubes, similar to those used for alveolar air, by manual pump."

The theory behind this is that the air in the "dead space" of conducting airways should be expelled first, and that very little "dead space" air should be coming out by the time the last 70 ml are collected as the "alveolar" air sample. On its face, this seems to be a reasonable procedure, but I know of no actual test of just how much admixture of dead space air might be contained in the "alveolar air" sampled in this way. Because of the uncertainties in the exposure estimates and other interpretive assumptions in the paper of Calleman et al. (1978), I believe this discrepancy should tentatively be resolved in favor of the observations of Brugnone et al. (1985), and the human model variants should stand as they are. Other research groups are now in the process of measuring hemoglobin adducts and exposure in workers (Frederica Perera, personal communication). The predictions of the models based on the Brugnone et al. (1985) data are that each day's exposure should produce much more hemoglobin adducts than found by Calleman et al. (1978). To avoid possible accelerated loss of red cells or hemoglobin adducts in vivo it would be best to do such measurements on new non-smoking workers just beginning their exposure to ethylene oxide.

4.3 Articulation of the Mouse Model

4.3.1 Calculation of "k2" for the Mouse Model Variants from Hemoglobin Alkylation Data

The equations for the basic mouse model (M-G3BL90) are reproduced in Table 4.10.

As for the human model variants, the lack of relatively high-dose absorption and exhalation data prevents us from making an independent assessment of "k_1" (the fraction of ethylene oxide metabolism accounted for by direct reaction with glutathione). Therefore, as before, the k_1 values for the corresponding rat model variants were used in the mouse models.

The "k_2" metabolism rates for the mouse model variants were set to correspond approximately at low doses to the average of the three lowest-dose hemoglobin alkylation observations recorded in Table 3.17. To represent intraperitoneal injection, a low dose of 2.175×10^{-7} moles of ethylene oxide (coresponding to 8.7 umole/kg, after the lower dose experiment of Segerback, 1983) was introduced into the livers of the model mice, and the blood concentration X time ultimately produced was observed. The level of k_2 was adjusted until the model mice showed a target blood concentration X time of about 8.7 umoles/kg * 1.23×10^{-5} (moles/liter)-min/(umole/kg) = 1.07×10^{-4} umoles/min. Table 4.11 shows the fits of the different model variants to this value, and the long term

Table 4.10
Equations for the Basic Mouse Model (M-G3BL90)

□ ARTERIAL_BLOOD = ARTERIAL_BLOOD - VRG_PERFUSION - LIVER_PERFUSION + LUNG_OUTPUT - FG_PERFUSION - MG_PERFUSION
INIT(ARTERIAL_BLOOD) = 0

□ BLOOD_CXT = BLOOD_CXT + BLOOD_DOSE_RATE
INIT(BLOOD_CXT) = 0 {initial value...}

□ BLOOD_GSH = BLOOD_GSH + BLOOD_GSH_GEN - BLOOD_GSH_LOSS
INIT(BLOOD_GSH) = 4.464E-7 {.72 ML AT .62 MICROMOLES PER ML. NOTE: OTHER BLOOD IS INCLUDED WITH THE VOLUMES OF VARIOUS ORGANS.}

□ FG = FG + FG_PERFUSION - FG_ELIMINATION
INIT(FG) = 0

□ LIVER = LIVER + LIVER_PERFUSION - LIVER_ELIMINATION - LIVER_METABOLISM
INIT(LIVER) = 0

□ LIVER_CXT = LIVER_CXT + LIVER_CONC
INIT(LIVER_CXT) = 0 {initial value...}

□ LUNG = LUNG - LUNG_OUTPUT + LUNG_PERFUSION + INFLOW - LUNG_METABOLISM - EXHALATION
INIT(LUNG) = 0

□ LUNG_CXT = LUNG_CXT + LUNG_CONC
INIT(LUNG_CXT) = 0 {initial value...}

□ LUNG_GSH = LUNG_GSH + LUNG_GSH_GEN - LUNG_GSH_LOSS
INIT(LUNG_GSH) = 1.76E-7 {.15 G OF LUNG AT 1.175 MICROMOLES/G. LUNG VOLUME TAKEN AS 1/10TH RAT LUNG VOLUME}

□ L_GSH = L_GSH - L_GSH_LOSS + L_GSH_GEN
INIT(L_GSH) = 7.28E-6 {Moles. Equal to 1.5 g liver tissue at 4.855 micromoles per gram, after McKelvey and Zemaitis.}

□ MG = MG + MG_PERFUSION - MG_ELIMINATION - MG_METABOLISM
INIT(MG) = 0

□ MIXED_VENOUS = MIXED_VENOUS + VRG_ELIMINATION + LIVER_ELIMINATION LUNG_PERFUSION + FG_ELIMINATION + MG_ELIMINATION - BLOOD_METAB
INIT(MIXED_VENOUS) = 0

□ M_GSH = M_GSH - M_GSH_LOSS + M_GSH_GEN
INIT(M_GSH) = 1.365E-5 {17.5 G MUSCLE GROUP TISSUE AT .78 MICROMOLES. G}{BASAL RATE DATA FROM GRIFFITH AND MEISTER, 1979}

□ RECOVERY = RECOVERY + EXHALATION
INIT(RECOVERY) = 0 {initial value...}

□ TOTAL_ABSORPTION = TOTAL_ABSORPTION + ABSORPTION
INIT(TOTAL_ABSORPTION) = 0 {initial value...}

□ TOTAL_METABOLISM = TOTAL_METABOLISM + LIVER_METABOLISM + MG_METABOLISM + LUNG_METABOLISM + VRG_METABOLISM + BLOOD_METAB
INIT(TOTAL_METABOLISM) = 0 {initial value...}

□ VRG = VRG + VRG_PERFUSION - VRG_ELIMINATION - VRG_METABOLISM
INIT(VRG) = 0

□ VRG_CXT = VRG_CXT + VRG_CONC
INIT(VRG_CXT) = 0 {initial value...}

□ VRG_GSH = VRG_GSH + VRG_GSH_GEN - VRG_GSH_LOSS
INIT(VRG_GSH) = 2.035E-6 {initial value...} {1.1 g at about 1.85 micromoles per gram}

○ ABSORPTION = IF (INFLOW > 0) THEN INFLOW ELSE 0

○ ALV_BLOOD_CONC = BLOOD_AIR*(CARDIAC_OUTPUT*VEN_CONC + V_ALV *(EXPOSURE *10^(-6)/25.45))/(CARDIAC_OUTPUT*BLOOD_AIR +V_ALV) { MOLES/LITER}

○ ART_BLOOD_VOL = .0024 {LITERS} {ARTERIAL BLOOD VOLUME}

○ BLOOD_AIR = 90

○ BLOOD_DOSE_RATE = (MIXED_VENOUS + ARTERIAL_BLOOD)/(ART_BLOOD_VOL + VENOUS_BLOOD) {CALCULATES TOTAL BLOOD CONCENTRATION}

○ BLOOD_GSH_GEN = 4.1515E-9 {MOLES/MIN. = .0093*4.464E-7 TO BALANCE LOSS RATE AT INITIAL EQUILIBRIUM IN THE ABSENSE OF EXPOSURE.}

Table 4.10, continued
Equations for the Basic Mouse Model (M-G3BL90)

- BLOOD_GSH_LOSS = .0093*BLOOD_GSH + .43*BLOOD_METAB
  {CAVEAT: BACKGROUND "BLOOD" GSH TURNOVER TAKEN FROM GRIFFITH AND MEISTER DATA ON PLASMA. THIS MAY NOT BE APPROPRIATE, AS IT WOULD EXCLUDE RED CELL GSH.}
- BLOOD_METAB = k2*BLOOD_DOSE_RATE*BLOOD_GSH {MOLES/MIN}
- CARDIAC_OUTPUT = VRG_FLOW + LIVER_FLOW + MG_FLOW + FG_FLOW {liters/minute}
- EXHALATION = IF (VEN_CONC > ALV_BLOOD_CONC) THEN CARDIAC_OUTPUT*(VEN_CONC - ALV_BLOOD_CONC) ELSE 0
- EXPOSURE = IF (TIME < 240) THEN 900 ELSE 0
- FG_ELIMINATION = (FG * FG_FLOW) / (.0025 * .44)
  {moles/minute} {FG/BLOOD = .44 BASED ON OIL/WATER SOLUBILITY RATIO OBSERVED BY CHAIGNEAU}
  { ([FG_BLOOD] * fF[FG]) / (fV[FG] * fL[FG\BLOOD]) }
- FG_FLOW = .00171 {liters/minute}
- FG_PERFUSION = ARTERIAL_BLOOD * FG_FLOW / ART_BLOOD_VOL
  {moles/minute}
  { [ARTERIAL_BLOOD] * fF[FG] / fV[arterial blood] }
- FRACT_ABSORB = IF (INFLOW ≥ 0) THEN
  INFLOW / (V_ALV * EXPOSURE * 10 ^(-6)/25.45) ELSE 0
- INFLOW = IF (ALV_BLOOD_CONC > VEN_CONC) THEN CARDIAC_OUTPUT*(ALV_BLOOD_CONC - VEN_CONC) ELSE 0 {MOLES/MIN}
- k2 = 135 {statement goes here...}
- LIVER_CONC = LIVER/.0015 {MOLES/LITER}
- LIVER_ELIMINATION = (LIVER * LIVER_FLOW) / (.0015 * .6)
  {moles/minute}
  { (LIVER * fF[LIVER]) / (fV[liver] * fL[LIVER\BLOOD]) }
- LIVER_FLOW = .00475 {liter/minute}
- LIVER_METABOLISM = k2*(LIVER)*(L_GSH/.0015) {BASIC SECOND ORDER RATE EQUATION.}
- LIVER_PERFUSION = ARTERIAL_BLOOD * LIVER_FLOW / ART_BLOOD_VOL
  {moles/minute}
  { fF[LIVER] * ARTERIAL_BLOOD / fV[arterial blood] }
- LUNG_CONC = LUNG/.00015 {MOLES/LITER}
- LUNG_GSH_GEN = 1.056E-9{EQUAL TO .006*1.76E-7 TO BALANCE LOSS AT INITIAL EQUILIBRIUM.}
- LUNG_GSH_LOSS = .006*LUNG_GSH +.43*LUNG_METABOLISM { T1/2 OF less than 2 HOURS, (M&Z DATA) 2 hr corresponds to .006. CAVEAT: DIRECT MEASUREMENTS BY GRIFFITH AND MEISTER SUGGEST TENFOLD LESS--5.7E-4
- LUNG_METABOLISM = k2*(LUNG)*(LUNG_GSH/.00015)
- LUNG_OUTPUT = LUNG * CARDIAC_OUTPUT /(.00015*1.07)
  {moles/minute}
  { [LUNG] * CARDIAC_OUTPUT / fV[lung blood] }
- LUNG_PERFUSION = MIXED_VENOUS * CARDIAC_OUTPUT / VENOUS_BLOOD
  {moles/minute}
  { MIXED_VENOUS * CARDIAC_OUTPUT / fV[venous blood] }
- L_GSH_GEN =.0088*7.28E-6
- L_GSH_LOSS = .0088*L_GSH + .43*LIVER_METABOLISM {MOLES/MIN.}
- MG_ELIMINATION = (MG * MG_FLOW) / (.0175 * .47)
  {moles/minute}
  { ([MG] * fF[MG]) / (fV[MG] * fL[MG\BLOOD]) }
- MG_FLOW = .00285 {liter/minute}
- MG_METABOLISM = k2*(M_GSH)*(MG/.0175) {BASIC SECOND ORDER RATE EQUATION.}
- MG_PERFUSION = ARTERIAL_BLOOD * MG_FLOW / ART_BLOOD_VOL {moles/minute}

Table 4.10, continued
Equations for the Basic Mouse Model (M-G3BL90)

- M_GSH_GEN = 4.641e-8{Moles/min. Equal to .0034*1.365E-5--turnover rate taken from Griffith and Meister, 1979}
- M_GSH_LOSS = .0034*M_GSH + .43*MG_METABOLISM
- VENOUS_BLOOD = .0048 {LITERS}
  {MIXED VENOUS BLOOD VOLUME}
- VEN_CONC = MIXED_VENOUS/VENOUS_BLOOD {MOLES/LITER}
- VRG_CONC = VRG/.0011 {MOLES/LITER}
- VRG_ELIMINATION = (VRG * VRG_FLOW) / (.0011 * .595)
  {moles/minute}{ VRG * ƒF[VRG] / ƒV[VRG blood] * ƒL[VRG\BLOOD] }{New value of .0011 for the volume of vrg is the old value of .00125 less .00015 for lung tissue.}
- VRG_FLOW = .00969 {liter/minute}
- VRG_GSH_GEN = 2.89e-8{Moles/min. = .0142*2.035E-6. Turnover rate is high, after kidney as measured by Griffith and Meister, even though the VRG contains many tissues with much lower turnover rates.}
- VRG_GSH_LOSS = .43*VRG_METABOLISM + .0142*VRG_GSH
- VRG_METABOLISM = k2*(VRG)*(VRG_GSH/.0011) {Basic bimolecular reaction kinetics.}
- VRG_PERFUSION = ARTERIAL_BLOOD * VRG_FLOW / ART_BLOOD_VOL
  {moles/minute}
  { ƒF[VRG] * ARTERIAL_BLOOD / ƒV[arterial blood] }
- V_ALV = .016 {liters/min.}

elimination half-lives indicated by the data*. The low-dose alveolar ventilation rates are derived in the following section.

4.3.2 Derivation of Low-Dose Alveolar Ventilation Rates for the Mouse Model from the Data of Ehrenberg et al. (1974)

The primary Ehrenberg et al. (1974) absorption data were reproduced in Table 3.16 (p. 58 above). Using the k_2 metabolism rate determined in the previous section, and incorporating a pattern of change in exposure levels reproducing the decline reported by Ehrenberg et al. 1974) for their closed-chamber experiments, I determined the alveolar ventilation rate that would give the reported absorption in each of the seven trials. Because the underlying data on absorption per ppm-min of exposure are quite variable, the calculated alveolar ventilation rates differed appreciably from trial to trial (see example in Table 4.12). Moreover, unlike the primary data in rats, these mouse data did not directly indicate any reduction in alveolar ventilation rates at the higher levels, although the data only go up to about 50 ppm. Therefore for exposure

---

*These elimination half lives were calculated by monitoring the concentration of ethylene oxide in the models' venous blood for pairs of time points beginning about 30 minutes after the end of exposure. The overall elimination constant (k_{el}) was found as

$$k_{el} = \frac{\ln(C_2/C_1)}{T_2 - T_1}$$

where C_2 and C_1 are the ethylene oxide concentrations in venous blood at time 2 and time 1 respectively. Then the elimination half life was calculated as:

$$T_{1/2} = (\ln 2)/k_{el}$$

Table 4.11
Ethylene Oxide Metabolism and Overall Long Term Elimination Rates
For Different Mouse Model Variants

.2175 umoles of Ethylene Oxide Delivered Directly to the Liver of the Model Mice at the Start of the Simulation

Model*	Alveolar Ventilation (l/min)	Final k_2	ETO Exhaled (umoles)	Blood C X T (umoles/l) -minutes	Elimination $T_{1/2}$ (minutes)
M-G3BL90	.0376	135	.0437	106.1	6.16
M-G3BL90-LV*	.0376	200/100	.0413	100.3	6.43
M-G3BL50-LV*	.0573	130/65	.1043	94.6	6.14
M-G3BL90-T*LV*	.0371	150/75	.0412	93.2	8.11

---

*See Table 4.3b on p. 85 for model terminology.

**For the "LV*" models the higher number represents the k_2 in the liver, and the other number represents the k_2 in other tissues.

Table 4.12
Model M-G3BL90--Derivation of Low Dose Alveolar Ventilation Rates from the Absorption Data of Ehrenberg et al. (1974)

Ave ppm (exposure range)*	time (min.)	ppm-min	absorption (umoles per 25g of mouse)	implied alv. vent. (l/min.)
1.15 (2.2 - .1)	75	86.25	.1125	.0504
3.5 (7 - 0)	107	374.5	.375	.0317
6.5 (9.7 - 3.3)	60	390	.3	.0224
6.5 (10 - 3)	75	487.5	.75	.0550
7.4 (9.7 - 5.1)	60	444	.325	.0213
29 (35 - 23)	82	2378	2.5	.033
33 (57 - 9)	75	2475	3.5	.0497
			AVERAGE	.0376

---

*During the period of exposure, the concentration of ethylene oxide in the chamber declined (reportedly approximately linearly) from the higher to the lower level given in the parentheses. In the modeling this was represented by an equation of the form:

EXPOSURE (ppm) = IF TIME LESS THAN [EXPOSURE PERIOD] THEN [HIGHEST EXPOSURE LEVEL]*(1 - TIME/[CONSTANT]) ELSE 0

where the "constant" was determined to give the desired range of exposures during the exposure period.

levels up to about 50 ppm I elected to use the average values determined by this procedure for each model.

For exposure levels of 100 ppm and above (see next section) I elected to assume that mice would decrease their alveolar ventilation rates to the same degree as was determined for the corresponding rat models in section 4.1. This is probably conservative, because in a number of cases in the past, such as formaldehyde, mice have tended to reduce their breathing rates as a function of dose to a greater extent than mice. Additionally, if mice really had no reduction in alveolar ventilation rates, the modeling suggests that McKelvey and Zemaitis (1986) would have observed a much larger reduction in tissue glutathione levels than they did.

One final point that should be noted is that the alveolar ventilation rate required to fit these absorption data is relatively high (57 ml/minute) if the blood/air partition coefficient is as low as 50. For comparison, Arms and Travis (1986) have recommended the use of 25 to 29 ml/minute as reference alveolar ventilation rates for pharmacokinetic modeling for mice. The highest of four measurements they cite of absolute minute volumes of unanesthetized mice is 52 ml/minute--which, with physiological dead space at 33%, would translate into an alveolar ventilation rate of only about 35 ml/minute. Therefore these data cast some doubt on the proposition that the blood/air partition coefficient could be as low as 50.

4.3.3 The Fit of the Models to the McKelvey and Zemaitis (1986) Data on Changes in Mouse Tissue Glutathione Levels

Given the assumptions listed above, Table 4.13 shows the predictions of the different models for the depression of glutathione levels immediately following four hour exposures of mice to various high doses of ethylene oxide. In this case it appears that the best overall correspondence is with the T*-LV* model, although the differences from the BL50-LV* and BL90-LV* models are not very great. The original G3-BL90 model appears farthest from the mark. This gives some additional support for the twofold increase in metabolism rates per glutathione level in the liver relative to other tissues.

4.4 Overall Conclusions From the Fit of the Models to Various Sets of Data

In general there should be considerable comfort in the conclusion that rat (and very probably mouse) alveolar ventilation rates must decline at higher levels of exposure to ethylene oxide.

With somewhat less certainty, I conclude that it is likely that the reaction between ethylene oxide and glutathione is not simply a passive bimolecular reaction, but is catalyzed by one or more enzymes. In parallel with the determination of differences in the k_2 "constant" (Table 4.14), there appears to be greater activity of metabolizing enzyme(s) in liver relative to other tissues, and in rodent tissues relative to human tissues. If the reaction were passive, k_2 should be

Table 4.13
Depletion of Glutathione in Mouse Tissues Immediately After 4 Hour Exposures To Various Concentrations of Ethylene Oxide

ppm (4 hrs)	Alveolar Ventilation (l/min)	----Percentage of Basal Glutathione Levels---- Blood	Lung	Vessel-Rich Group	Liver
Observations					
100	Not Measured	91.3	78.1	Incomplete	80.7
450	Not Measured	50.4	35.5	Incomplete	41.3
900	Not Measured	39.8	14.1	About 77	16.3
Model M-G3-BL90 (Blood/Air = 90, k_1 = .43, k_2 = 135)					
100	.029	70.9	60.8	85.3	80.9
450	.0201	30.7	20.8	53.0	43.2
900	.0160	13.6	8.5	29.1	20.8
Model M-G3-BL90-LV* [Bloood/Air = 90, rate constant for reaction of glutathione with ETO in the liver is set at twice the value for other tissues, k_1 = .4, k_2 = 130 (liver) or 65 (other tissues)]					
100	.0294	78.2	69.9	89.3	75.7
450	.0204	39.9	28.7	62.4	35.2
900	.0163	19.6	12.6	38.8	16.2
Model M-G3-BL50-LV* [Bloood/Air = 50, rate constant for reaction of glutathione with ETO in the liver is set at twice the value for other tissues, k_1 = .395, k_2 = 172 (liver) or 86 (other tissues)]					
100	.0435	80.2	72.8	90.6	77.4
450	.0304	44.2	32.8	66.5	39.0
900	.0243	25.2	16.8	46.4	21.1
Model M-G3-BL90-T*-LV* [Bloood/Air = 90, tissue/blood partition coefficients are the new set presented in the last line of Table 3.11 (p. 45) (with liver set equal to kidney, but fat maintained at its original value of .44); additionally, the rate constant for reaction of glutathione with ETO in the liver is set at twice the value for other tissues, k_1 = .42, k_2 = 110 (liver) or 55 (other tissues)]					
100	.029	82.3	79.5	89.6	76.2
450	.0202	46.9	41.4	63.1	36.0
900	.016	24.6	20.1	39.7	16.8

Table 4.14
Apparent Differences in k_2

Model Series (named for rat model)	Values of k_2*		
	Mouse	Rat	Human
G3BL90 (plain vanilla)	135	80	18
G3BL90-LV* (2X increase in liver metabolism)	200 (liver) 100 (elsewhere)	130 (liver) 65 (elsewhere)	28 (liver) 14 (elsewhere)
G3BL50-LV* (Blood/air of 50, 2X increase in liver metabolism)	130 (liver) 65 (elsewhere)	172 (liver) 86 (elsewhere)	58 (liver) 29 (elsewhere)
G3BL90-LV*-T* (T* set of tissue/blood partition coefficients, 2X increase in liver metabolism)	150 (liver) 75 (elsewhere)	110 (liver) 55 (elsewhere)	19.8 (liver) 9.9 (other)

---

*The units of k_2 are "fraction of tissue ethylene oxide metabolized per minute per mole per liter of tissue glutathione concentration".

uniform across tissues and species. Particularly if the blood/air partition coefficient is 90, the only way the human k_2 values could be comparable with the rodent k_2 values is if the Brugnone et al. (1985) measurements of alveolar absorption were grossly affected by contamination with air from the respiratory "dead space". Additional data relevant to this issue will be discussed in Section 5.1 below. However, although the interspecies difference in k_2 is quite significant for determining risk, the precise allocation of ethylene oxide metabolism among the tissues (e.g. the "vanilla" vs. "LV*"models) makes almost no difference in the final calculation of human internal dosage and therefore human risk (see Table 4.9).

Third, although in some cases the modeling data appear somewhat more consistent with a blood/air partition coefficient of 90 than one of 50, the latter cannot be firmly excluded based on existing information.

Finally, the data provide little basis to choose between the original set of tissue/blood partition coefficients and the "T*" set. However, as was seen in Table 4.9 and will be illustrated further in Section 5, the differences in sets of tissue/blood partition coefficients produce almost no change in the ultimate predicted doses delivered to animal and human tissues. Even the major difference between a blood/air partition coefficient of 90 and one of 50 makes only about a two-fold difference in the projected concentration X time dose to human blood. Therefore in the following section I will only do full risk projections for the "BL90LV*" and "BL50LV*" series of models.

5. CONCLUSIONS--INTERSPECIES COMPARISON OF THE CONCENTRATION X TIME PRODUCT OF ETHYLENE OXIDE IN THE BLOOD--AND IMPLICATIONS FOR HUMAN RISK

5.1 Interspecies Comparison of Metabolism and Estimated Tissue Doses

Table 4.14 on page 118 has already compared the metabolism of different species in terms of our "k_2" model parameter. A related comparison whose implications may be more readily understandable is of long-term elimination half-lives for ethylene oxide in the body after low dose* exposures (Table 5.1). Other things being equal, the longer it takes to eliminate the average molecule of ethylene oxide from the body, the greater the internal dose (expressed in units of concentration X time) and the more opportunity there will be for reaction with DNA.

It can be seen in Table 5.1 that all of the series of models indicate that ethylene oxide is eliminated much more slowly in humans than in rats or mice--suggesting that per mole of absorbed dose, one should expect a greater concentration X time of ethylene oxide to be available in humans. Table 5.2 shows the results of putting these data into the standard allometric scaling equation (Adolf, 1949):

$$T_{1/2} = K\ (\text{Body Weight})^m$$

---

*At higher doses, where glutathione is appreciably depleted, ethylene oxide will be eliminated more slowly (longer half-life). The low-dose calculations for Table 5.1 were generally based on exposures to 1 ppm in humans, 11 ppm in rats, or simulated intraperitoneal injection of 2.175×10^{-7} moles of ethylene oxide in mice. None of the models shows appreciable depletion of glutathione under these conditions, nor is there any difference between inhalation and intraperitoneal exposure in the elimination half life calculated by observing the long term decline in ethlyene oxide concentrations in venous blood.

Table 5.1
Apparent Differences in Low Dose Elimination Half-Lives ($T_{1/2}$)
for Ethylene Oxide In Different Species

Model Series (named for rat model)	Values of $T_{1/2}$ (min.) Mouse	Rat	Human
G3BL90 (plain vanilla)	6.16	8.84	39.6
G3BL90-LV* (2X increase in liver metabolism)	6.43	9.21	40.8
G3BL50-LV* (Blood/air of 50, 2X increase in liver metabolism)	6.14	6.84	22.1
G3BL90-LV*-T* (T* set of tissue/blood partition coefficients, 2X increase in liver metabolism)	8.11	11.52	54.8

Table 5.2
Allometric Scaling Equations for Elimination Half-Lives for Ethylene Oxide In Different Species

Model Series named for rat model)	Regression Coefficients* log K	m	r	Predicted $T_{1/2}$ for 17.5 Kg Dogs
G3BL90 (plain vanilla)	1.14	.240	.9948	27.5 min.
G3BL90-LV* (2X increase in liver metabolism)	1.16	.239	.9949	28.4 min.
G3BL50-LV* (Blood/air of 50, 2X increase in liver metabolism)	1.01	.170	.9781	16.6 min.
G3BL90-LV*-T* (T* set of tissue/blood partition coefficients, 2X increase in liver metabolism)	1.27	.247	.9937	37.5 min.

---

*For the equation, $\log(T_{1/2}) = m \log(\text{Body Weight})$

For the models with a blood/air partition coefficient of 90, there are excellent linear fits. Moreover the m's that result are very close to the scaling factor of 1/4 that would be expected if, according to the theory of Boxenbaum (1982), elimination rates for chemicals tend to scale with metabolic energy density (metabolic rates per unit of mass).

The conclusion that the elimination half life for ethylene oxide in humans is longer than in rodents differs markedly from the conclusion of Calleman et al. (1978) who inferred from their data that the elimination half-life in humans was similar to that in mice. I have already discussed (pp. 55-7 and 102-106 above) the reasons why the human models were based on the absorption data of Brugnone et al. (1985) rather than the hemoglobin adduct data of Calleman et al. (1978). There is, however, an additional set of data relevant to this issue that has not been used up until this point. Martis et al. (1982) measured the clearance of ethylene oxide from plasma in four 17-19 kg dogs following intravenous administration of each of two doses--75 or 25 mg/kg. At the higher dose level he measured an average elimination half life of 36.5 +/- 18.5 (SD) min., while at the lower dose level the average half life measured was 29.3 +/- 5.7 min. As can be seen in the last column of Table 5.2 the latter result at the lower dose is in good agreement with the half life predicted from the mouse, rat, and human model results using the allometric equation for my "best estimate" G3BL90-LV* series of models. This strenthens the conclusion that the longer elimination half life predicted by the human model is likely to be correct.

Table 5.3 shows the implications of the models for the overall internal dosage that can be expected in humans for brief exposures to relatively low air levels of ethylene oxide. It can be seen that because

Table 5.3

Expected Blood and Tissue Doses Following
5 Minute Exposures of Different Species to 1 ppm Ethlene Oxide

Best Estimate Models*

Species	----------Absorption-------- (Moles/kg)	(Moles/kg$\cdot^{75}$)	Blood C X T (Moles/l)-min
Human	3.13×10^{-8}	9.04×10^{-8}	4.36×10^{-6}
Rat	8.53×10^{-8}	6.03×10^{-8}	2.57×10^{-6}
Mouse	2.74×10^{-7}	1.09×10^{-7}	3.77×10^{-6}

The names of these models are: Human--GSH3-LV; Rat--g3BL90-LV*; and Mouse--Mg3BL90-LV*. In all three models, the "LV*" designation indicates that the rate constant for metabolism in the liver has been set at a level twice that in other tissues (to better conform to observations of glutathione depletion in different tissues).

**This is the ultimate amount exhaled by several hours after the 5 minute exposures--after all ethylene oxide absorbed has been disposed of either through metabolism/reaction or exhalation. The approximate half lives of ethylene oxide in the three species are: Human--41 minutes; Rat--9.2 minutes; Mouse--6.4 minutes.

humans breathe less per unit of body weight, they absorb substantially less than mice or rats per body weight. This lower absorption rate per body weight almost exactly offsets the longer elimination half life, so that the models indicate that the three species will experience quite a similar internal concentration X time from a given low external air level X time.

5.2 Risk Assessment for Human Occupational Exposures

There is a substantial body of data available on the carcinogenic response of rats and mice to ethylene oxide. In both species, for several different organs significant excesses of tumors have been observed in groups exposed to ethylene oxide compared to controls.

Below (Section 5.2.1) I will first show the delivered dosages implied by the different pharmacokinetic models for the rodent carcinogenesis bioassays. Then (Section 5.2.2) I will derive the animal dose response relationships by standard procedures, using (1) the delivered dose measures implied by the pharmacokinetic models (2) net absorption of ethylene oxide [analogous to the approach used in an earlier risk assessment by EPA (1985)] and (3) raw ppm X time external exposures. Next (Section 5.2.3) I will compare the predictions for human occupational risk for these three approaches for defining dose, and draw inferences about the appropriate interspecies scaling of cancer risk for ethylene oxide. Finally (Section 5.2.4) I will show the implications of the models for different time patterns of human external exposure.

5.2.1 Measures of Delivered "Dose" for the Rodent Carcinogenesis Bioassays

For rats, there are two separate experiments available--one by Snellings et al. (1984) using 6 hour/day, 5 day/week exposures for both males and females--and one by Lynch et al. (1984) using 7 hour per day exposures for males only. Table 5.4 shows the net absorption of ethylene oxide and the tissue concentration X time predictions of the various models for the Snellings et al. (1984) rat bioassay, Table 5.5 shows similar information for two models for the Lynch (1984) rat bioassay, and Table 5.6 provides delivered dosage for the recent NTP (1987) mouse bioassay.

It can be seen in Tables 5.4 and 5.6 that there are relatively modest differences in the predictions of the different models. Because of this, I will simplify the subsequent discussion by confining the analysis to the "best estimate" G3BL90-LV* series of models and the models with a reduced blood/air partition coefficient of 50. The latter model, by predicting somewhat lower delivered (Concentration X Time) doses in the animal experiments will lead to a larger estimate of the potency of ethylene oxide. As will become apparent later, however, this effect will be offset when we turn to the ultimate human risk projection, because the expected human delivered doses are also reduced in relation to environmental exposure levels. Under these conditions, retaining the G3BL50-LV* series of models in the analysis merely provides some sense of the sensitivity of the conclusions to different assumptions about the blood/air partition coefficient.

Table 5.4
Daily* Net Absorption and Tissue C X T Doses Predicted by the Different Models for the Snellings et al. (1984) Rat Carcinogenesis Bioassays

ppm (6 hrs)	Alveolar Ventilation (l/min)	Net Absorption During Exposure (umoles/day)	Tissue Doses (umoles/liter)-minutes/day* Liver	Vessel-Rich Group	Blood
Model G3-BL90 (Blood/Air = 90, k_1 = .43, k_2 = 80)					
10	.117	13.94	1,139	1,203	1,965
33	.1035	41.34	3,453	3,638	5,947
100	.09	110.4	9,750	10,220	16,740
Model G3-BL90-LV* [Bloood/Air = 90, rate constant for reaction of glutathione with ETO in the liver is set at twice the value for other tissues, k_1 = .4, k_2 = 130 (liver) or 65 (other tissues)]					
10	.115	13.82	1,036	1,152	1,871
33	.1015	40.86	3,148	3,481	5,661
100	.09	110.8	9,168	10,020	16,330
Model G3-BL50-LV* [Bloood/Air = 50, rate constant for reaction of glutathione with ETO in the liver is set at twice the value for other tissues, k_1 = .395, k_2 = 172 (liver) or 86 (other tissues)]					
10	.125	13.82	797	914	1,473
33	.110	41.06	2,432	2,773	4,474
100	.095	109.5	6,958	7,817	12,650
Model G3-BL90-T*-LV* [Bloood/Air = 90, tissue/blood partition coefficients are the new set presented in the last line of Table 3.11, p. 45 (with liver set equal to kidney, but fat maintained at its original value of .44); additionally, the rate constant for reaction of glutathione with ETO in the liver is set at twice the value for other tissues, k_1 = .42, k_2 = 110 (liver) or 55 (other tissues)]					
10	.112	13.74	1,136	1,280	1,643
33	.0998	40.91	3,472	3,894	5,001
100	.0875	109.7	9,976	11,050	14,240

---

*These are the expected delivered doses for the five days per week that the animals were exposed.

Table 5.5
Daily* Net Absorption and Tissue C X T Doses Predicted by the Different Models for the Lynch et al. (1984) Rat Carcinogenesis Bioassays

ppm (7 hrs)	Alveolar Ventilation (l/min)	Net Absorption During Exposure (umoles/day)	Tissue Doses (umoles/liter)-minutes/day* Liver	Vessel-Rich Group	Blood
Model G3-BL90-LV* [Bloood/Air = 90, rate constant for reaction of glutathione with ETO in the liver is set at twice the value for other tissues, k_1 = .4, k_2 = 130 (liver) or 65 (other tissues)]					
50	.0975	69.53	5,501	6,056	9,857
100	.09	129.0	10,830	11,800	19,250
Model G3-BL50-LV* [Bloood/Air = 50, rate constant for reaction of glutathione with ETO in the liver is set at twice the value for other tissues, k_1 = .395, k_2 = 172 (liver) or 86 (other tissues)]					
50	.104	69.09	4,201	4,763	7,693
100	.095	127.4	8,211	9,119	14,890

---

*These are the expected delivered doses for the five days per week that the animals were exposed.

Table 5.6
Blood and Tissue C X T Doses Predicted by the Different Models for the Daily Exposures Used in the Mouse Carcinogenesis Bioassays

ppm (6 hrs)	Alveolar Ventilation (l/min)	Net Absorption During Exposure (umoles/day)	Tissue Doses (umoles/liter)-minutes/day* Liver	Vessel-Rich Group	Blood
Model M-G3-BL90 (Blood/Air = 90, k_1 = .43, k_2 = 135)					
50	.0376	20.30	8,322	9,038	14,730
100	.029	32.73	14,400	15,540	25,390
Model M-G3-BL90-LV* [Bloood/Air = 90, rate constant for reaction of glutathione with ETO in the liver is set at twice the value for other tissues, k_1 = .4, k_2 = 130 (liver) or 65 (other tissues)]					
50	.0376	20.35	7,922	9,016	14,630
100	.0294	33.14	13,930	15,670	25,500
Model M-G3-BL50-LV* [Bloood/Air = 50, rate constant for reaction of glutathione with ETO in the liver is set at twice the value for other tissues, k_1 = .395, k_2 = 172 (liver) or 86 (other tissues)]					
50	.0573	18.42	10,690	11,640	19,090
100	.0435	31.29	19,540	21,100	34,680
Model M-G3-BL90-T*-LV* [Bloood/Air = 90, tissue/blood partition coefficients are the new set presented in the last line of Table 3.11 (p. 45) (with liver set equal to kidney, but fat maintained at its original value of .44); additionally, the rate constant for reaction of glutathione with ETO in the liver is set at twice the value for other tissues, k_1 = .42, k_2 = 110 (liver) or 55 (other tissues)]					
50	.0371	20.18	9,869	11,240	14,470
100	.029	32.84	17,330	19,520	25,210

---

*These are the expected delivered doses for the five days per week that the animals were exposed.

I will also simplify the subsequent analysis by including only blood dosage, excluding the liver and VRG data. If one divides the liver and VRG doses by the blood doses in Tables 5.4 and 5.6 it can be seen that the ratios of tissue dose to blood dose are always expected to be relatively constant in the dose range used for the bioassays. For example for the Snellings rats and NTP Mice in the LV* series of models one obtains:

	Ratio of Liver to Blood C X T Doses	Ratio of VRG to Blood C X T Doses
Snellings Rats		
10 ppm	.554	.616
33 ppm	.556	.615
100 ppm	.561	.614
NTP Mice		
50 ppm	.541	.616
100 ppm	.546	.614

As it happens, the different tissues all eliminate a relatively small proportion of the ethylene oxide on each passage of blood through from the arterial to the venous circulation, and therefore tissue doses in relation to blood doses depend primarily on the tissue/blood partition coefficient. If metabolism were a more important factor in determining tissue dose, and if there were major depletion of glutathione (and hence slowed metabolism) in specific tissues at doses within the range studied in the bioassays, this result would have been different and it might have been informative to investigate the tumor response of specific organs in relation to the predicted C X T dosage in those same organs. However, with the proportions of tissue and blood doses being so consistent at different exposure levels, one might as well use the blood dose as a proxy for the

relevant tissue doses for simplicity.

5.2.2 Measures of "Dose" and Dose Response Relationships for Carcinogenesis in Animals

The detailed analytical tables beginning on the following page (Tables 5.7 through 5.22) are divided into two parts. The upper portions of the tables juxtapose the raw animal tumor bioassay results observed in the various studies with different measures of external exposure or internal dose. The lower portions of these tables show the results of using the alternative measures of dose in standard multistage carcinogenesis risk projections using Howe and Crump's (1982) "Global82" computer program*. In these tables, the blood concentration X time dosages given in Tables 5.4 through 5.6 have been further transformed to "equivalent continuous ethylene oxide concentration" in micromoles per liter. (To do this, the numbers in the parent tables were divided by 1440 minutes per day and multiplied by 5/7 to represent the five days of exposure per week.) I believe that this measure provides the simplest comparison of delivered dosage across species and time patterns of exposure.

---

*This program calculates maximum likelihood estimates (MLE) for the "q" coefficients in the equation:

$$P(d) = 1 - e^{-(q_0 + q_1 d + q_2 d^2 + \ldots q_k d^k)}$$

Where P(d) is the expected tumor incidence at a particular dose (d). The "q_0" term determines the background tumor incidence, the "q_1" determines the size of the linear dose response term, and q_k's determine the contributions of higher powers of dose. The program also calculates sets of "q" coefficients for predicting upper 95% confidence limits on induced tumor incidence (UCL), based solely on statistical sampling-error uncertainties in the experimental data. All the "q" coefficients are constrained to be positive or zero.

Table 5.7
Leukemias in Male Fischer 344 Rats in the Study of Lynch et al., 1984

CAVEAT: THE APPARENT EXCESS OF THIS TUMOR IN THIS SEX WAS EVALUATED BY EPA (1985) AS NOT STATISTICALLY SIGNIFICANT. ON THE OTHER HAND, THE RESULTS ARE ALSO COMPATIBLE WITH AN INTERPRETATION OF EQUAL CARCINOGENIC POTENCY AS OBSERVED IN FEMALE RATS (SEE TABLE 5.9).

A. Alternative Expressions of "Dose" and Tumor Response:

Animals and Exposure Level	Net Absorption (umoles per day of exposure) BL90 model	Equivalent Contin. Blood ETO Conc. umoles/liter BL90 model	BL50 model	----Observed Incidence	Tumor Response---- "hits"* animal	"excess hits" animal **
Control	0	0	0	24/77	.374	-
50 ppm	69.53	4.89	3.82	38/79	.656	.282
100 ppm	129.0	9.55	7.38	30/76	.502	.128

B. Use of Alternative Expressions of Dose in Global82 Multistage Dose Response Modeling:

Expression for "Dose"		Model Coefficients q_0	q_1	q_2	Measures of Model Fit "chi^2"	degrees freedom	P *****
ppm in air	MLE***	.429	.00155	0	3.47	1	.05 - .1
	UCL****	.344	.00384	-			
Net Absorption umoles/day BL90 model	MLE	.422	.00129	0	3.26	1	.05 - .1
	UCL	.337	.00303				
Equiv. Contin. ETO Blood Conc. umoles per liter, BL90 (Best estimate model)	MLE	.427	.0166	0	3.41	1	.05 - .1
	UCL	.342	.0405				
Equiv. Contin. ETO Bood Conc. umoles per liter, BL50 (Alternative model)	MLE	.426	.0217	0	3.37	1	.05 - .1
	UCL	.341	.0525				

---

*See p. 147 below for notes to these tables.

Table 5.8
Leukemias in Male Fischer 344 Rats in the Study of Snellings et al., 1984

CAVEAT: THE APPARENT EXCESS OF THIS TUMOR IN THIS SEX WAS EVALUATED BY EPA (1985) AS NOT STATISTICALLY SIGNIFICANT. ON THE OTHER HAND, THE RESULTS ARE ALSO COMPATIBLE WITH AN INTERPRETATION OF EQUAL CARCINOGENIC POTENCY AS OBSERVED IN FEMALE RATS (SEE TABLE 5.9).

A. Alternative Expressions of "Dose" and Tumor Response:

Animals and Exposure Level	Net Absorption (umoles per day of exposure) BL90 model	Equivalent Contin. Blood ETO Conc. umoles/liter BL90 model	BL50 model	----Observed Tumor Incidence	Response---- "hits"* animal	"excess hits" animal **
Control	0	0	0	38/234	.177	-
10 ppm	13.82	.928	.731	21/79	.309	.132
33 ppm	40.86	2.81	2.22	25/81	.369	.192
100 ppm	110.8	8.10	6.27	26/119	.247	.070

B. Use of Alternative Expressions of Dose in Global82 Multistage Dose Response Modeling:

Note: Because of the poor fit of models to the data including the highest dose point (chi^2 over eight, P less than .02) the following results have been obtained after excluding the highest dose point:

Expression for "Dose"		Model Coefficients q_0	q_1	q_2	Measures of Model Fit "chi^2"	degrees freedom	P *****
ppm in air	MLE***	.187	.00638	0	1.13	1	.2 - .5
	UCL****	.168	.0108	-			
Net Absorption umoles/day BL90 model	MLE	.185	.00518	0	.90	1	.2 - .5
	UCL	.166	.00870	-			
Equiv. Contin. ETO Blood Conc. umoles per liter, BL90 (Best estimate model)	MLE	.185	.0752	0	.95	1	.2 - .5
	UCL	.166	.127	-			
Equiv. Contin. ETO Bood Conc. umoles per liter, BL50 (Alternative model)	MLE	.186	.0952	0	.96	1	.2 - .5
	UCL	.167	.160	-			

---

*See p. 147 below for notes to these tables.

Table 5.9
Leukemias in Female Fischer 344 Rats
in the Study of Snellings et al., 1984

A. Alternative Expressions of "Dose" and Tumor Response:

Animals and Exposure Level	Net Absorption (umoles per day of exposure) BL90 model	Equivalent Contin. Blood ETO Conc. umoles/liter BL90 model	BL50 model	----Observed Tumor Response---- Incidence	"hits"* animal	"excess hits" animal **
Control	0	0	0	22/186	.126	-
10 ppm	13.82	.928	.731	14/71	.220	.094
33 ppm	40.86	2.81	2.22	24/72	.405	.280
100 ppm	110.8	8.10	6.27	28/73	.484	.357

B. Use of Alternative Expressions of Dose in Global82 Multistage Dose Response Modeling:

Expression for "Dose"		Model Coefficients q_0	q_1	q_2	Measures of Model Fit "chi^2"	degrees freedom	P *****
ppm in air	MLE***	.147	.00427	0	4.32	2	.1 - .2
	UCL****	.129	.00610	-			
Net Absorption umoles/day BL90 model	MLE	.142	.00386	0	3.35	2	.1 - .2
	UCL	.124	.00546	-			
Equiv. Contin. ETO Blood Conc. umoles per liter, BL90 (Best estimate model)	MLE	.144	.0529	0	3.85	2	.1 - .2
	UCL	.126	.0751	-			
Equiv. Contin. ETO Bood Conc. umoles per liter, BL50 (Alternative model)	MLE	.144	.0683	0	3.69	2	.1 - .2
	UCL	.126	.0969	-			

---

*See p. 147 below for notes to these tables.

Table 5.10
Peritoneal Mesotheliomas in Male Fischer 344 Rats
in the Study of Lynch et al., 1984

A. Alternative Expressions of "Dose" and Tumor Response:

Animals and Exposure Level	Net Absorption (umoles per day of exposure) BL90 model	Equivalent Contin. Blood ETO Conc. umoles/liter BL90 model	BL50 model	----Observed Tumor Incidence	Response---- "hits"* animal	"excess hits" animal **
Control	0	0	0	3/78	.039	-
50 ppm	69.53	4.89	3.82	9/79	.121	.082
100 ppm	129.0	9.55	7.38	21/79	.309	.270

B. Use of Alternative Expressions of Dose in Global82 Multistage Dose Response Modeling:

Expression for "Dose"		Model Coefficients q_0	q_1	q_2	Measures of Model Fit "chi^2"	degrees freedom	P *****
ppm in air	MLE***	.039	5.71E-4	2.13E-5	No test possible--no		
	UCL****	.027	.00321	-	degrees of freedom		
Net Absorption umoles/day BL90 model	MLE	.039	1.05E-4	1.54E-5	No test possible--no		
	UCL	.028	.00236	-	degrees of freedom		
Equiv. Contin. ETO Blood Conc. umoles per liter, BL90 (Best estimate model)	MLE	.039	.00461	.00248	No test possible--no		
	UCL	.027	.0331	-	degrees of freedom		
Equiv. Contin. ETO Bood Conc. umoles per liter, BL50 (Alternative model)	MLE	.039	.00513	.00426	No test possible--no		
	UCL	.027	.0426	-	degrees of freedom		

---

*See p. 147 below for notes to these tables.

Table 5.11
Peritoneal Mesotheliomas in Male Fischer 344 Rats
in the Study of Snellings et al., 1984

A. Alternative Expressions of "Dose" and Tumor Response:

Animals and Exposure Level	Net Absorption (umoles per day of exposure) BL90 model	Equivalent Contin. Blood ETO Conc. umoles/liter BL90 model	BL50 model	----Observed Tumor Response---- Incidence	"hits"* animal	"excess hits" animal **
Control	0	0	0	4/187	.022	-
10 ppm	13.82	.928	.731	3/88	.035	.013
33 ppm	40.86	2.81	2.22	7/82	.089	.068
100 ppm	110.8	8.10	6.27	22/96	.260	.239

B. Use of Alternative Expressions of Dose in Global82 Multistage Dose Response Modeling:

Expression for "Dose"		Model Coefficients q_0	q_1	q_2	Measures of Model Fit "chi^2"	degrees freedom	P *****
ppm in air	MLE***	.021	.00171	6.84E-6	.06	1	over .5
	UCL****	.016	.00316	-			
Net Absorption umoles/day BL90 model	MLE	.021	.00119	8.90E-6	.07	1	over .5
	UCL	.016	.00270	-			
Equiv. Contin. ETO Blood Conc. umoles per liter, BL90 (Best estimate model)	MLE	.021	.0187	.00136	.08	1	over .5
	UCL	.016	.0380	-			
Equiv. Contin. ETO Bood Conc. umoles per liter, BL50 (Alternative model)	MLE	.021	.0232	.00242	.07	1	over .5
	UCL	.016	.0487	-			

---

*See p. 147 below for notes to these tables.

Table 5.12
Brain Tumors in Male Fischer 344 Rats in the Study of Lynch et al., 1984

A. Alternative Expressions of "Dose" and Tumor Response:

Animals and Exposure Level	Net Absorption (umoles per day of exposure) BL90 model	Equivalent Contin. Blood ETO Conc. umoles/liter BL90 model	BL50 model	----Observed Tumor Response---- Incidence	"hits"* animal	"excess hits" animal **
Control	0	0	0	0/76	0	-
50 ppm	69.53	4.89	3.82	2/77	.026	.026
100 ppm	129.0	9.55	7.38	5/79	.065	.065

B. Use of Alternative Expressions of Dose in Global82 Multistage Dose Response Modeling:

Expression for "Dose"		Model Coefficients q_0	q_1	q_2	Measures of Model Fit "chi^2"	degrees freedom	P *****
ppm in air	MLE***	0	3.99E-4	2.55E-6	No test possible--no		
	UCL****	0	.00107	-	degrees of freedom		
Net Absorption umoles/day BL90 model	MLE	0	2.28E-4	2.16E-6	No test possible--no		
	UCL	0	8.02E-4	-	degrees of freedom		
Equiv. Contin. ETO Blood Conc. umoles per liter, BL90 (Best estimate model)	MLE	0	.00384	3.14E-4	No test possible--no		
	UCL	0	.0111	-	degrees of freedom		
Equiv. Contin. ETO Bood Conc. umoles per liter, BL50 (Alternative model)	MLE	0	.00478	5.53E-4	No test possible--no		
	UCL	0	.0143	-	degrees of freedom		

---

*See p. 147 below for notes to these tables.

Table 5.13
Brain Tumors in Male Fischer 344 Rats
in the Study of Snellings et al., 1984

A. Alternative Expressions of "Dose" and Tumor Response:

Animals and Exposure Level	Net Absorption (umoles per day of exposure) BL90 model	Equivalent Contin. Blood ETO Conc. umoles/liter BL90 model	BL50 model	----Observed Tumor Incidence	Response---- "hits"* animal	"excess hits" animal **
Control	0	0	0	1/181	.0055	-
10 ppm	13.82	.928	.731	1/92	.011	.005
33 ppm	40.86	2.81	2.22	5/85	.061	.055
100 ppm	110.8	8.10	6.27	7/87	.084	.078

B. Use of Alternative Expressions of Dose in Global82 Multistage Dose Response Modeling:

Expression for "Dose"		Model Coefficients q_0	q_1	q_2	Measures of Model Fit "chi^2"	degrees freedom	P *****
ppm in air	MLE***	.0059	9.54E-4	0	1.55	2	.2 - .5
	UCL****	.0040	.00155	-			
Net Absorption umoles/day BL90 model	MLE	.0055	8.35E-4	0	1.28	2	over .5
	UCL	.0038	.00134	-			
Equiv. Contin. ETO Blood Conc. umoles per liter, BL90 (Best estimate model)	MLE	.0057	.0116	0	1.44	2	.2 - .5
	UCL	.0039	.0188	-			
Equiv. Contin. ETO Bood Conc. umoles per liter, BL50 (Alternative model)	MLE	.0056	.0149	0	1.38	2	over .5
	UCL	.0039	.0241	-			

---

*See p. 147 below for notes to these tables.

Table 5.13
Brain Tumors in Male Fischer 344 Rats
in the Study of Snellings et al., 1984

A. Alternative Expressions of "Dose" and Tumor Response:

Animals and Exposure Level	Net Absorption (umoles per day of exposure) BL90 model	Equivalent Contin. Blood ETO Conc. umoles/liter BL90 model	BL50 model	----Observed Tumor Response---- Incidence	"hits"* animal	"excess hits" animal **
Control	0	0	0	1/181	.0055	-
10 ppm	13.82	.928	.731	1/92	.011	.005
33 ppm	40.86	2.81	2.22	5/85	.061	.055
100 ppm	110.8	8.10	6.27	7/87	.084	.078

B. Use of Alternative Expressions of Dose in Global82 Multistage Dose Response Modeling:

Expression for "Dose"		Model Coefficients q_0	q_1	q_2	Measures of Model Fit "chi^2"	degrees freedom	P *****
ppm in air	MLE***	.0059	9.54E-4	0	1.55	2	.2 - .5
	UCL****	.0040	.00155	-			
Net Absorption umoles/day BL90 model	MLE	.0055	8.35E-4	0	1.28	2	over .5
	UCL	.0038	.00134	-			
Equiv. Contin. ETO Blood Conc. umoles per liter, BL90 (Best estimate model)	MLE	.0057	.0116	0	1.44	2	.2 - .5
	UCL	.0039	.0188	-			
Equiv. Contin. ETO Bood Conc. umoles per liter, BL50 (Alternative model)	MLE	.0056	.0149	0	1.38	2	over .5
	UCL	.0039	.0241	-			

---

*See p. 147 below for notes to these tables.

Table 5.14
Brain Tumors in Female Fischer 344 Rats
in the Study of Snellings et al., 1984

A. Alternative Expressions of "Dose" and Tumor Response:

Animals and Exposure Level	Net Absorption (umoles per day of exposure) BL90 model	Equivalent Contin. Blood ETO Conc. umoles/liter BL90 model	BL50 model	----Observed Tumor Response---- Incidence	"hits"* animal	"excess hits" animal **
Control	0	0	0	1/188	.005	-
10 ppm	13.82	.928	.731	1/94	.011	.005
33 ppm	40.86	2.81	2.22	3/92	.033	.028
100 ppm	110.8	8.10	6.27	4/80	.051	.046

B. Use of Alternative Expressions of Dose in Global82 Multistage Dose Response Modeling:

Expression for "Dose"		Model Coefficients q_0	q_1	q_2	Measures of Model Fit "chi^2"	degrees freedom	P *****
ppm in air	MLE***	.0059	5.40E-4	0	.45	2	over .5
	UCL****	.0038	.00104	-			
Net Absorption umoles/day BL90 model	MLE	.0056	4.76E-4	0	.32	2	over .5
	UCL	.0036	9.04E-4	-			
Equiv. Contin. ETO Blood Conc. umoles per liter, BL90 (Best estimate model)	MLE	.0057	.00660	0	.39	2	over .5
	UCL	.0037	.0126	-			
Equiv. Contin. ETO Bood Conc. umoles per liter, BL50 (Alternative model)	MLE	.0057	.00849	0	.36	2	over .5
	UCL	.0037	.0162	-			

---

*See p. 147 below for notes to these tables.

Table 5.15
Malignant and Benign Lung Tumors in Male B6C3F1 Mice (NTP, 1987)
(Alveolar/Bronchiolar Carcinomas and Adenomas)

A. Alternative Expressions of "Dose" and Tumor Response:

Animals and Exposure Level	Net Absorption (umoles per day of exposure) BL90 model	Equivalent Contin. Blood ETO Conc. umoles/liter BL90 model	BL50 model	----Observed Tumor Response---- Incidence	"hits"* animal	"excess hits" animal **
Control	0	0	0	11/50	.248	-
50 ppm	20.35	7.26	9.47	19/50	.478	.230
100 ppm	33.14	12.65	17.2	26/50	.734	.486

B. Use of Alternative Expressions of Dose in Global82 Multistage Dose Response Modeling:

Expression for "Dose"		Model Coefficients q_0	q_1	q_2	Measures of Model Fit "chi^2"	degrees freedom	P *****
ppm in air	MLE***	.248	.00433	5.27E-6	No test possible--no		
	UCL****	.192	.00740	-	degrees of freedom		
Net Absorption umoles/day BL90 model	MLE	.248	.00592	2.63E-4	No test possible--no		
	UCL	.190	.0206	-	degrees of freedom		
Equiv. Contin. ETO Blood Conc. umoles per liter, BL90 (Best estimate model)	MLE	.248	.0225	.00125	No test possible--no		
	UCL	.190	.0557	-	degrees of freedom		
Equiv. Contin. ETO Bood Conc. umoles per liter, BL50 (Alternative model)	MLE	.248	.0194	5.15E-4	No test possible--no		
	UCL	.190	.0416	-	degrees of freedom		

---

*See p. 147 below for notes to these tables.

Table 5.16
Malignant and Benign Lung Tumors in Female B6C3F1 Mice (NTP, 1987)
(Alveolar/Bronchiolar Carcinomas and Adenomas)

A. Alternative Expressions of "Dose" and Tumor Response:

Animals and Exposure Level	Net Absorption (umoles per day of exposure) BL90 model	Equivalent Contin. Blood ETO Conc. umoles/liter BL90 model	BL50 model	----Observed Tumor Response---- Incidence	"hits"* animal	"excess hits" animal **
Control	0	0	0	2/49	.042	-
50 ppm	20.35	7.26	9.47	5/48	.110	.068
100 ppm	33.14	12.65	17.2	22/49	.596	.554

B. Use of Alternative Expressions of Dose in Global82 Multistage Dose Response Modeling:

Expression for "Dose"		Model Coefficients q_0	q_1	q_2	Measures of Model Fit "chi^2"	degrees freedom	P *****
ppm in air	MLE***	.034	0	5.08E-5	1.02	1	.2 - .5
	UCL****	.031	.00284	-			
Net Absorption umoles/day BL90 model	MLE	.033	0	4.15E-4	3.00	1	.05 - .1
	UCL	.031	.00733	-			
Equiv. Contin. ETO Blood Conc. umoles per liter, BL90 (Best estimate model)	MLE	.033	0	.00297	2.21	1	.1 - .2
	UCL	.031	.0198	-			
Equiv. Contin. ETO Bood Conc. umoles per liter, BL50 (Alternative model)	MLE	.033	0	.00164	1.79	1	.1 - .2
	UCL	.031	.0150	-			

---

*See p. 147 below for notes to these tables.

Table 5.17
Harderian Gland Papillary Cystadenomas in Male B6C3F1 Mice (NTP, 1987)

A. Alternative Expressions of "Dose" and Tumor Response:

Animals and Exposure Level	Net Absorption (umoles per day of exposure) BL90 model	Equivalent Contin. Blood ETO Conc. umoles/liter BL90 model	BL50 model	----Observed Tumor Response---- Incidence	"hits"* animal	"excess hits" animal **
Control	0	0	0	1/43	.024	-
50 ppm	20.35	7.26	9.47	9/44	.229	.205
100 ppm	33.14	12.65	17.2	8/42	.211	.188

B. Use of Alternative Expressions of Dose in Global82 Multistage Dose Response Modeling:

Expression for "Dose"		Model Coefficients q_0	q_1	q_2	Measures of Model Fit "chi^2"	degrees freedom	P *****
ppm in air	MLE***	.030	.00250	0	2.04	1	.1 - .2
	UCL****	.017	.00396	-			
Net Absorption umoles/day BL90 model	MLE	.026	.00721	0	1.12	1	.2 - .5
	UCL	.016	.0112	-			
Equiv. Contin. ETO Blood Conc. umoles per liter, BL90 (Best estimate model)	MLE	.028	.0192	0	1.40	1	.2 - .5
	UCL	.016	.0301	-			
Equiv. Contin. ETO Bood Conc. umoles per liter, BL50 (Alternative model)	MLE	.043	.00913	0	4.08	1	.02 - .05
	UCL	.021	.0156	-			

---

*See p. 147 below for notes to these tables.

Table 5.18
Harderian Gland Papillary Cystadenomas in Female B6C3F1 Mice (NTP, 1987)

A. Alternative Expressions of "Dose" and Tumor Response:

Animals and Exposure Level	Net Absorption (umoles per day of exposure) BL90 model	Equivalent Contin. Blood ETO Conc. umoles/liter BL90 model	BL50 model	----Observed Tumor Response---- Incidence	"hits"* animal	"excess hits" animal **
Control	0	0	0	1/46	.022	-
50 ppm	20.35	7.26	9.47	6/46	.140	.118
100 ppm	33.14	12.65	17.2	8/47	.186	.165

B. Use of Alternative Expressions of Dose in Global82 Multistage Dose Response Modeling:

Expression for "Dose"		Model Coefficients q_0	q_1	q_2	Measures of Model Fit "chi^2"	degrees freedom	P *****
ppm in air	MLE***	.024	.00184	0	.31	1	over .5
	UCL****	.014	.00302	-			
Net Absorption umoles/day BL90 model	MLE	.023	.00524	0	.06	1	over .5
	UCL	.014	.00853	-			
Equiv. Contin. ETO Blood Conc. umoles per liter, BL90 (Best estimate model)	MLE	.023	.0140	0	.12	1	over .5
	UCL	.014	.0229	-			
Equiv. Contin. ETO Bood Conc. umoles per liter, BL50 (Alternative model)	MLE	.023	.0104	0	.17	1	over .5
	UCL	.014	.0170	-			

---

*See p. 147 below for notes to these tables.

Table 5.19
Malignant Lymphomas in Male B6C3F1 Mice (NTP, 1987)

CAVEAT: THE APPARENT EXCESS OF THIS TUMOR IN THIS SEX WAS EVALUATED BY THE AUTHORS AS NOT STATISTICALLY SIGNIFICANT

A. Alternative Expressions of "Dose" and Tumor Response:

Animals and Exposure Level	Net Absorption (umoles per day of exposure) BL90 model	Equivalent Contin. Blood ETO Conc. umoles/liter BL90 model	BL50 model	----Observed Tumor Response---- Incidence	"hits"* animal	"excess hits" animal **
Control	0	0	0	1/50	.020	-
50 ppm	20.35	7.26	9.47	3/50	.062	.042
100 ppm	33.14	12.65	17.2	3/50	.062	.042

B. Use of Alternative Expressions of Dose in Global82 Multistage Dose Response Modeling:

Expression for "Dose"		Model Coefficients q_0	q_1	q_2	Measures of Model Fit "chi^2"	degrees freedom	P *****
ppm in air	MLE***	.024	.00049	0	.29	1	over .5
	UCL****	.012	.00127	-			
Net Absorption umoles/day BL90 model	MLE	.022	.00147	0	.15	1	over .5
	UCL	.011	.00363	-			
Equiv. Contin. ETO Blood Conc. umoles per liter, BL90 (Best estimate model)	MLE	.022	.00386	0	.20	1	over .5
	UCL	.011	.00970	-			
Equiv. Contin. ETO Bood Conc. umoles per liter, BL50 (Alternative model)	MLE	.023	.00284	0	.22	1	over .5
	UCL	.012	.00722				

---

*See p. 147 below for notes to these tables.

Table 5.20
Malignant Lymphomas in Female B6C3F1 Mice (NTP, 1987)

A. Alternative Expressions of "Dose" and Tumor Response:

Animals and Exposure Level	Net Absorption (umoles per day of exposure) BL90 model	Equivalent Contin. Blood ETO Conc. umoles/liter BL90 model	BL50 model	----Observed Tumor Response---- Incidence	"hits"* animal	"excess hits" animal **
Control	0	0	0	9/49	.203	-
50 ppm	20.35	7.26	9.47	6/48	.134	-.069
100 ppm	33.14	12.65	17.2	22/49	.596	.393

B. Use of Alternative Expressions of Dose in Global82 Multistage Dose Response Modeling:

Expression for "Dose"		Model Coefficients q_0	q_1	q_2	Measures of Model Fit "chi^2"	degrees freedom	P *****
ppm in air	MLE***	.151	0	3.71E-5	3.49	1	.05 - .1
	UCL****	.143	.00240	-			
Net Absorption umoles/day BL90 model	MLE	.153	0	2.98E-4	5.21	1	.02 - .05
	UCL	.148	.00695	-			
Equiv. Contin. ETO Blood Conc. umoles per liter, BL90 (Best estimate model)	MLE	.152	0	.00215	4.56	1	.02 - .05
	UCL	.146	.0182	-			
Equiv. Contin. ETO Bood Conc. umoles per liter, BL50 (Alternative model)	MLE	.151	0	.00119	4.20	1	.02 - .05
	UCL	.145	.0135	-			

---

*See p. 147 below for notes to these tables.

Table 5.21
Mammary Tumors in Female B6C3F1 Mice (NTP, 1987)
(Adenocarcinomas and Adenosquamous Carcinomas)

A. Alternative Expressions of "Dose" and Tumor Response:

Animals and Exposure Level	Net Absorption (umoles per day of exposure) BL90 model	Equivalent Contin. Blood ETO Conc. umoles/liter BL90 model	BL50 model	----Observed Tumor Response---- Incidence	"hits"* animal	"excess hits" animal **
Control	0	0	0	1/49	.021	-
50 ppm	20.35	7.26	9.47	8/48	.182	.162
100 ppm	33.14	12.65	17.2	6/49	.131	.110

B. Use of Alternative Expressions of Dose in Global82 Multistage Dose Response Modeling:

Expression for "Dose"		Model Coefficients q_0	q_1	q_2	Measures of Model Fit "chi²"	degrees freedom	P *****
ppm in air	MLE***	.029	.00161	0	3.03	1	.05 - .1
	UCL****	.015	.00279	-			
Net Absorption umoles/day BL90 model	MLE	.025	.00478	0	2.01	1	.1 - .2
	UCL	.014	.00799	-			
Equiv. Contin. ETO Blood Conc. umoles per liter, BL90 (Best estimate model)	MLE	.026	.0127	0	2.32	1	.1 - .2
	UCL	.014	.0213	-			
Equiv. Contin. ETO Bood Conc. umoles per liter, BL50 (Alternative model)	MLE	.027	.00935	0	2.53	1	.1 - .2
	UCL	.014	.0159	-			

---

*See p. 147 below for notes to these tables.

Table 5.22
Uterine Tumors in Female B6C3F1 Mice (NTP, 1987)
(Adenomas or Adenocarcinomas)

A. Alternative Expressions of "Dose" and Tumor Response:

Animals and Exposure Level	Net Absorption (umoles per day of exposure) BL90 model	Equivalent Contin. Blood ETO Conc. umoles/liter BL90 model	BL50 model	----Observed Tumor Response---- Incidence	"hits"* animal	"excess hits" animal **
Control	0	0	0	0/49	0	-
50 ppm	20.35	7.26	9.47	2/47	.043	.043
100 ppm	33.14	12.65	17.2	5/49	.108	.108

B. Use of Alternative Expressions of Dose in Global82 Multistage Dose Response Modeling:

Expression for "Dose"		Model Coefficients q_0	q_1	q_2	Measures of Model Fit "chi^2"	degrees freedom	P *****
ppm in air	MLE***	0	6.63E-4	4.13E-6	No test possible--no		
	UCL****	0	.00176	-	degrees of freedom		
Net Absorption umoles/day BL90 model	MLE	0	3.69E-4	8.68E-5	No test possible--no		
	UCL	0	.00484	-	degrees of freedom		
Equiv. Contin. ETO Blood Conc. umoles per liter, BL90 (Best estimate model)	MLE	0	.00260	4.67E-3	No test possible--no		
	UCL	0	.0131	-	degrees of freedom		
Equiv. Contin. ETO Bood Conc. umoles per liter, BL50 (Alternative model)	MLE	0	.00255	2.15E-4	No test possible--no		
	UCL	0	.00983		degrees of freedom		

---

*See p. 147 below for notes to these tables.

Notes for Tables 5.7 Through 5.22

*Assuming, for this calculation, a simple "one hit" dose response relationship. From the poisson distribution, the probability of an animal remaining tumor free (1 - tumor incidence) is e^{-m} where "m" is the number of "hits" per animal. Therefore the numbers in this column represent -ln(1 - tumor incidence).

**The numbers in this column are after subtraction of the "background" hits/animal.

***Maximum likelihood estimates.

****Coefficients for calculating the 95% upper confidence limit on induced risk at low doses. To arrive at these numbers a specific low dose was selected--one thousanth of the lowest dose used in the animal bioassay.

*****This is the probability that the data would be expected to depart from the model by as large an amount as was observed purely by chance, on the basis of statisical sampling error, even if the model were a completely accurate description of the underlying dose response relationship. Higher P values indicate better fits than lower P values, although the reader should be cautioned that only very large differences are likely to be "statistically significant" by usual standards. P values below .01 or .05 are conventionally taken to indicate an unsatisfactory fit between the model and the data.

With some exceptions, the tumor sites considered "positive" in these tables, the number of animals with tumors, and the number of animals at risk for tumors have been kept consistent with the analysis done previously by EPA (1985). The exceptions are

(1) Although they are very difficult to interpret, for the moment I have retained in the analysis the leukemias observed in the male animals in both the Lynch et al. (1984) and the Snellings et al. (1984) studies. The relatively high background in the male rats in these experiments evidently prevents the data from showing a statistically significant increase in the exposed groups. However, the simple "one hit" analysis in Tables 5.7 through 5.9 indicates that at least at doses up to 50 ppm the data in male rats are entirely consistent with the expectation that ethylene oxide has the same potency for inducing these tumors as is seen in female rats in the Snellings et al. (1984) study. In the presence of the result in the female animals, who exhibit many fewer "background" leukemias, I am reluctant to apply the baseline "null hypothesis" of no leukemogenic effect as the starting point for analysis of the male data.

(2) For the brain tumors in the Snellings et al. (1984) study I have used the denominators given by the authors in a later publication (Garman et al., 1986) reflecting the numbers of animals alive and therefore at risk at the time that the first brain tumor was observed.

(3) The new NTP (1987) mouse results were not available when the risk analysis was done by EPA (1985).

It can be seen in Tables 5.7 - 5.22 that in general reasonable fits were obtained using all of the available data.* Because the pharmacokinetic models predict only small deviations from linearity in the relationship between external dose and delivered dose, the various measures of dose lead to only minor differences in the "goodness of fit" statistics. Fit to a one- or two-stage carcinogenesis model therefore provides no information that can be used to choose among the various dose metrics. The subsequent analysis of risks across species therefore uses

---

*However, in the case of malignant lymphomas in female mice, the data suggest more nonlinearity than can be accommodated within a dose^2 model. See below for further discussion of the leukemia data for male rats.

each of the measures in turn to evaluate the overall carcinogenic risk of ethylene oxide in rats and mice.

There was also a distinct failure of the fit of the models for the leukemias in the Snellings et al. (1984) males. In the light of this, following standard procedure (EPA, 1985), I discarded the highest-dose point and reestimated the models to obtain the risk coefficients shown in Table 5.7. Conceivably the high dose animals might not have develeoped as many tumors as would be expected from the points at lower doses because of competing mortality from other tumors, etc. This result also meant that the analogous Lynch et al. (1984) results should be reexamined in the same light. Although the fits in that case were not quite poor enough to be rejected at the .05 level, it is clear that the data show the same trend seen in the more extensive data of Snellings et al. (1984). If one excludes the 100 ppm data point in the Lynch et al. (1984) leukemia data, the estimated q_1 potency of ethylene oxide would be comparable to that observed with the Snellings et al. (1984) data (Table 5.23). In the end, however, these ambiguities and complexities in interpreting the male rat data are great enough that in making interspecies projections of carcinogenic risk, I will focus on the data from female rats and male and female mice. Tables 5.24 through 5.27 in turn use each of the four measures of "dose" to analyze these remaining data.

Table 5.23
Overall Carcinogenic Risk in Male Rats, Expressing "Dose" in PPM
(Based on 6 hour/day, 5 day/week exposures)**

CAVEAT: BECAUSE OF THE AMBIGUITIES IN INTERPRETING THESE DATA, THEY ARE EXCLUDED FROM THE SUBSEQUENT ANALYSIS OF RISKS IN DIFFERENT SPECIES

Sex Species Site and Study		---Risk Coefficients---- MLE q_1	q_2	UCL q_1	Overall Induced Cacrcinogenic Transformations per Animal at 1 ppm MLE	"UCL"*
Male Rats [Lynch et al. (1984) and Snellings et al., (1984)]						
Leukemias (excluding high dose point)	Ly	.00484	0	.00872		
	Sn	.00638	0	.0108		
Mesothel-iomas	Ly	4.89E-4	1.56E-5	.00275		
	Sn	.00171	6.84E-6	.00316		
Brain	Ly	3.42E-4	1.87E-6	9.17E-4		
	Sn	9.54E-4	0	.00155		
Subtotal, Male Rats (Excluding Leukemias)						
	Ly	.000831	1.75E-5	.00367		
	Sn	.00266	6.84E-6	.00471		
	Average	.00182	1.22E-5	.00419	.00183	.00419
Total, Male Rats (Including Leukemias)						
	Ly	.00567	1.75E-5	.0124		
	Sn	.00904	6.84E-6	.0155		
	Average	.00736	1.22E-5	.0137	.00737	.0137

---

*Strictly, this "upper confidence limit", representing the sum of the 95% upper confidence limits seen for a number of different tumor sites, is somewhat more "conservative" (lower probability) than would be obtained by a Monte Carlo simulation of the statistical errors implied for the component data sets.

**For the Lynch data, which were based on 7 hour exposures, the q_1's were multiplied by 6/7 and the q_2's by $(6/7)^2$.

Table 5.24
Interspecies Comparison of Overall Carcinogenic Dose Response
--Expressing "Dose" in PPM (6 hrs/day, 5 days/week)

Sex, Species and Site	---Risk Coefficients---- MLE q1	MLE q2	UCL q1	Overall Induced Cacrcinogenic Transformations per Animal at 1 ppm MLE	"UCL"*
Female Rats (Snellings et al., 1984)					
Leukemias	.00427	0	.00610		
Brain	.00054	0	.00104		
Total	.00481	0	.00714	.00481	.00714
Male Mice (NTP, 1987)					
Lung	.00433	5.27E-6	.00740		
Harderian Gland	.00250	0	.00396		
Lymphomas	.00049	0	.00127		
Total	.00732	5.27E-6	.0126	.00732	.0126
Female Mice (NTP, 1987)					
Lung	0	5.08E-5	.00284		
Harderian Gland	.00184	0	.00302		
Lymphomas	0	3.71E-5	.00240		
Mammary	.00161	0	.00279		
Uterus	.00066	4.13E-6	.00176		
Total	.00411	9.20E-5	.0128	.00420	.0128

*Strictly, this "upper confidence limit", representing the sum of the 95% upper confidence limits seen for a number of different tumor sites, is somewhat more "conservative" (lower probability) than would be obtained by a Monte Carlo simulation of the statistical errors implied for the component data sets.

Table 5.25
Interspecies Comparison of Overall Carcinogenic Dose Response
--Expressing "Dose" in Micromoles/Day Absorbed Per Animal
(On the 5 of 7 days per week when exposures were given)

Sex, Species and Site	---Risk Coefficients---- MLE q_1	q_2	UCL q_1	Overall Induced Cacrcinogenic Transformations per Animal at 1 ppm* MLE	"UCL"**
Female Rats (Snellings et al., 1984)					
Leukemias	.00386	0	.00546		
Brain	.00048	0	.00090		
Total	.00434	0	.00636	.00601	.00880
Male Mice (NTP, 1987)					
Lung	.00592	2.63E-4	.0206		
Harderian Gland	.00721	0	.0112		
Lymphomas	.00147	0	.00363		
Total	.0146	2.63E-4	.0354	.00616	.0148
Female Mice (NTP, 1987)					
Lung	0	4.15E-4	.00733		
Harderian Gland	.00524	0	.00853		
Lymphomas	0	2.98E-4	.00695		
Mammary	.00478	0	.00799		
Uterus	.00037	8.68E-5	.00484		
Total	.0104	8.00E-4	.0356	.00449	.0149

*Computed at the equivalent of 1 ppm--approximately 1.384 umoles/day of net absorption for the rats, and .4187 umoles/day for mice.

**Strictly, this "upper confidence limit", representing the sum of the 95% upper confidence limits seen for a number of different tumor sites, is somewhat more "conservative" (lower probability) than would be obtained by a Monte Carlo simulation of the statistical errors implied for the component data sets.

Table 5.26
Interspecies Comparison of Overall Carcinogenic Dose Response
--Expressing "Dose" in Average Internal Micromoles/Liter
As Estimated by the "Best Estimate" BL90 Series of Models

Sex, Species and Site	---Risk Coefficients---- MLE q_1	MLE q_2	UCL q_1	Overall Induced Cacrcinogenic Transformations per Animal at 1 ppm* MLE	"UCL"**
Female Rats (Snellings et al., 1984)					
Leukemias	.0529	0	.0751		
Brain	.00660	0	.0126		
Total	.0595	0	.0877	.00547	.00807
Male Mice (NTP, 1987)					
Lung	.0225	.00125	.0557		
Harderian Gland	.0192	0	.0301		
Lymphomas	.00386	0	.0097		
Total	.0456	.00125	.0955	.00618	.0129
Female Mice (NTP, 1987)					
Lung	0	.00297	.0198		
Harderian Gland	.0140	0	.0229		
Lymphomas	0	.00215	.0182		
Mammary	.0127	0	.0213		
Uterus	.0026	.00467	.0131		
Total	.0293	.00979	.0953	.00413	.0129

---

*Computed at the equivalent to 1 ppm of approximately .092 umoles/liter long term average internal ETO concentration for rats, and .135 umoles/liter for mice.

**Strictly, this "upper confidence limit", representing the sum of the 95% upper confidence limits seen for a number of different tumor sites, is somewhat more "conservative" (lower probability) than would be obtained by a Monte Carlo simulation of the statistical errors implied for the component data sets.

Table 5.27
Interspecies Comparison of Overall Carcinogenic Dose Response
--Expressing "Dose" in Average Internal Micromoles/Liter
As Estimated by the "Alternative" BL50 Series of Models

Sex, Species and Site	---Risk Coefficients---- MLE q_1	q_2	UCL q_1	Overall Induced Cacrcinogenic Transformations per Animal at 1 ppm* MLE	"UCL"**
Female Rats (Snellings et al., 1984)					
Leukemias	.0683	0	.0969		
Brain	.00849	0	.0162		
Total	.0768	0	.113	.00557	.00819
Male Mice (NTP, 1987)					
Lung	.0194	5.15E-4	.0416		
Harderian Gland	.00913	0	.0156		
Lymphomas	.00284	0	.00722		
Total	.0314	5.15E-4	.0644	.00573	.0117
Female Mice (NTP, 1987)					
Lung	0	.00164	.0150		
Harderian Gland	.0104	0	.0170		
Lymphomas	0	.00119	.0135		
Mammary	.00935	0	.0159		
Uterus	.00255	.00022	.00983		
Total	.0223	.00304	.0712	.00415	.0130

---

*Computed at the equivalent to 1 ppm--approximately .0725 umoles/liter long term average internal ETO concentration for rats, and .182 umoles/liter for mice.

**Strictly, this "upper confidence limit", representing the sum of the 95% upper confidence limits seen for a number of different tumor sites, is somewhat more "conservative" (lower probability) than would be obtained by a Monte Carlo simulation of the statistical errors implied for the component data sets.

5.2.2.1 Interspecies Comparison of Risks, Using PPM as the Dose Metric

It can be seen in Table 5.24 (and in the limited comparisons that are possible with the male rat data in Table 5.23) that even when dose is expressed simply in terms of ppm in air, overall carcinogenic risks are reasonably consistent between the different sex and species groups. Given the difficulties of comparing different experiments showing excesses of somewhat different groups of tumors, agreement within a factor of two should be considered quite satisfactory. Averaging the results for male and female mice at 1 ppm, one obtains risks that exceed the corresponding value for female rats by only 20% (MLE) and 78% (UCL).

5.2.2.2 Interspecies Comparison of Risks, Using Net Absorption as the Dose Metric

This is the metric that is most closely related to the absorbed doses used in the risk assessment by EPA (1985). A similar overall corresponence of risks at 1 ppm can be seen in this case (Table 5.25) as was seen when ppm external air level was used as the dose metric. Here, however, the average MLE risk for the mice at 1 ppm is projected at about 11% less than the corresponding figure for mice, wheras the UCL at 1 ppm is about 69% more for the mice than for the rats. These slightly divergent results for the MLE and UCL at 1 ppm are produced by the $(dose)^2$ dependence of some of the maximum likelihood estimates of some of the tumors in mice.

For appropriate comparison, and to facilitate later projections to humans, the "q_1" and "q_2" coefficients in Table 5.25 (overall absorption in micromoles per animal) require some correction for the differing body weights of the different species. EPA most commonly divides by a measure of body surface area [(Body weight)$\cdot^{75}$] whereas OSHA and some industry researchers tend to favor simply dividing by body weight. In previous work (Hattis et al., 1986) I found that correcting for metabolic rates per body weight [(body weight)$\cdot^{75}$] was more attractive on basic theoretical grounds (Boxenbaum, 1982) and performed somewhat better in reconciling overall carcinogenic risks for perchloroethylene between rats and mice. Table 5.28 shows how the three different body weight correction rules do in reconciling the summary equations for overall carcinogenic risk per absorbed dose between female rats and male and female mice. Because both q_1's and q_2's are involved in the mice but not in the rats, the MLE estimates in this table are difficult to compare--and any comparison of projected risks depends on the dose considered. The UCL estimates are more readily compared, and these are most similar across species for the (body weight)$\cdot^{75}$ correction--although as usual the difference between this and the surface area correction is very small.

The data in Table 5.28 allows another approximate comparison. The earlier modeling work for perchloroethylene (Hattis et al., 1986) calculated the carcinogenic potency of perchloroethylene oxide in rats and mice. The indicated q_1's per (body weight)$\cdot^{75}$ for this material were:

Table 5.28
Transformation of the "q" Risk Coefficients in Table 5.25 Using Three Different Body Weight Correction Rules

	Female Rats	Male Mice	Female Mice
Umoles Absorbed Per Kg Body Weight:*			
MLE q_1	.00108	.000365	.000260
MLE q_2	0	1.64E-7	5.00E-7
UCL q_1	.00159	.000885	.000890
Umoles Absorbed Per (Kg Body Weight)$^{.75}$ ("Metabolic Energy Density")*			
MLE q_1	.00153	.000918	.000654
MLE q_2	0	1.04E-6	3.16E-6
UCL q_1	.00225	.00222	.00224
Umoles Absorbed Per (Kg Body Weight)$^{2/3}$ ("Surface Area")*			
MLE q_1	.00172	.00125	.000889
MLE q_2	0	1.92E-6	5.85E-6
UCL q_1	.00252	.00303	.00304

---

*For these purposes female rats were assumed to weigh .25 kg, and both male and female mice were assumed to weigh .025 kg. To obtain the data shown, the q_1 coefficients from Table 5.25 were multiplied by .25 (rats) or .025 (mice) whereas the q_2 coefficients were multiplied by $(.25)^2$ (rats) or $(.025)^2$ (mice). For the metabolic energy density and body surface area corrections, this process was repeated, substituting the body weights to the .75 or .6666667 power respectively.

	Rats (Average of Male and Female) (Leukemias)	Male Mice (Hepatocellular Carcinomas)
MLE q_1	.00506	.00600
UCL q_1	.0113	.0109

The indication is, therefore, that the active metabolites of prchloroethlene may be several fold more potent in inducing tumors than ethylene oxide.

5.2.2.3 Interspecies Comparison of Risks, Using As the Dose Metric "Long Term Average ETO Concentration for the Best Estimate Series of Models (BL90-LV*)"

The thought behind the construction of this "average internal concentration" metric was that no further corrections for body weight among species would be required. Because the rate of DNA reaction at low doses should be directly proportional to the internal concentration, this metric should provide the closest analogy to the dose metrics used in radiation--"rads" represent absorbed energy (and therefore initial DNA change capacity) per gram of tissue.

It can be seen in Table 5.26 that "q_1" coefficients, which determine low-dose risks, are reasonably consistent across the species. The average maximum likelihood estimate of q_1 for the two sexes in mice is 63% of the value derived for female rats. The upper confidence limit q_1 for the mice is very similar (9% more) to the rat value. The small difference in the MLE q_1's is likely to be due primarily to the

influence of the positive q_2 coefficient in the MLE models for some of the tumor sites in mice.

5.2.2.4 Interspecies Comparison of Risks, Using As the Dose Metric "Long Term Average ETO Concentration for the Alternative Series of Models (BL50-LV*)"

These comparisons are shown in Table 5.27. In this case the average MLE q_1 coefficient for the two sexes in mice is projected to be about 35% of the corresponding risk in female rats. The average UCL q_1 coefficient for the mice is risk is a little closer at 60% of the rat value. The greater consistency seen for the q_1 coefficients for the BL90 models in the previous section gives a small additional reason to prefer them in projecting human risks. In general, however, with the coefficients and projected risks so consistent across all of the comparisons in rodents, these data add little additional weight to the judgement that the blood/air partition coefficient is likely to be closer to 90 than 50.

5.2.3 Projection of Human Risks for Constant 8-Hour Occupational Exposures

Table 5.29 consolidates the results of the previous section in the form that is helpful in making my "best estimate" and "plausible upper limit" calculations of human risk. The "best estimate" coefficients in

this table represent the arithmetic averages of the q_1 and q_2 coefficients for female rats with the averages for both sexes of mice. The "plausible upper limit" coefficients represent the highest 95% upper confidence limit q_1's seen in the three species-sex trials. All of the coefficients from Tables 5.24 - 5.28 were multiplied by 45/70 to represent 45 working years over an assumed 70 year human lifetime. In addition, the ppm coefficients were multiplied by 8/6 to represent eight hours of exposure per day rather than six. Finally for the "net absorption" coefficients, the "best estimate" column reflects a (body weight)$^{.75}$ correction while the "plausible upper limit" column reflects a (body weight)$^{2/3}$ correction.

Having derived the risk coefficients, I now need to give the human delivered dose measures to go with them. Table 5.30 shows the relationships predicted by the human models between external exposure levels and internal doses.

It can be seen that relatively little nonlinearity can be expected at continuous 8 hour exposure levels below 100 ppm. This is basically because if (as the models assume) glutathione concentrations in human tissues are similar to those in rat tissues, the initial store of glutathione in the body is quite large--about .044 moles. Since it takes at least one mole of ethylene oxide to react with one mole of glutathione (neglecting reactions with other sulfhydryls and the continuous replacement of glutathione), a relatively large air concentration for an 8 hour day is required to produce appreciable depletion. For example, at 10 ppm, the approximately 5.44 cubic meters of air taken into the alveoli in an 8 hour work day contains about

Table 5.29
Final Coefficients for Making Human Risk Projections
For Different Dose Metrics*

Based on Exposure for 45 Years Out of A Lifetime of 70 Years

Dose Metric	"Best Estimate" Risk Coefficients		"Plausible Upper Limit" Risk Coefficient
	q_1	q_2	q_1
PPM in Air (8 hours per day, 5 days/week)	.00451	2.08E-5	.0128 (from female mice)
Net Absorption (Umoles/day) / (Body Weight)^{n}**	7.44E-4	6.75e-7	.00304 (from female mice)
Best Estimate BL90LV* Models Umoles/liter long term average blood ETO conc.	.0312	.00177	.0955 (from male mice)
Alternative BL50LV* Models Umoles/liter long term average blood ETO conc.	.0333	8.89E-4	.113 (from female rats)

---

*See the text for the basis and assumptions used in these calculations.

**Where n is .75 for the "Best Estimate" risk coefficient and 2/3 for the "Plausible Upper Limit" coefficient, and where absorption refers to the ethylene oxide absorbed per day on each of 5 days per week of exposure.

Table 5.30
Net Absorption and Blood C X T Doses for Humans Predicted
for Constant 8-Hour Occupational Exposures

ppm (8 hrs per day)	Net Absorption During Exposure (moles/day)	Exhalation of Unchanged ETO After Exposure (moles/day)	Blood C X T (mole/liter)-min per day of exposure	Average Weekly Blood Concentration (umoles/liter) for 5 days exposure/week
Best-Estimate Model (GSH3-LV*--Blood/air partition coefficient = 90*)				
1	.0001666	5.948E-6	.0004143	.2055
10	.001665	6.041E-5	.004162	2.064
100	.01649	7.073E-4	.04370	21.68
1000	.1472	28.37 E-3	.7480	371.0
Alternative Model (GSH3BL50-LV*--Blood/air partition coefficient = 50*)				
1	.0001658	2.779E-6	.0002139	.1061
10	.001656	2.823E-5	.002149	1.066
100	.01638	3.325E-4	.02250	11.16
1000	.1390	17.87 E-3	.4011	199.0

---

*See the footnote to Table 4.7, p. 99 for other model specifications.

(5443 liters)*(10^{-5} moles/25.45 liters at 10 ppm) = 2.1 X 10^{-3} moles ETO

Thus an 8 hour exposure to 10 ppm ethylene oxide is unlikely to produce more than about a 5% depletion of the overall store of glutathione in the body. If, as assumed in my models, this is the chief likely source of nonlinearity*, it follows that there can be only relatively modest nonlinearities in the exposure region up to 10 ppm.

In summarizing risks and making the final comparisons across different dose metrics I will therefore only provide estimates at one exposure level--1 ppm time-weighted average over an eight-hour period. Risks for other exposure levels within several fold above and at any level below this value will be in higher or lower in proportion. Table 5.31 shows these final risk projections, based on the risk coefficients in Table 5.29 and the measures of human delivered dose provided in Table 5.30.

In the end it can be seen that in this case the different dose metrics used in the analysis do not lead to markedly divergent estimates of human risk. Even the simplest exposure measure considered--external air ppm X exposure time--leads to expected risks that are well within a two-fold range of the "best estimate" risks inferred from the pharmacokinetic modeling. At least for a simple direct-acting alkylating agent such as ethylene oxide, the traditional approaches for dose and risk projection across species appear to be sustained by the more elaborate pharmacokinetic-based analysis.

---

*Conceivably enzyme saturation could also produce nonlinearities. However if enzyme saturation were appreciable in rodents at lower doses than required for appreciable glutathione depletion I should not have been able to fit the glutathione depletion results of McKelvey and Zemaitis (1986) as well as I did without including this additional factor.

Table 5.31
"Best Estimates" and "Plausible Upper Limits" for Overall Cancer Risk from Occupational Exposure to 1 ppm Ethylene Oxide

(Exposure for 8 Hours/Day, 5 Days/Week for 45 Years)

Probability Per Individual of Developing at Least One Additional Cancer		
Dose Metric	"Best Estimate"	"Plausible Upper Limit"
PPM in Air (8 hours per day, 5 days/week)	.0045	.013
Net Absorption (Umoles/day) / (Body Weight)^{n}*	.0051	.029
Best Estimate BL90LV* Models Umoles/liter long term average blood ETO conc.	.0065	.019
Alternative BL50LV* Models Umoles/liter long term average blood ETO conc.	.0035	.012

*Where n is .75 for the "Best Estimate" risk and 2/3 for the "Plausible Upper Limit" risk, and where absorption refers to the ethylene oxide absorbed per day on each of 5 days per week of exposure.

This result was foreshadowed by the comparisons in Tables 5.1 - 5.3 above. Tables 5.1 and 5.2 indicated that the internal rates of metabolism of ethylene oxide scale nicely with overall metabolic rates per body weight [the elimination half lives are longer in humans than in mice, rats, and dogs, with elimination half lives proportional to (body weight)$^{.25}$]. This leads to greater persistence and therefore greater tissue dose in humans relative to rodents per mole of ethylene oxide absorbed. On the other hand, because alveolar ventilation rates also must scale approximately with metabolic rates, humans absorb appreciably less ethylene oxide per unit body weight at similar ppm air levels of exposure. As seen in Table 5.3, the longer persistence of absorbed ethylene oxide in humans and the lesser absorption per body weight nearly exactly offset one another--leading to an expectation of approximately equal internal concentration X time for a given low dose ppm X time of external exposure.

Another conclusion from Table 5.31 is of course that the projected risk from working lifetime exposure at the proposed OSHA 8-hour time-weighted-average standard of 1 ppm is appreciable in relation to other cancer risks that have been the subjects of control action in the past. In the light of the mandate of the OSHAct, consideration of the feasibility of a stricter standard is warranted.

5.2.4 Comparison with Risks Estimated by EPA (1985) From Human Epidemiological Information

I have not independently analysed the human epidimiological literature. Classically, the difficulties in estimating past human

exposure, eliminating confoundng from exposure to extraneous risk factors, and projecting lifetime risks from limited periods of observation and limited numbers of cases, make the task of drawing quantitative inferences of human risk directly from human observations very complex.

Nevertheless based on the available studies of a sterilizing plant by Hogstedt, in a group where two leukemias were observed when .03 cases would have been expected, EPA (1985) estimated that the potency of ethylene oxide for inducing leukemia in humans was about .5 per lifetime continuous exposure to 1 ppm (95% confidence interval .07 to 2.5). If we translate this into terms comparable with those used in Table 5.31--8 hours/day, 5 days/week, for 45 years, the comparable "best estimate" q_1 would be

$$(.5)*(8/24)*(5/7)*(45/70) = .076$$

with 95% confidence limits of .011 to .38. EPA's "best estimate" risk from the human epidemiology is therefore about tenfold higher than the maximum likelihood estimate of .0065 from my pharmacokinetic-based projection from animals. The inferred 95% confidence interval from the human data, however, at least overlaps with the range included within the "plausible upper limit" of the animal projection. In any event, the very limited inference of quantitative risk from the human data do not suggest that the risks implied by Table 5.31 are overstated.

5.2.5 Comparison with Risks Estimated for Perchloroethylene

Previously I have made the comparison of the apparent potency of perchloroethylene oxide with ethylene oxide. However only a small proportion of inhaled perchloroethylene is metabolized to this active agent--the bulk is exhaled unchanged. How does the expected potency of perchloroethylene itself for humans compare with the risks projected in Table 5.31 for ethylene oxide?

From earlier pharmacokinetic work (Hattis et al., 1986), the "best estimate" and "plausible upper limit" estimates of carcinogenic risks from 45 year occupational exposure to 1 ppm perchloroethylene were 6.7×10^{-4} and .013, respectively. Thus the best estimate for risk from low dose exposure to perchloroethylene is only tenfold less than the best estimate of risk from a comparable exposure to ethylene oxide, and the "plausible upper limit" risks are within two-fold. In the light of the fact that relatively high level exposure to perchloroethylene in dry cleaning is very widespread, this reinforces the desirability of further efforts to assess and control risks from perchloroethylene exposure.

5.2.6 Dose-Rate Effects Expected in Humans

Table 5.32 compares the blood concentration X time doses of ethylene oxide that can be expected for constant eight hour exposures with a parallel series of acute high-level 15 minute exposures presenting the same numbers of external air ppm-hours. It can be seen for both models (and all of the other model variants I explored) that at least in the

Table 5.32
Comparison of Predicted Delivered Doses for Constant 8-Hour vs.
High-Level 15 Minute Exposures Presenting the Same External PPM-Hours

ppm	Net Absorption During Exposure (moles/day)	Exhalation of Unchanged ETO After Exposure (moles/day)	Blood C X T (mole/liter)-min per day of exposure	Average Weekly Blood Concentration (umoles/liter) for 5 days exposure/week
Best-Estimate Model (GSH3-LV*. Blood/air partition coefficient = 90*)				
480 minute exposures:				
1	.0001666	5.948E-6	.0004143	.2055
10	.001665	6.041E-5	.004162	2.064
100	.01649	7.073E-4	.04370	21.68
1000	.1472	28.37 E-3	.7480	371.0
15 minute exposures delivering the same ppm-hours/day:				
32	.0002044	4.326E-5	.0004156	.2062
320	.002044	4.353E-4	.004177	2.072
3200	.02044	4.640E-3	.04408	21.86
32000	.2044	9.027E-2	.7917	392.7
Alternative Model (GSH3BL50-LV*. Blood/air partition coefficient = 50*)				
480 minute exposures:				
1	.0001658	2.779E-6	.0002139	.1061
10	.001656	2.823E-5	.002149	1.066
100	.01638	3.325E-4	.02250	11.16
1000	.1390	17.87 E-3	.4011	199.0
15 minute exposures delivering the same ppm-hours/day:				
32	.0001975	3.399E-5	.0002146	.1064
320	.001975	3.423E-4	.002157	1.070
3200	.01975	3.679E-3	.02273	11.27
32000	.1971	8.339E-2	.4373	216.9

---

*See the footnote to Table 4.7, p. 99 for other model specifications.

range contemplated for current standard-setting for ethylene oxide, the effects of more rapid presentation are quite modest. The reason for this is basically the same as for the relative linearity of internal dose in the 1 - 100 ppm range--it takes a great deal of ethylene oxide to deplete glutathione enough that the elimination half-life of ethylene oxide is appreciably prolonged. I am therefore reasonably confident that current efforts to measure hemoglobin adduct formation in workers will detect no significant differences in adduct formation per ppm-hour of exposure between workers exposed relatively continuously and workers exposed in short high-level bursts.

The fact that emissions from sterilizers and the resulting worker exposures may often occur primarily in short bursts (e.g. when the sterilizers are opened for unloading) suggests that monitoring procedures and control efforts may be usefully directed at limiting the peaks of emissions and worker exposure. Also, in enforcing workplace standards, designing 15 minute limits, to be evaluated at known times of high level exposure, rather than 8-hour time weighted averages, could lead to important savings in the time required for OSHA industrial hygeinists to collect samples. I would suggest that these engineering and administrative considerations should be the driving factors in evaluating the desirability of short term exposure limits for ethylene oxide, rather than biological/pharmacokinetic considerations.

5.3 Prospects for Further Research

The modeling in this report rests upon an extensive and diverse body of research data from different species, but also on quite a number of simplifying assumptions and projections where data were not directly available. The assumptions/projections include:

- The measurements of absorption of ethylene oxide from alveolar air of Brugnone et al. (1985) were used to calibrate human metabolism rates for ethylene oxide, rather than the hemoglobin adduct measurements of Calleman et al. (1978). Using the latter would have led to expectations of several fold lower human doses and risks, but both the exposure data and some of the interpretive assumptions of Calleman et al. (1978) were considered to be doubtful. Still, it would be useful to check both observations in future work. Also, the interpretive assumptions of Calleman et al. (1978) (that ethylene oxide hemoglobin adducts are stable *in vivo* and are lost with the same kinetics as the red cells that carry them) need to be subjected to careful quantitative testing. This would be best studied by periodic blood and air monitoring of nonsmoking workers over several months, starting from their initial occupational exposure to ethylene oxide. Another useful test would be to expose red blood cells to ethylene oxide *in vitro*, reinject them into the same individual, and measure the loss of hemoglobin adducts over time.

- Glutathione concentrations in human tissues were assumed to be similar to those in corresponding rat tissues. Glutathione turnover rates in human tissues were scaled from rat turnover rates in proportion to metabolic rates. (Note: because of the small degree of glutathione depletion expected at moderate ethylene oxide exposure levels, the latter assumption does not appreciably affect the interspecies scaling of ethylene oxide metabolism).

- The response to glutathione depletion in tissues was assumed to be a simple reduction in other processes leading to first-order loss of glutathione. No induction of enhanced synthesis was assumed over six-eight hour exposure periods.

- Tissue partition coefficients were projected from work of Fiserova-Bergerova et al. (1986), and measurements of the partition coefficient between oil and air and water and air. It would be preferable to have direct measurements of these parameters, although the modeling results were shown not to be very sensitive to them.

- In the final models, reaction ethylene oxide with glutathione was assumed to proceed with the same rate constant in all tissues except the liver. The gluthatione depletion data were better fit by an assumption that the reaction proceeded twice as fast in the liver as in other tissues. It was also assumed that reaction with glutathione and other sulfhydryl compounds is the primary route of metabolism, that sulfhydryl compounds other than glutathione are present in concentrations proportional to the concentration of glutathione, and that these other sulfhydryl's are depleted by ethylene oxide at comparable rates.

It is of basic scientific interest to fill some of these data gaps. And conceivably major changes in the assumptions cited in the first bullet could lead to appreciable changes in projected human risks. However, the sensitivity analysis of modeling assumptions on tissue/blood partition coefficients and the tissue distribution of ethylene oxide metabolism generally led to very small differences in projected delivered doses in animals or people. This was because these assumptions basically form background for the fitting of metabolic rates to observed absorption, exhalation and hemoglobin adduct data. Because of this insensitivity to modeling assumptions, and because of the small differences in the ultimate risks projected from the pharmacokinetic modeling from those that would be expected from simpler assumptions of equivalent risk per ppm-hour of exposure (Table 5.31), I think it is unlikely that changes in the other assumptions in the light of new data will significantly alter the human risk assessment.

6. REFERENCES

Adkins, B., Stee, E. W. Van, Simmons, J. E., and Eustis, S. L. (1986). "Oncogenic response of strain A/J mice to inhaled chemicals," J. Toxicol. Environ. Hlth., vol. 17, pp. 311-322.

Adolph, E.F. (1949). "Quantitative relations in the physiological constitutions of mammals," Science, vol. 109, pp. 579-585.

Alarie, Y. (1981). "Dose-response analysis in animal studies: Prediction of human responses," Environ. Health Perspect., vol. 42, pp. 9-13.

Boxenbaum, H. (1982). "Interspecies scaling, allometry, physological time, and the ground plan of pharmacokinetics," J. Pharmaco. Biopharm., vol. 10, pp. 201-227.

Brugnone, F., Perbelline, L., Gaffuri, E., and Apostoli, P. (1980). "Biomonitoring of industrial solvent exposures in workers' alveolar air," Int. Arch. Occup. Environ. Hlth., vol. 47, pp. 245-261.

Brugnone, F., Perbellini, L., and Gaffuri, E. (1980). "N-N-Dimethylformamide concentration in environmental and alveolar air in an artificial leather factory," Brit. J. of Industrial Medicine, vol. 37, pp. 185-188.

Brugnone, F., Perfellini, L, Faccini, G., and Pasini, F. (1985). "Concentration of ethylene oxide in the alveolar air of occupationally exposed workers," Am J. Indust. Med., vol. 8, pp. 67-72.

Brugnone, F., Perbellini, L., Faccini, G. B., Pasini, F., Bartolucci, G. B., and DeRosa, E. (1986). "Ethylene oxide exposure. Biological monitoring by analysis of alveolar air and blood," Int. Arch. Occup. Environ. Health, vol. 58, pp. 105-112.

Calleman, C.J., Ehrenberg, L., Jansson, B., Osterman-Golkar, S., Segerback, D., Svensson, K., and Wachtmeister, C.A. (1978). "Monitoring and risk assessment by means of alkyl groups in hemoglobin in persons occupationally exposed to ethylene oxide," J. Environ. Path. and Toxicol., vol. 2, pp. 427-442.

Chaigneau, M. (1985). "Sur les solubilites de l'oxyde d'ethylene," Ann. Pharmaceutiques Francaises, vol. 43, pp. 193-194.

Dodd, D. E., Bus, J. S., and Barrow, C. S. (1982). "Nonprotein sulfhydryl alterations in F-344 rats following acute methyl chloride inhalation," Toxicol. Appl. Pharmacol., vol. 62, pp. 228-236.

Ehrenberg, I., Hiesche, K.D., Osterman-Golkar, S., and Wennberg, I. (1974). "Evaluation of genetic risks of alkylating agents: Tissue doses in the mouse from air contaminated with ethylene oxide," Mutation Research, vol. 24, pp. 83-103.

Ehrenberg, L., Osterman-Golkar, S., Segerback, D., Svensson, K., and Calleman, C. J. (1977). "Evaluation of genetic risks of alkylating agents. III. Alkylation of haemoglobin after metabolic conversion of ethene to ethene oxide in vivo," Mutat. Res., vol. 45, p. 175.

Ehrenberg, L. (1979). "Risk assessment of ethylene oxide and other compounds," Assessng Chemical Mutagens, the Risk to Humans, V. McEhlen and S. Abramson, eds., vol. 1979, pp. 151-190.

Environmental Protection Agency, Office of Health and Environment al Assessment (1985). Health Assessment Document for Ethylene Oxide--Final Report. Washington, D. C.: Environmental Protection Agency, Office of Health and Environment al Assessment, June.

Filser, J. G. and Bolt, H. M. (1984). "Inhalation pharmacokinetics based on gas uptake studies. VI. Comparative evaluation of ethylene oxide and butadiene monoxide as exhaled reactive metabolites of ethylene and 1,3-butadiene in rats," Arch. Toxicol., vol. 55, pp. 219-223.

Fiserova-Bergerova, V. and Diaz, M. L. (1986). "Determination and prediction of tissue-gas partition coefficients," Int. Arch. Occup. Environ. Health, vol. 58, pp. 75-87.

Garman, R. H., Snellings, W. M., and Maronpot, R. R. (1986). "Frequency, size and location of brain tumors in F-344 rats chronically exposed to ethylene oxide," Fd. Cehm. Toxic., vol. 24, pp. 145-153.

Gehring, P. J., Watanabe, P. G., and Park, C. N. (1978). "Resolution of dose-response toxicity data for chemicals requiring metabolic activation: Example--vinyl chloride," Toxicol. Appl. Pharmacol., vol. 44, pp. 581-591.

Generoso, W. M., Cain, K. T., Hughes, L. A., Sega, G. A., Braden, P. W., Gosslee, D. G., and Shelby, M. D. (1986). "Ethylene oxide dose and dose-rate effects in the mouse dominant-lethal test," Environ. Mutagenesis, vol. 8, pp. 1-7.

Griffith, O. W. and Meister, A. (1979). "Glutathione: Interorgan translocation, turnover, and metabolism," Proc. Natl. Acad. Sci. USA, vol. 76, pp. 5606-5610.

Hattis, D., Tuler, S., Finkelstein, L., and Luo, Z. Q. (1986). A Pharmacokinetic/Mechanism-Based Analysis of the Carcinogenic Risk of Perchloroethylene. Cambridge, Mass.: M.I.T. Center for Technology, Policy and Industrial Development, No. CTPID 86-7, September.

Hogstedt, C., Aringer, L., and Gustavsson, A. (1986). "Epidemologic support for ethylene oxide as a cancer-causing agent," JAMA, vol. 255, pp. 1575-1578.

Howe, R. B. and Crump, K. S. (1982). "Global 82--A computer program to extrapolate quantal animal toxicity data to low doses," Report by K.S. Crump and Company to Office of Carcinogen Standard s, OSHA, May.

Jones, A.R. and Wells, G. (1981). "The comparative metabolism of 2-bromoethanol and ethylene oxide in the rat," Xenobiotica, vol. 11, pp. 763-770.

Joshi, U. M., Dumas, M, and Mehendale, H. M. (1986). "Glutathione turnover in perfused rabbit lung. Effect of external gluthathione," Biochem. Pharmacol., vol. 35, pp. 3409-3412.

Kane, L. E. and Alarie, Y. (1977). "Sensory irritation to formaldehyde and acrolein during single and repeated exposures in mice," Am. Ind. Hyg. Ass. J., vol. 38, pp. 509-522.

Kane, L. E., Barrow, C. S., and Alarie, Y. (1979). "A short-term test to predict acceptable levels of exposure to airborne sensory irritants," Am. Ind. Hyg. Ass. J., vol. 40, pp. 207-229.

Kane, L. E., Dombroske, R., and Alarie, Y. (1980). "Evaluation of sensory irritation from some common industrial solvents," Am. Ind. Hyg. Ass. J., vol. 41, pp. 451-455.

Kaplowitz, N., Aw, T. Y., and Ookhtens, M. (1985). "The regulation of hepatic gluthathione," Ann. Rev. Pharmacol. Toxicol., vol. 25, pp. 715-744.

Kline, S. A., Solomon, J.J., and Duuren, B.L. Van (1978). "Synthesis and reactions of chloroalkene epoxides," J. Org. Chem., vol. 43, pp. 3596-3600.

Kolman, A., Naslund, M., and Calleman, C. J. (1986). "Commentary--Genotoxic effects of ethylene oxide and their relevance to human cancer," Carcinogenesis, vol. 7, pp. 1245-1250.

Lauterburg, B. H. and Mitchell, J. R. (1981). "Regulation of hepatic glutathione turnover in rats in vivo and evidence for kinetic homogeneity of the hepatic glutathione pool," J. Clin. Invest., vol. 67, pp. 1415-1424.

Lewis, T. (1987). NTP Technical Report on the Toxicology and Carcinogenesis Studies of Ethylene Oxide (CAS No. 75-21-8) in B6C3F1 Mice (Inhalation Studies). RTP, North Carolina: National Toxicology Program.

Lynch, D.W., Lewis, T.R., Moorman, W.J., Burg, J.R., Groth, D.H., Khan, A., Ackerman, L.J., and Cockrell, B.Y. (1984). "Carcinogenic and toxicologic effects of inhaled ethylene oxide and propylene oxide in F344 rats," Toxicol. Appl. Pharmacol., vol. 76, pp. 69-84.

Mann, A. M. and Darby, F. J. (1985). "Effects of 1,2-dibromoethane on glutathione metabolism in rat liver and kidney," Biochem. Pharmacol., vol. 34, pp. 2827-2830.

Martis, L., Kroes, R., Darby, T. D., and Woods, E. F. (1982). "Disposition kinetics of ethylene oxide, ethylene glycol, and 2-chlorethanol in the dog," J. Toxicol. Environ. Hlth., vol. 10, pp. 847-856.

McKelvey, J. A. and Zemaitis, M. A. (1986). "The effects of ethylene oxide (EO) exposure on tissue glutathione levels in rats and mice," Drug and Chemical Toxicology, vol. 9, pp. 51-66.

Morton, S. and Mitchell, M. C. (1985). "Effects of chronic ethanol feeding on glutathione turnover in the rat," Biochem. Pharmacol., vol. 34, pp. 1559-1563.

Osterman-Golkar, S., Ehrenberg, L., Segerback, D., and Hallstrom, I. (1976). "Evaluation of genetic risks of alkylating agents. II. Haemoglobin as a dose monitor," Mutat. Res., vol. 34, pp. 1-10.

Osterman-Golkar, S., Farmer, P. B., Segerback, D., Bailey, E., Calleman, C. J., Svensson, K., and Ehrenberg, L. (1983). "Dosimetry of ethylene oxide in the rat by quantitation of alkylated histidine in hemoglobin," Teratogenesis, Carcinogenesis, and Mutagenesis, vol. 3, pp. 395-405.

Pero, R.W., Widegren, B., Hogstedt, B., and Mintelman, F. (1981). "In vivo and in vitro ethylene oxide exposure of human lyphocytes assessed by chemical stimulation of unscheduled DNA synthesis," Mutation Research, vol. 83, pp. 271-289.

Pierson, J. L. and Mitchell, M. C. (1986). "Increased hepatic efflux of glutathione after chronic ethanol feeding," Biochem. Pharmacol., vol. 35, pp. 1533-1537.

Politzer, P., Laurence, P.R., and Jayasuriya, K. (1985). "Halogenated olefins and their epoxides: factors underlying carcinogenic activity," Molecular Basis of Cancer, Part A: Macromolecular Structure, pp. 227-237.

Ramsey, J.C. and Andersen, M.E. (1984). "A physiologically based description of the inhalation pharmacokinetics of styrene in rats and humans," Toxicol. Appl. Pharmacol., vol. 73, pp. 159-175.

Reed, D. J. (1986). "Regulation of reductive processes by glutathione," Biochem. Pharmacol., vol. 35, pp. 7-13.

Riggs, D. S. (1963). The Mathematical Approach to Physiological Problems--A Critical Primer. Cambridge, Mass.: MIT Press.

Schmiedel, G., Filser, J. G., and Bolt, H. M. (1983). "Rat liver microsomal transformation of ethene to oxirane in vitro," Toxicology Letters, vol. 19, pp. 293-297.

Segerback, D. (1983). "Alkylation of DNA and hemoglobin in the mouse following exposure to ethene and ethene oxide," Chem. Biol. Interactions, vol. 45, pp. 139-151.

Seybold, P. G., May, M. A., Vargas, M. L., and Andersen, M. E., (1986) "Modeling blood and tissue solubilities of halogenated methane-, ethane-, and ethylene." The Toxicologist, Vol. 6, No.1, 25th anniversary meeting of the Society of Toxicology, March 3-7, 1986, New Orleans, La., Abstract No. 1046.

Snellings, W. M., Weil, C. S., and Maronpot, R. R. (1981). "Final report, ethylene oxide, two years inhalation study," Report to the Environmental Protection Agency, cited by EPA, 1985.

Snellings, W., Weil, C., and Maronpot, R. (1984). "A two-year inhalation study of the carcinogenic potential of ethylene oxide in Fischer 344 rats," Toxicol. Appl. Pharmacol., vol. 75, pp. 105-117.

Sun, M. (1986). "Study estimates higher risk from ethylene oxide exposure," Science, vol. 231, p. 448.

Tornqvist, M., Osterman-Golkar, S., Kautiainen, A., Jensen, S., Farmer, P. B., and Ehrenberg, L. (1986). "Tissue doses of ethylene oxide in cigarette smokers determined from adduct levels in hemoglobin," Carcinogenesis, vol. 7, pp. 1519-1521.

Tyler, T. R. and McKelvey, J. A. (1983). "Dose dependent disposition of 14C labeled ethylene oxide in rats," Bushy Run Research Center, Union Carbide, February.

Wendel, A. and Jaeschke, H. (1981). "Drug-induced lipid peroxidation in mice--III. Glutathione content of liver, kidney and spleen after intravenous administration of free and liposomally entrapped glutathione," Biochem. Pharmacol., vol. 31, pp. 3607-3611.

APPENDIX A

Exerpts From

Hattis, D., Tuler, S., Finkelstein, L., and Luo, Z. Q. (1986). A Pharmacokinetic/Mechanism-Based Analysis of the Carcinogenic Risk of Perchloroethylene. Cambridge, Mass.: M.I.T. Center for Technology, Policy and Industrial Development, No. CTPID 86-7, September.

2.1 Definition of Compartments

To simplify pharmacokinetic analyses, tissues with similar kinetic behavior are combined into "compartments." The single most important characteristic used to define expected kinetic behavior for these purposes is the ratio of blood flow through the tissue to tissue volume.

To see why this is so, consider a simple salt that is equally soluble in blood and a particular tissue, and assume that the concentration of the salt in blood flowing through the tissue is in rapid equilibrium with the concentration of the salt in the tissue. In that case the rate of output of the salt from the tissue (dC/dt) will be simply the concentration in the tissue (C) times the tissue blood flow (Q) divided by the tissue volume (V):

$$\frac{dC}{dt} = \frac{CQ}{V} \qquad (1)$$

or

$$\frac{dC}{C} = \frac{Q\,dt}{V} \qquad (2)$$

Integrating, we find that the concentration in the tissue will decrease according to a simple exponential rate equation with a rate constant equal to Q/V:

$$C = C_0 e^{-(Q/V)t} \qquad (3)$$

(assuming that the blood flowing <u>into</u> the tissue has none of the salt in question).

Traditionally, compartments have been constructed using the heuristic that processes of first-order kinetics are experimentally distinguishable only if rate constants for different tissues differ by at least a factor of five [Fiserova-Bergerova (1983), Vol. 1, pg. 88]. However, it is not necessary to place all tissues with similar rate constants into the same compartment and in general those tissues/organs that are important in metabolizing foreign substances are placed in distinct compartments.

For our human models, tissues are divided into the following five groups:

- Vessel Rich Group containing the brain, kidney, coronary, adrenals, and thyroid tissues as well as additional small viscera,
- Vessel Poor Group containing the skeletal bone and connective tissue,
- Muscle Group containing the lean body tissue: muscle, skin, and tongue,
- Fat Group containing the perirenal and subcutaneous fat and the marrow, and
- Liver Group. This organ is placed by many researchers in the same category as the tissues in the vessel rich group, however, in our models it was placed into a seperate compartment because of its key role in metabolism.

Table 2.1 shows the volumes and perfusion rates of these groups of tissues used in our "base" human model under conditions of relatively low waking activity ("sitting"--alveolar ventilation of about 7 liters/minute). For comparison, Tables 2.2 and 2.3 show the tissue volumes and flows for our basic rat and mouse models. The derivation of these numbers will be discussed in more detail in Section 3. What can be noted here is that (1) intrinsic clearance rates for most tissues are faster in the rodent species than in humans, however (2) the clearance rates for all tissues do not appear to change proportionately among the three species--there is

Table 2.1
Human Tissue Group Volumes and Flows for "Sitting" Level of Activity

Compartment	Volume* (V) (liters)	Blood Flow (Q) (liters/min.)	Intrinsic Clearance Rate (Q/V) (min^{-1})
Vessel Rich Group	6.04	3.38	0.56
Liver	2.48	1.34	0.54
Muscle Group	34.76	1.5	0.043
Fat Group	15.02	0.34	0.023
Vessel Poor Group	12.5	.1	0.008
Total	70.8	6.66	

---

*All volumes include the blood associated with the different tissue groups. In addition, the volume of the vessel rich group includes the blood in the lung and the arterial and venous circulation.

Table 2.2
Rat Tissue Group Volumes and Flows

Compartment	Volume* (V) (milliliters)	Blood Flow (Q) (ml/min.)	Intrinsic Clearance Rate (Q/V) (min^{-1})
Vessel Rich Group	12.5	47.9	3.83
Liver	10	23.5	2.35
Muscle Group	187.5	14.1	0.0752
Fat Group	17.5	8.5	0.486
Total	227.5	94	

Table 2.3
Mouse Tissue Group Volumes and Flows

Compartment	Volume* (V) (milliliters)	Blood Flow (Q) (ml/min.)	Intrinsic Clearance Rate (Q/V) (min^{-1})
Vessel Rich Group	1.25	9.69	7.75
Liver	1.5	4.75	3.17
Muscle Group	17.5	2.85	0.163
Fat Group	2.5	1.71	0.684
Total	22.75	19.0	

very little difference between the two rodent species in the ratio of volume to flow for the fat group but a comparatively large difference beween the rodents and people (over twenty fold) By contrast the intrinsic clearance rates for the muscle group for the three species differ by only about four fold, and in this case the rats are about at the logarthmic midpoint between humans and mice (differing from each by about two fold. If these data are correct, no simple scaling rule can fully capture the pharmacokinetic differences between humans and rodents.

2.2 The Role of Partition Coefficients

2.2.1 The Dynamics of Exchange Between Blood and Tissues

Unlike the hypothetical simple salt discussed in the previous section, of course, most chemicals are not equally soluble in blood and tissues. We can define a partition coefficient, $L_{tissue/blood}$, as the equilibrium ratio of the concentration of a particular chemical in a specific tissue and the concentration in blood. In that case, by analogy with equation 1 above, the output of chemical from the tissue becomes

$$\frac{dC}{dt} = \frac{CQ}{VL_{tissue/blood}} \qquad (4)$$

Other things being equal, if the chemical has a much higher affinity for the tissue than it has for blood, the blood flowing out will carry a smaller proportion of the chemical contained in the tissue. Effectively, the volume of the tissue relative to the blood flowing through is increased by the factor $L_{tissue/blood}$, and of couse the time constant for the exponential loss of chemical from the tissue is correspondingly reduced:

$$C = C_0 e^{-(Q/VL_{tissue/blood})t} \qquad (5)$$

As it happens, perchloroethylene is very hydrophobic compared with most other solvents and anesthetics that have been the subjects of pharmacokinetic study to date in humans and animals (Table 2.4). Because tissues generally contain much more lipid material than blood, this means that $L_{tissue/blood}$ coefficients for perchloroethylene are particularly

Table 2.4
Partition Coefficients at 37°C For Different Pairs of Media

Chemical	$L_{water/gas}$	$L_{Oil/Gas}$	Calclulated $L_{Oil/Water}$
Ethylene oxide	62**	---	(0.5)***
Vinyl Chloride	(2.3)****	20	(9)****
Dichloromethane	7.2	152	21
1,2-Dichloroethane (EDC)	11.7	447	40
1,1-Dichloroethane	2.7	187	69
cis-1,2-Dichloroethlene	2.9	270	93
Chloroform	3.75	400.5	107
Enflurane	.78	98	128
Benzene	2.8	476.5	170
Methoxyflurane	4.5	950	211
Halothane	.79	220	279
1,1,1-Trichloroethane	.93	356	383
Trichloroethylene	1.5	819	546
Toluene	2.2	1425.5	648
Perchloroethylene	.43	1917	4458

---

*Source for water/gas and oil/gas partition coefficients:
Fiserova-Bergerova (1983), Vol. 1, pp 16-20

**From Filser and Bolt (1984).

***Octanol/water partition coefficient from Hansch and Leo, 1979.

****Calculated from the oil/gas partiton coefficient from Fiserova-Bergerova (1983) and the blood/gas partition coefficient of 2.9 given by Bolt et al. (1977).

large, and intrinsic rates of desorption from tissues are quite slow relative to most other chemicals. The opposite seems likely to be true for the more hydrophilic ethylene oxide, vinyl chloride and ethylene dichloride.

2.2.2 The Initial Dynamics of Absorption Through the Lungs

We can demonstrate the application of these mass conservation principles further by deriving the equations for absorption of chemical from the aleveolar air to the arterial blood. First, it is clear that

$$\text{Inflow to lung} = Q*C_{ven} + C_{exp}*V_{alv} \qquad (6)$$

Where Q is the rate of blood flow through the lung, C_{ven} is the concentration of the chemical in the mixed pool of venous blood, C_{exp} is the concentration of the chemical in external air, and V_{alv} is the aleveolar ventilation rate (all rates are in liters per minute and all concentrations are in moles per liter). Similarly,

$$\text{Outflow from the lung} = Q*C_{art} + C_{alv}*V_{alv} \qquad (7)$$

Where C_{art} is the concentration of the chemical in arterial blood leaving the lung, and C_{alv} is the concentration of the chemical in air leaving the alveoli.

Now as before we can define a partition coefficient, $L_{blood/air}$, that depends on the physical/chemicial characteristics of the chemical and measures the relative affinity of the chemical for blood and air. If a rapid equilibrium is established between arterial blood and alveolar air,

then

$$C_{art} = C_{alv} * L_{blood/air} \qquad (8)$$

This allows us to substitute $(C_{art}/L_{blood/air}$ for C_{alv} in equation (7). Then because the outflow from the lung must equal the total inflow to the lung,

$$C_{art} = \frac{Q*C_{ven} + C_{exp}*V_{alv}}{Q + V_{alv}/L_{blood/air}} \quad \text{or} \qquad (9)$$

$$C_{art} = \frac{L_{blood/air}*(Q*C_{ven} + C_{exp}*V_{alv})}{Q*L_{blood/air} + V_{alv}} \qquad (10)$$

This is one of the equations that is directly incorporated into our models.

Using equation (8) another way, we can calculate the fraction of incoming chemical that is absorbed from the alveolar air, at least under initial conditions where $C_{ven} = 0$. Under these circumstances, equating lung input with lung output yields

$$\begin{aligned} C_{exp}*V_{alv} &= Q*C_{art} + C_{alv}*V_{alv} \\ &= Q*C_{alv}*L_{blood/air} + C_{alv}*V_{alv} \end{aligned} \qquad (11)$$

and therefore the fraction of incoming chemical that is absorbed $(1 - C_{alv}/C_{exp})$ becomes

$$1 - \frac{C_{alv}}{C_{exp}} = 1 - \frac{V_{alv}}{QL_{blood/air} + V_{alv}}$$

or,

$$\text{Fract. Absorbed} = \frac{Q L_{\text{blood/air}}}{Q L_{\text{blood/air}} + V_{\text{alv}}} \qquad (12)$$

Therefore, other things being equal, the initial absorption rate is directly dependent on a chemical's blood/air partition coefficient and the relationship of total cardiac output (Q) to alveolar ventilation. Table 2.5 shows the results of calculations of the initial percentage of different chemicals absorbed under basal (sleeping) conditions, and for light to moderate exercise. It can be seen that the initial absorption of perchloroethylene and ethylene oxide are expected to be quite large, whereas the percentage absorption of ethylene can be expected to be quite small. Vinyl chloride is intermediate, falling to somewhat less than 60% initial absorption under conditions of "light exercise."

Table 2.5
Expected Fraction of Different Chemicals Absorbed from Alveolar Air*
Initial Exposure Conditions--Venous Concentration = 0

Chemical	$L_{blood/air}$ ***	% Absorbed at Rest** Q/V = 1.3	% Absorbed with "Light Activty"** Q/V = 0.45
Ethylene	0.15	16	6
Ethyl Chloride	1.9	71	46
Enflurane	1.9	71	46
1,1,1-Trichloroethane	2.35	75	51
Halothane	2.5	76	53
Vinyl Chloride	2.9*****	79	57
1,1-Dichloroethane	5.1	87	70
Benzene	7.4	91	77
Dichloromethane	8	91	78
cis-1,2-Dichloroethlene	9.2	92	81
Chloroform	9.3	92	81
Trichloroethylene	9.4	92	81
Methoxyflurane	13	94	85
Perchloroethylene	14	95	86
Toluene	14.5	95	87
1,2-Dichloroethane (EDC)	20	96	90
Ethylene oxide	(68)****	99	97

---

*Calculations from Equation 10--see text.

**According to Astrand [in Fiserova-Bergerova, (1983) vol. II, pp. 108-27) the perfusion/ventilation ratio is about 1.3 at rest, but falls to 0.4-0.5 with light to heavy exercise (50 W to 150 W, with 50 W corresponding to 1 l/min oxygen uptake, 7-12 l/min perfusion, and 17-22 l/minute of alveolar ventilation).

***Data from Fiserova-Bergerova, 1983 unless otherwise noted.

****Calculated from the data in Table 2.4, and the regression relationship for human blood/air partition coefficients derived in Section 3.2 below.

*****From Bolt et al. (1977).

2.4 Computer Implementation*

Our models were developed using "STELLA**" an Apple Macintosh microcompter version of the "DYNAMO" system dynamics modeling language developed at M.I.T. "System dynamics" is helpful for exploring the complex behavior of any system governed by feedback mechanisms. The concept of feedback refers to the transmission and return of information in a dynamic system. An important premise of System Dynamics is that the cause and effect relationships in a system's behavior are primarily a function of the underlying feedback structure and not of any one or group of external parameters.

In pharmacokinetic modeling there are many examples of feedback in the relationships between rates of absorption and desorption and concentrations of a substance in body tissue. For example, the rate of exhalation of a substance during desorption depends on the concentration of the substance in the tissue. As the exhalation rate changes, the tissue concentration changes, thus creating a feedback loop as the new tissue concentration further modifies the exhalation rate. Additional examples of feedback loops occur between the rate of metabolism and substance concentration in the liver tissue, the rate of tissue absorption/desorption and tissue concentration, and the rates of exchange of a substance between blood and air and between tissue and blood.

It has been shown that all dynamic systems can be represented using the concepts of stocks and flows: stocks represent accumulations through

---

*The basic reference for this section is Weigand, (1986), "A STELLA Solution," The MACazine, May 1986, pp. 52-56.

**"Structured Thinking, Experimental Learning Laboratory with Animation"

time; flows represent the movement of stock per unit time. STELLA allows one to construct a model on the terminal screen as an explicit structural diagram element by element. It facilitates the investigation of simulations through the animation of diagrams, plotting of graphs, and the generation of tables of numerical data.

A major advantage of these modeling packages is their requirement that the relationships of all components be made explicit. Figure 2.1 is an example of a STELLA diagram window. On the left side is the "tool box" containing all the elements needed to construct a model: the "Hand" functions as a cursor to select and position elements; the "Accumulator" or stock; the "flow regulator" functions as a "faucet" to regulate stock inflows and outflows according to the logic defined in its equations; the "converter" processes input logic converting information to control signals; the "link" is used to connect data paths between structural elements; the "ghost" is used to reproduce elements and their associated logic and parameters in order to reduce cluttering of interconnecting links; and the "dynamite" is used to remove elements from a diagram. "Clouds" at the beginning or end of a flow regulator serve as infinite sources or sinks and help to define the boundary of a model. Associated with each major element (accumulators, flow regulators, and converters) are dialog boxes (figure 2.2) which are used to define the logic governing their relationship with other elements.

Simulations in STELLA are run with user defined time steps and integration routines. The maximum size of the time step required to obtain accurate computations is determined by the time constants used in the model. In STELLA the hueristic used is that the time step must be no more than one fifth of the smallest time constant in order to avoid

Figure 2.1
STELLA Diagram Window

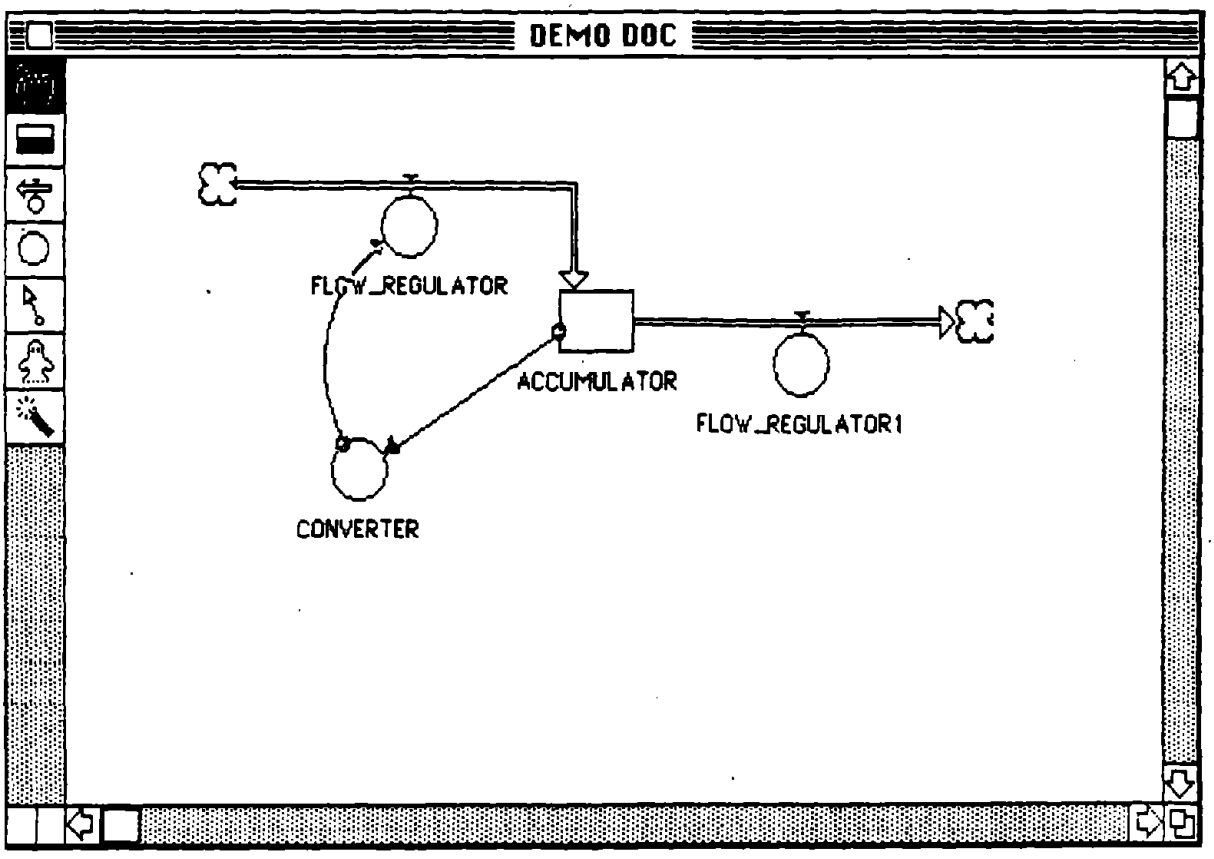

ACCUMULATOR: representation of levels of stock under analysis. They reflect conditions prevailing within the system at every point in time.

FLOW REGULATOR: provide dynamic behavior to accumulators. Flow regulators use 'decision rules' to compute flows from/to accumulators at each computation step given input from accumulators and/or converters.

CONVERTER: allow information from other system components and constant parameters to be input into flow regulator decision rules.

Figure 2.2
An Example of a STELLA Dialog Box

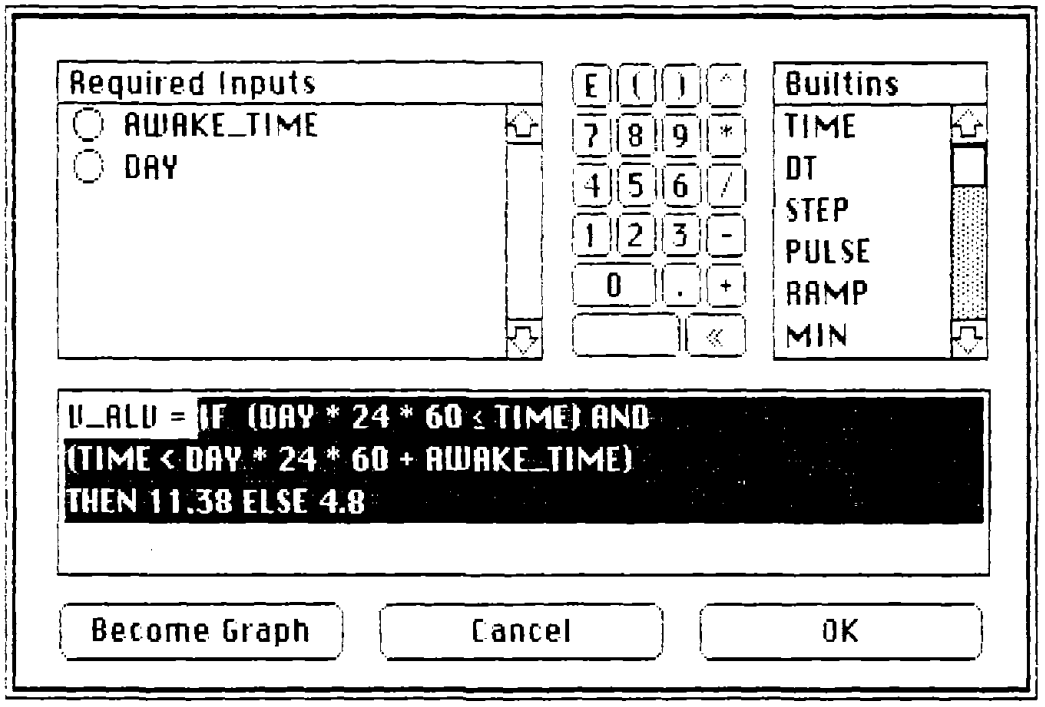

rounding errors. Our models are run using a time step of one minute (at this rate, our longest two week simulations take approximately 10 hours each to run)*. Tissue compartment levels are calculated at the end of each time step. All inflows and outflows are integrated with respect to time step and the result is added to the previous amount retained in the compartment.

The basic structure of flows to and from various tissue compartments for the rat model is shown in Figure 2.3. At the bottom of Figure 2.3 can be seen the way the model provides for gavage exposure. Material given by gavage (quantitatively defined by the initial value of the UNABSORBED compartment) is delivered to the blood flowing into the liver by at a rate that undergoes a simple exponential decay with the declining amount of material in the UNABSORBED compartment.

In our models time is expressed in minutes and chemical amounts are expressed in moles. Thus, all rates are in moles/minute and chemical levels are in moles. Other model parameters expressed either as accumulators or converters are in units of concentration -- moles/liter, with the exception of external air concentrations, defined in parts per million (ppm). To convert to units of moles/liter for inhalation input to the system, the external air ppm value is multiplied by the ratio of $10^{-6}/25.45$ (a mole of gas at body temperature of 37°C has a volume of about 25.45 liters).

This conversion, and the calculation of a number of other miscellaneous parameters are performed in a separate part of the model. Relationships among the various miscellaneous parameters for the human

---

*In order to achieve processing at this rate, it was necessary to represent the relationships between external air, the lung, arterial and venous circulations by equations rather than by compartments.

Figure 2.3
Flows To And From Compartments in the Base Rat Gavage Model

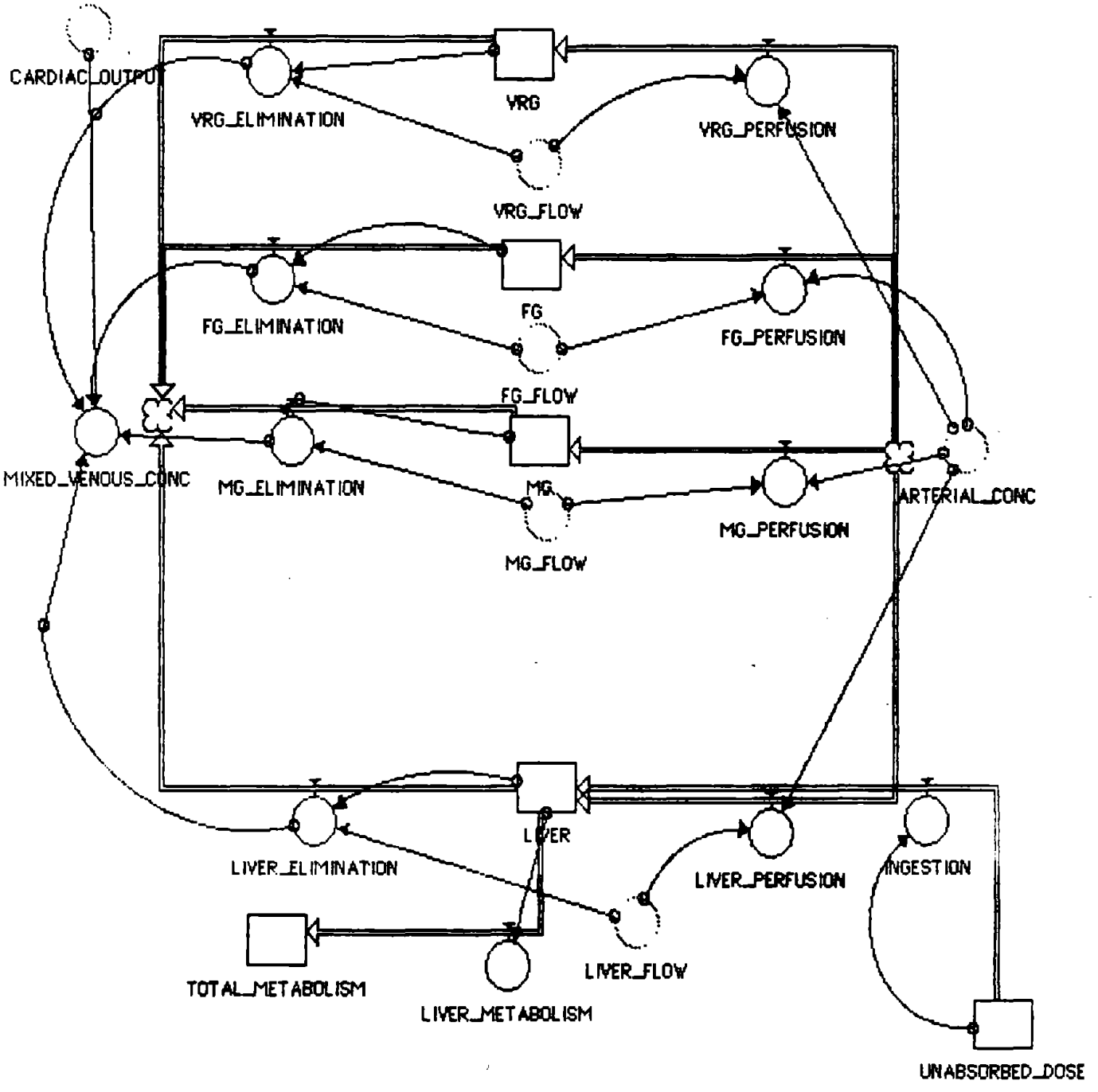

Figure 2.4
Diagrams for Calculation of Miscellaneous Parameters

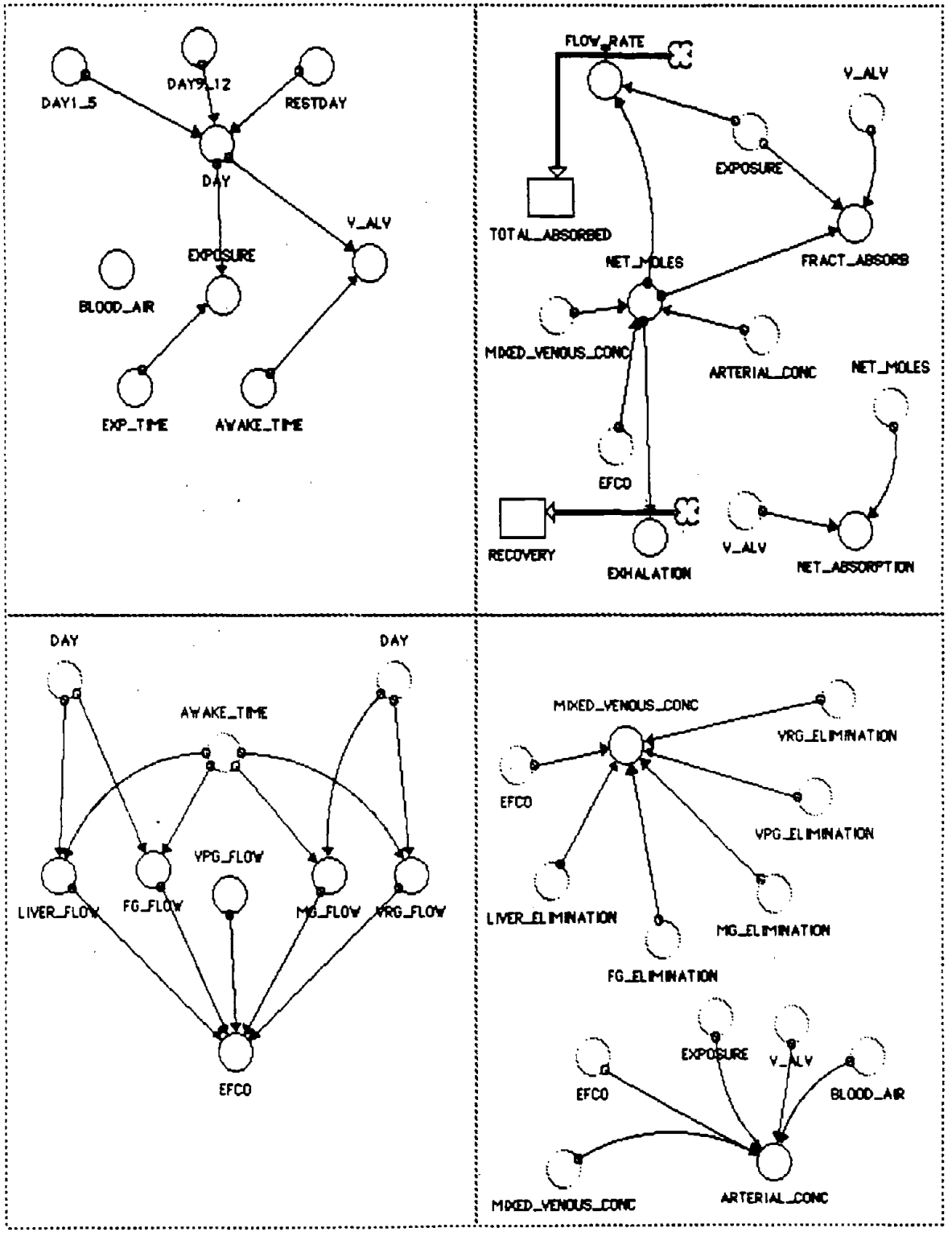

models are shown in Figure 2.4. Starting in the upper right box of Figure 2.4, these parameters include the total absorption during a simulation (TOTAL_ABSORBED), the fraction of chemical in the alveolar air that is absorbed at any specific time, (FRACT_ABSORB), the total moles exhaled during a simulation (RECOVERY), and the ppm of perchloroethylene in exhaled alveolar air at any specific time (somewhat misleadingly named NET ABSORPTION). Turning to the lower right hand box, the equation defining arterial concentration (ARTERIAL_CONC) was derived in Section 2.2.2 above, based on the alveolar ventilation ($\dot{V}$_ALV), venous concentration (MIXED VENOUS_CONC), and cardiac output (EFCO). Venous concentration is defined in turn as the sum of the moles of material eliminated from each of the tissue compartments divided by cardiac output. The calculations diagrammed in the upper left and lower left of Figure 2.4 provide for changes in air exposure level, alveolar ventilation, and tissue flows according to the day of the week (workday vs. restday) and the time of day (relative to EXP_TIME, the duration of exposure, and AWAKE_TIME, the duration of waking activity).

Figures 2.5 and 2.6 show printouts of the equations used in the basic human and rat models. Equations preceded by a square are for level variables (compartments) whose values are based in part on the contents of the compartment in the previous time step. By contrast, equations for flow regulators and miscellaneous parameters are preceded by a circle.

Figure 2.5
Equations for the Basic Human Model
("Ohitsu+" Metabolism Parameters)
("Shoeworker" Activity Level)

```
□ FG = FG + FG_PERFUSION - FG_ELIMINATION
  INIT(FG) = 0
□ LIVER = LIVER + LIVER_PERFUSION - LIVER_ELIMINATION -
  LIVER_METABOLISM
  INIT(LIVER) = 0
□ MG = MG + MG_PERFUSION - MG_ELIMINATION
  INIT(MG) = 0
□ RECOVERY = RECOVERY + EXHALATION
  INIT(RECOVERY) = 0
□ TOTAL_ABSORBED = TOTAL_ABSORBED + FLOW_RATE
  INIT(TOTAL_ABSORBED) = 0
□ TOTAL_METABOLISM = TOTAL_METABOLISM + LIVER_METABOLISM
  INIT(TOTAL_METABOLISM) = 0
□ VPG = VPG - VPG_ELIMINATION + VPG_PERFUSION
  INIT(VPG) = 0
□ VRG = VRG + VRG_PERFUSION - VRG_ELIMINATION
  INIT(VRG) = 0
○ ARTERIAL_CONC = BLOOD_AIR * (EFCO * MIXED_VENOUS_CONC + V_ALV *(
  EXPOSURE * 10^(-6)/25.45))
  / (EFCO*BLOOD_AIR + V_ALV) (moles/liter)
○ AWAKE_TIME = 960 (minutes)
○ BLOOD_AIR = 13.71
○ DAY = DAY1_5 + RESTDAY + DAY9_12 - 1
○ DAY1_5 = IF (TIME≥0) AND (TIME<1440) THEN 1 ELSE IF (TIME ≥ 1440 ) AND (
  TIME< 2880) THEN 2 ELSE IF (TIME ≥ 2880) AND (TIME < 4320) THEN 3 ELSE
  IF (TIME ≥ 4320)AND (TIME<5760) THEN 4 ELSE IF (TIME≥5760) AND (TIME<
  7200) THEN 5 ELSE 0
○ DAY9_12 = IF (TIME ≥ 11520) AND (TIME < 12960) THEN 9 ELSE IF (TIME ≥
  12960 ) AND (TIME< 14400) THEN 10 ELSE IF (TIME ≥ 14400) AND (TIME <
  15840) THEN 11 ELSE IF (TIME ≥ 15480)AND (TIME<17280) THEN 12 ELSE 0
○ EFCO = LIVER_FLOW + FG_FLOW + MG_FLOW + VPG_FLOW + VRG_FLOW
○ EXHALATION = IF (NET_MOLES < 0)
    THEN NET_MOLES*(-1) ELSE 0
○ EXPOSURE = IF (DAY * 24*60 ≤ TIME) AND (TIME < DAY * 24*60 + EXP_TIME)
   AND (DAY ≤4) THEN 100 ELSE IF (DAY * 24*60 ≤ TIME) AND (TIME < DAY *
  24*60 + EXP_TIME) AND (DAY ≥8) AND (DAY<12) THEN 20 ELSE 0 (ppm)
○ EXP_TIME = 450 (minutes)
○ FG_ELIMINATION =
  (FG * FG_FLOW) / (15.024 * 104.2)
   (moles / minute)
○ FG_FLOW = IF (DAY * 24 * 60 ≤ TIME) AND
  (TIME < DAY * 24 * 60 + AWAKE_TIME)
  THEN .49 ELSE .25
○ FG_PERFUSION = ARTERIAL_CONC * FG_FLOW
  (moles / minute)
○ FLOW_RATE = IF (EXPOSURE > 0) THEN NET_MOLES ELSE 0
○ FRACT_ABSORB =
```

Figure 2.5, Continued
Equations for the Basic Human Model
("Ohitsu+" Metabolism Parameters)

```
    NET_MOLES / (V_ALV * (EXPOSURE * (10^(-6)) / 25.45))
○ LIVER_ELIMINATION =
    (LIVER * LIVER_FLOW) / (2.476 * 4.73)
    {moles/minute}
○ LIVER_FLOW = IF (DAY * 24 * 60 ≤ TIME) AND
    (TIME < DAY * 24 * 60 + AWAKE_TIME)
    THEN 1.224 ELSE 1.4
○ LIVER_METABOLISM = (9.12* 10^(-7) * (LIVER/2.476)) /
        (1.273 * 10^(-4) + (LIVER/2.476))
    {moles/minute}
○ LIVER_PERFUSION =
    ARTERIAL_CONC * LIVER_FLOW {moles/minute}
○ MG_ELIMINATION =
    (MG * MG_FLOW) / (34.756 * 3.56) {moles / minute}
○ MG_FLOW = IF (DAY * 24 * 60 ≤ TIME) AND
    (TIME < DAY * 24 * 60 + AWAKE_TIME)
    THEN 2.155 ELSE 1.1
○ MG_PERFUSION = ARTERIAL_CONC * MG_FLOW
    {moles / minute}
○ MIXED_VENOUS_CONC =
    (VRG_ELIMINATION + FG_ELIMINATION + MG_ELIMINATION +
    VPG_ELIMINATION + LIVER_ELIMINATION) / EFCO
○ NET_ABSORPTION = IF (NET_MOLES < 0) THEN
      (NET_MOLES * (-1) / V_ALV) * 25.45 * 10^6
    ELSE 0
○ NET_MOLES =
    EFCO * (ARTERIAL_CONC - MIXED_VENOUS_CONC)
     {moles/minute}
○ RESTDAY = IF (TIME ≥ 7200) AND (TIME<8640) THEN 6 ELSE IF (TIME ≥ 8640)
    AND (TIME<10080) THEN 7 ELSE IF (TIME ≥ 10080) AND (TIME<11520) THEN
    8 ELSE IF (TIME≥17280) AND (TIME<18720) THEN 13 ELSE IF (TIME ≥ 18720)
    THEN 14 ELSE 0
○ VPG_ELIMINATION =
    (VPG * VPG_FLOW) / (12.5 * 8.0) {moles / minute}
○ VPG_FLOW = 0.1 {liter/minute}
○ VPG_PERFUSION = ARTERIAL_CONC * VPG_FLOW
    {moles / minute}
○ VRG_ELIMINATION =
    (VRG * VRG_FLOW) / (6.037 * 2.05) {moles / minute}
○ VRG_FLOW = IF (DAY * 24 * 60 ≤ TIME) AND
    (TIME < DAY * 24 * 60 + AWAKE_TIME)
    THEN 4.421 ELSE 2.95
○ VRG_PERFUSION = ARTERIAL_CONC * VRG_FLOW
    {moles / minute}
○ V_ALV = IF (DAY * 24 * 60 ≤ TIME) AND
    (TIME < DAY * 24 * 60 + AWAKE_TIME)
    THEN 11.38 ELSE 4.8
```

Figure 2.6
Equations for the Basic Rat Model

```
□ FG = FG + FG_PERFUSION - FG_ELIMINATION
  INIT(FG) = 0
□ LIVER = LIVER + LIVER_PERFUSION - LIVER_ELIMINATION -
  LIVER_METABOLISM + INGESTION
  INIT(LIVER) = 0
□ MG = MG + MG_PERFUSION - MG_ELIMINATION
  INIT(MG) = 0
□ RECOVERY = RECOVERY + EXHALATION
  INIT(RECOVERY) = 0
□ TOTAL_ABSORBED = TOTAL_ABSORBED + FLOW_RATE
  INIT(TOTAL_ABSORBED) = 0
□ TOTAL_METABOLISM = TOTAL_METABOLISM + LIVER_METABOLISM
  INIT(TOTAL_METABOLISM) = 0
□ UNABSORBED_DOSE = UNABSORBED_DOSE - INGESTION
  INIT(UNABSORBED_DOSE) = 1.507E-6
□ VRG = VRG + VRG_PERFUSION - VRG_ELIMINATION
  INIT(VRG) = 0
○ ARTERIAL_CONC = BLOOD_AIR * (CARDIAC_OUTPUT *MIXED_VENOUS_CONC +
  V_ALV * (EXPOSURE * 10^(-6)/25.45))
   / (CARDIAC_OUTPUT*BLOOD_AIR +V_ALV)     {moles/liter}
○ BLOOD_AIR =  18.9
○ CARDIAC_OUTPUT = FG_FLOW + MG_FLOW + LIVER_FLOW + VRG_FLOW    {
  liters/minute}
○ EXHALATION = IF (NET_MOLES < 0)  THEN
       NET_MOLES * (-1)  ELSE  0
○ EXPOSURE = IF (0 ≤TIME) AND (TIME < 0+360)
   THEN  0 ELSE  0
○ FG_ELIMINATION = (FG * FG_FLOW) / (.0175 * 109)
  {moles/minute}
  { ([FG] * fF[FG]) / (fV[FG] * fL[FG\BLOOD]) }
○ FG_FLOW = .0085 {liters/minute}
○ FG_PERFUSION = ARTERIAL_CONC * FG_FLOW
  {moles/minute}
  { [ARTERIAL_BLOOD] * fF[FG] / fV[arterial blood] }
○ FLOW_RATE = IF (EXPOSURE > 0) THEN  NET_MOLES
  ELSE  0
○ FRACT_ABSORB =
  NET_MOLES / (V_ALV * (EXPOSURE * (10^(-6)) / 25.45))
○ INGESTION = .01*UNABSORBED_DOSE
○ LIVER_ELIMINATION = (LIVER * LIVER_FLOW) / (.01 * 3.72)
  {moles/minute}
  { (LIVER * fF[LIVER] ) / (fV[liver] * fL[LIVER\BLOOD]) }
○ LIVER_FLOW = .0235 {liter/minute}
○ LIVER_METABOLISM = (8.6* 10^(-8)) * (LIVER/.01) /
      (1.52*10^(-4) +  (LIVER/.01))
  {moles/minute}
○ LIVER_PERFUSION = ARTERIAL_CONC * LIVER_FLOW {moles/minute}
```

Figure 2.6, Continued
Equations for the Basic Rat Model

{ ƒF[LIVER] * ARTERIAL_BLOOD / ƒV[arterial blood] }
○ MG_ELIMINATION = (MG * MG_FLOW) / (.1875 * 1.06)
{moles/minute}
{ ([MG] * ƒF[MG]) / (ƒV[MG] * ƒL[MG\BLOOD]) }
○ MG_FLOW = .0141 {liter/minute}
○ MG_PERFUSION = ARTERIAL_CONC * MG_FLOW
{moles/minute}
{ [ARTERIAL_BLOOD] * ƒF[MG] / ƒV[arter}
○ MIXED_VENOUS_CONC =
(VRG_ELIMINATION + FG_ELIMINATION + MG_ELIMINATION +
LIVER_ELIMINATION) / CARDIAC_OUTPUT
○ NET_ABSORPTION = IF (NET_MOLES < 0) THEN
(NET_MOLES * (-1) / V_ALV) * 25.45 * 10^6
ELSE 0
○ NET_MOLES =
CARDIAC_OUTPUT * (ARTERIAL_CONC - MIXED_VENOUS_CONC)
○ VRG_ELIMINATION = (VRG * VRG_FLOW) / (.0125 * 3.72)
{moles/minute}
{ VRG * ƒF[VRG] / ƒV[VRG blood] * ƒL[VRG\BLOOD] }
○ VRG_FLOW = .0479 {liter/minute}
○ VRG_PERFUSION = ARTERIAL_CONC * VRG_FLOW
{moles/minute}
{ ƒF[VRG] * ARTERIAL_BLOOD / ƒV[arterial blood] }
○ V_ALV = 0.133 {liters/minute}

Figure 2.7
Equations for the Basic Mouse Model

□ FG = FG + FG_PERFUSION - FG_ELIMINATION
INIT(FG) = 0
□ LIVER = LIVER + LIVER_PERFUSION - LIVER_ELIMINATION -
LIVER_METABOLISM + INGESTION
INIT(LIVER) = 0
□ MG = MG + MG_PERFUSION - MG_ELIMINATION
INIT(MG) = 0
□ RECOVERY = RECOVERY + EXHALATION
INIT(RECOVERY) = 0
□ TOTAL_ABSORBED = TOTAL_ABSORBED + FLOW_RATE
INIT(TOTAL_ABSORBED) = 0
□ TOTAL_METABOLISM = TOTAL_METABOLISM + LIVER_METABOLISM
INIT(TOTAL_METABOLISM) = 0
□ UNABSORBED = UNABSORBED - INGESTION
INIT(UNABSORBED) = 0
□ VRG = VRG + VRG_PERFUSION - VRG_ELIMINATION
INIT(VRG) = 0
○ ARTERIAL_CONC = BLOOD_AIR * (CARDIAC_OUTPUT *MIXED_VENOUS_CONC +
V_ALV * (EXPOSURE * 10^(-6)/25.45))
/ (CARDIAC_OUTPUT*BLOOD_AIR +V_ALV) {moles/liter}
○ BLOOD_AIR = 18.9
○ CARDIAC_OUTPUT = FG_FLOW + MG_FLOW + LIVER_FLOW + VRG_FLOW {
liters/minute}
○ EXHALATION = IF (NET_MOLES < 0) THEN
NET_MOLES * (-1) ELSE 0
○ EXPOSURE = IF (0 ≤TIME) AND (TIME < 360) OR (1440≤TIME) AND (TIME<1800)
OR (2880≤TIME) AND (TIME<3240) OR
(4320≤TIME) AND (TIME<4680) OR (5760≤TIME) AND (TIME<6120) THEN 200
ELSE 0
○ FG_ELIMINATION = (FG * FG_FLOW) / (.0025 *109)
{moles/minute}
{ ([FG_BLOOD] * ƒF[FG]) / (ƒV[FG] * ƒL[FG\BLOOD]) }
○ FG_FLOW = .00171 {liters/minute}
○ FG_PERFUSION = ARTERIAL_CONC * FG_FLOW
{moles/minute}
{ [ARTERIAL_BLOOD] * ƒF[FG] / ƒV[arterial blood] }
○ FLOW_RATE = IF (EXPOSURE > 0) THEN NET_MOLES
ELSE 0
○ FRACT_ABSORB =
NET_MOLES / (V_ALV * (EXPOSURE * (10^(-6)) / 25.45))
○ INGESTION = .01*UNABSORBED
○ LIVER_ELIMINATION = (LIVER * LIVER_FLOW) / (.0015 * 3.72)
{moles/minute}
{ (LIVER * ƒF[LIVER]) / (ƒV[liver] * ƒL[LIVER\BLOOD]) }
○ LIVER_FLOW = .00475 {liter/minute}
○ LIVER_METABOLISM = (1.13* 10^(-8)) * (LIVER/.0015) /
(1.5*10^(-5) + (LIVER/.0015))

Figure 2.7, Continued
Equations for the Basic Mouse Model

(moles/minute)
○ LIVER_PERFUSION = ARTERIAL_CONC * LIVER_FLOW {moles/minute}
{ fF[LIVER] * ARTERIAL_BLOOD / fV[arterial blood] }
○ MG_ELIMINATION = (MG * MG_FLOW) / (.0175 * 1.06)
{moles/minute}
{ ([MG] * fF[MG]) / (fV[MG] * fL[MG\BLOOD]) }
○ MG_FLOW = .00285 {liter/minute}
○ MG_PERFUSION = ARTERIAL_CONC * MG_FLOW
{moles/minute}
{ [ARTERIAL_BLOOD] * fF[MG] / fV[arter}
○ MIXED_VENOUS_CONC =
(VRG_ELIMINATION + FG_ELIMINATION + MG_ELIMINATION +
LIVER_ELIMINATION) / CARDIAC_OUTPUT
○ NET_ABSORPTION = IF (NET_MOLES < 0) THEN
(NET_MOLES * (-1) / V_ALV) * 25.45 * 10^6
ELSE 0
○ NET_MOLES =
CARDIAC_OUTPUT * (ARTERIAL_CONC - MIXED_VENOUS_CONC)
○ VRG_ELIMINATION = (VRG * VRG_FLOW) / (.00125 * 3.72)
{moles/minute}
{ VRG * fF[VRG] / fV[VRG blood] * fL[VRG\BLOOD] }
○ VRG_FLOW = .00969 {liter/minute}
○ VRG_PERFUSION = ARTERIAL_CONC * VRG_FLOW
{moles/minute}
{ fF[VRG] * ARTERIAL_BLOOD / fV[arterial blood] }
○ V_ALV = 0.0158 {liters/minute}

50272-101

REPORT DOCUMENTATION PAGE	1. REPORT NO.	2.	3. PB88-188784

4. Title and Subtitle
A Pharmacokinetic/Mechanism-Based Analysis of the Carcinogenic Risk of Ethylene Oxide

5. Report Date
87/08/00

6.

7. Author(s)
Hattis, D.

8. Performing Organization Rept. No.
CTPID 87-1

9. Performing Organization Name and Address
Center for Technology, Policy and Industrial Development, Massachusetts Institute of Technology, Cambridge, Massachusetts

10. Project/Task/Work Unit No.

11. Contract(C) or Grant(G) No.
(C)
(G)

12. Sponsoring Organization Name and Address

13. Type of Report & Period Covered

14.

15. Supplementary Notes

16. Abstract (Limit: 200 words)

An attempt was made to build an integrated series of pharmacokinetic models for low molecular weight alkylating agents in efforts to expand the understanding of risk assessment for various occupational carcinogens. The purpose was to allow for better assessment of biologically effective doses of activated metabolites delivered to target tissues and to arrive at a better translation of such units between species. The approach to pharmacokinetic modeling of ethylene-oxide (75218) was defined, and specific results were presented. Longer elimination was predicted to increase internal dose, so that greater internal doses would be expected in man compared to rodents. Lower respiration per body weight in man would decrease absorption rate, offsetting the higher predicted internal dose. In terms of human cancer risk, it is stated that substantial data is available showing carcinogenic response of rats and mice to ethylene-oxide. Equations were presented showing the risk resulting for different sites, species, and sexes using the measure of delivered dose in a multistage model. Implications for overall human cancer risk from 45 year 8 hour per day occupational exposures to 1 part per million ethylene-oxide were presented. Doses used in analysis did not yield markedly divergent estimates of human risk. The authors conclude that for a simple direct acting alkylator like ethylene-oxide, traditional approaches for dose and risk projection across species are supported by pharmacokinetic based analysis.

17. Document Analysis a. Descriptors

b. Identifiers/Open-Ended Terms

Computer-models, Kinetics, Exposure-levels, Ethylenes, Oxides, Disinfectants, Humans, Occupational-exposure, Carcinogenesis, Laboratory-animals, Metabolic-study, Risk-analysis

c. COSATI Field/Group

18. Availability Statement	19. Security Class (This Report)	21. No. of Pages
	20. Security Class (This Page)	22.